ROMA TRE
UNIVERSITÀ DEGLI STUDI

SCUOLA DOTTORALE IN BIOLOGIA MOLECOLARE E CELLULARE

XXXII CICLO

Le amino ossidasi in Arabidopsis, espresse nei tessuti e nelle cellule coinvolte nel trasporto idrico e nella perdita di acqua, svolgono un ruolo nella chiusura stomatica e nella plasticità fenotipica dello xilema dopo trattamenti ormonali o in condizioni di stress abiotico

---

The Arabidopsis amine oxidases expressed in tissues and cells involved in water transport and water loss play a role in stomatal closure and xylem phenotypic plasticity under hormone treatments and abiotic stress

ILARIA FRAUDENTALI

Tutor:
Prof.ssa ALESSANDRA CONA

Coordinatore:
Prof. PAOLO MARIOTTINI

A.A. 2019/2020

TABLE OF CONTENTS

ABBREVIATIONS

ABA	Abscissic acid
AO	Amine oxidase
AtCuAO	*Arabidopsis thaliana* copper-containing amine oxidase
AtPAO	*Arabidopsis thaliana* polyamine oxidase
AUR	Amplex ultra red
CuAO	Copper-containing amine oxidase
DMTU	*N*,*N*^{1}-dimethylthiourea
GFP	Green fluorescent protein
GLR	Glutamate like-receptor
GUS	β-glucuronidase
IAA	Indole-3-acetic acid
JA	Jasmonic acid
LM	Light microscope
LSCM	Laser-scanning confocal microscope
MeJA	Methyl jasmonate
MS	Murashige and Skoog
PAO	Polyamine oxidase
PCD	Programmed cell death
PI	Propidium iodide
Put	Putrescine
PA	Polyamine
RT-qPCR	Reverse transcription quantitative PCR
SA	Salicylic acid
Spd	Spermidine
Spm	Spermine
Ther-Spm	Thermospermine
TPQ	2,4,5-trihydroxyphenylalanine quinone cofactor
WT	Wild type

RIASSUNTO

Le poliammine (PA) sono composti alifatici a basso peso molecolare presenti in tutti gli organismi viventi ed essenziali per la crescita e il differenziamento cellulare. La fine regolazione delle loro vie biosintetiche e cataboliche, nonché i processi di coniugazione e trasporto, assicurano il mantenimento dell'omeostasi dei livelli cellulari delle PA, supportando la rilevanza biologica di questi composti. Nelle piante, le PA più comuni sono la triamina spermidina (Spd), la tetramina spermina (Spm) e il loro precursore diamminico putrescina (Put). Per quanto riguarda il loro ruolo fisiologico, è stato riportato che le PA svolgono ruoli importanti in molti processi di sviluppo, tra cui la morfogenesi, la crescita, il differenziamento e la senescenza. Le PA sono catabolizzate da due classi di enzimi appartenenti alla famiglia delle ammine ossidasi (AO), le poliammino ossidasi monomeriche contenenti FAD (PAO) e le ammino ossidasi omodimeriche contenenti rame (CuAO). Nell'organismo modello *Arabidopsis thaliana*, sono presenti dieci geni putativi annotati come *CuAO* (*AtCuAO*), di cui solo cinque sono stati caratterizzati per la specificità del substrato, la localizzazione subcellulare e la regolazione dell'espressione genica: AtCuAOβ (precedentemente AtAO1; At4g14940) e AtCuAOγ1 (precedentemente AtCuAO1; At1g62810) con localizzazione apoplastica, AtCuAOα2 (precedentemente AtCuAO8; At1g31690), AtCuAOα3 (precedentemente AtCuAO2; At1g31710) e AtCuAOζ (precedentemente AtCuAO3; At2g42490) con localizzazione perossisomiale, tutte ossidano la Spd a livello del gruppo amminico primario con un'affinità paragonabile a quella della Put (AtCuAOγ1, AtCuAOα2 and AtCuAOα3) o di poco inferiore (AtCuAOβ and AtCuAOζ). Oltre a regolare la concentrazione delle PA nelle cellule vegetali, le AO contribuiscono ad importanti processi fisiologici attraverso i loro prodotti di reazione, fra i cui l'H_2O_2, composto condiviso in tutte le reazioni catalizzate dalle AO che svolge un ruolo chiave durante i processi di sviluppo e nelle risposte di difesa contro gli stress biotici e abiotici. Nel dettaglio, le AO localizzate nella parete cellulare sono coinvolte nelle risposte di difesa (sia costitutive, sia inducibili) contro gli stress biotici, inducendo eventi di irrigidimento della parete attraverso la produzione di H_2O_2 nell'apoplasto, e rappresentano quindi dei mediatori coinvolti nelle fasi finali di differenziazione dello xilema, nella deposizione della parete secondaria e nei processi di morte cellulare programmata. Inoltre, in risposta agli stress biotici e abiotici, l'ABA induce la produzione di H_2O_2 nelle cellule di guardia portando alla chiusura stomatica. Nonostante una fonte indiscussa di H_2O_2 nella parete cellulare delle cellule di

guardia sia rappresentata dalle NADPH ossidasi della membrana plasmatica, recentemente è stato dimostrato che anche l'H_2O_2 prodotta dall'ossidazione delle PA può essere coinvolta in questo processo.

Lo scopo del presente lavoro è stato quello di evidenziare i ruoli fisiologici svolti dall'ossidazione delle PA mediata da sei CuAO di Arabidopsis (codificate dai rispettivi geni *AtCuAOα2, AtCuAOα3, AtCuAOβ, AtCuAOγ1, AtCuAOγ2 e AtCuAOδ*) nelle risposte allo stress. A tal fine, sono state analizzate piante transgeniche di Arabidopsis esprimenti i costrutti *AtCuAO::proteina fluorescente verde-β-glucuronidasi (GFP-GUS),* nonché mutanti inserzionali con perdita di funzione *Atcuaoβ* e *Atcuaoδ*. In particolare, al fine di porre le basi per future ricerche sui ruoli fisiologici delle AtCuAO, è stato svolto uno studio completo dei *pattern* di espressione delle sei AtCuAO in studio mediante analisi quantitative (RT-qPCR) e approcci qualitativi (piante transgeniche AtCuAO-promotore: GFP-GUS), in piante trattate con diversi ormoni legati allo stress (ABA, MeJA, SA) e IAA, e in piante sottoposte a stress abiotici come la ferita e la disidratazione. Per quanto riguarda i ruoli fisiologici, l'espressione riportata precedentemente di *AtCuAOβ* nelle cellule di guardia, insieme alla sua espressione inducibile dal MeJA nei tessuti xilematici della radice, suggeriscono un ruolo di questo gene nei meccanismi omeostatici che portano a un equilibrio tra l'apporto idrico dipendente dallo xilema e la perdita d'acqua dipendente gli stomi in condizioni di stress. La chiusura stomatica può rappresentare una risposta rapida alle lesioni seguita dal rimodellamento del tessuto xilematico che consente l'acclimatazione delle piante in condizioni avverse. In considerazione di ciò, è stato studiato il coinvolgimento di AtCuAOβ nella chiusura stomatica e nel differenziamento dello xilema in piante sottoposte alla ferita della foglia o della radice, con particolare attenzione al suo possibile coinvolgimento nelle risposte sistemiche. Inoltre, il ruolo noto svolto dal vacuolo nella chiusura stomatica indotta dall'ABA, insieme al verificarsi di un'espressione di AtCuAOδ inducibile dall'ABA nelle cellule di guardia, ci hanno portato ad analizzare il possibile coinvolgimento dell'enzima vacuolare AtCuAOδ nel controllo del movimento stomatico.

Per quanto riguarda *AtCuAOβ*, i dati qui riportati mostrato un aumento dei suoi livelli di espressione dopo la ferita sia della foglia, sia della radice e dopo il trattamento con il MeJA, ormone che segnala la ferita, supportando quindi un ruolo di primo piano di questa ammino ossidasi nelle risposte ai danni meccanici. Inoltre, i saggi istochimici svolti su piante *prom-AtCuAOβ::GFP-GUS* dimostrano che il trattamento con il MeJA, così come la ferita della foglia e della radice, inducono l'espressione di AtCuAOβ nelle

cellule di guardia, supportandone il ruolo nel controllo del movimento stomatico. Coerentemente, i risultati di questo lavoro indicano il coinvolgimento dell'H_2O_2 prodotta dall'ossidazione delle PA mediata da AtCuAOβ nella chiusura stomatica indotta da MeJA e dalla ferita. Per quanto riguarda le risposte più brevi, è interessante notare che le piante WT rispondono alla ferita della foglia o della radice sia con una segnalazione locale che sistemica, rivelando il verificarsi di risposte AtCuAOβ-dipendenti nei tessuti distali, come è evidenziato dalla non responsività dei mutanti *Atcuaoβ* nelle stesse condizioni di trattamento. Complessivamente, questi risultati supportano il coinvolgimento di AtCuAOβ nella chiusura stomatica indotta dal MeJA e dalla ferita con una comunicazione radice-foglia a lunga distanza estremamente rapida. Questi dati ci permettono di ipotizzare un'azione sia locale che sistemica di AtCuAOβ nella regolazione dell'omeostasi del bilancio idrico mediato dalla chiusura stomatica. Per quanto riguarda la comunicazione distale fra foglia e radice, le analisi qui riportate sulla crescita delle radici, sulla posizione del protoxilema e sulla dimensione del meristema nelle piante WT ferite nell'aera fogliare, mostrano una differenziazione precoce del protoxilema reversibile dal trattamento con lo *scavenger* dell' H_2O_2 DMTU, che si verifica dopo la ferita, senza comportare variazioni osservabili nella dimensione del meristema e nella crescita delle radici, confermando il coinvolgimento di AtCuAOβ nel differenziamento precoce dello xilema che si verifica in condizioni di stress, come appunto la ferita. Nel complesso, l'espressione di *AtCuAOβ* nei tessuti e nelle strutture che regolano l'approvvigionamento idrico e la perdita d'acqua come le cellule di guardia degli stomi e lo xilema, il suo ruolo nel differenziamento precoce del protoxilema e nella chiusura stomatica indotti dalla ferita, suggeriscono un ruolo di questo enzima nell'omeostasi dell'equilibrio idrico mediante la modulazione coordinata di riarrangiamenti anatomici e funzionali del tessuto xilematico e dei livelli di apertura delle cellule di guardia nelle piante sottoposte a ferita.

Per quanto riguarda AtCuAOδ, i dati mostrano che la sua espressione genica è indotta dall'ABA e che i mutanti inserzionali *Atcuaoδ* risultano meno sensibili a questo ormone, mostrando una chiusura stomatica ridotta dopo il trattamento con ABA rispetto alle piante WT. Inoltre, gli inibitori delle CuAO, così come il DMTU, revertono quasi completamente la chiusura stomatica indotta dall'ABA nelle piante WT. Nel complesso, i dati suggeriscono quindi che AtCuAOδ è coinvolto nella produzione dell'H_2O_2 che media la chiusura stomatica indotta da ABA.

Infine, i dati riportati delle analisi di espressione genica quantitativa e tessuto-specifica svolte tramite RT-qPCR e colorazione istochimica (GUS) in condizioni di stress o dopo i trattamenti con ormoni o PA, hanno rivelato che l'espressione di *AtCuAOα2*, *AtCuAOα3*, *AtCuAOγ1* e *AtCuAOγ2* è indotta in seguito alla disidratazione, alla ferita e al trattamento con IAA e la Put. L'espressione di questi quattro geni nei tessuti vascolari e negli idatodi, strutture coinvolte nell'approvvigionamento e/o nella perdita d'acqua, e l'induzione della loro espressione dopo disidratazione, suggeriscono un ruolo nell'omeostasi dell'equilibrio idrico. In aggiunta, la localizzazione riscontrata in zone in cui è stato osservato un massimo di auxina insieme all'induzione della loro espressione da parte dell'IAA, supportano un ruolo di questi enzimi nella maturazione dei tessuti e nel differenziamento dello xilema.

ABSTRACT

Polyamines (PAs) are ubiquitous, low-molecular-weight aliphatic compounds, present in all living organisms and essential for cell growth and differentiation. The fine regulation of their biosynthetic and catabolic pathways as well as conjugation and transport processes ensure an accurate homeostasis of PA cellular levels, supporting the biological relevance of these compounds. In plants, the most common PAs are the triamine spermidine (Spd), the tetramine spermine (Spm) and their diamine precursor putrescine (Put). Regarding their physiological role, it has been suggested that PAs play important roles in many developmental processes, including morphogenesis, growth, differentiation and senescence. PAs are catabolized through terminal or back-conversion metabolism giving rise to an amine moiety, an amino-aldehyde and H_2O_2, by two different classes of enzymes belonging to the amine oxidase (AO) family, the monomeric FAD-containing polyamine oxidases (PAOs) and the homodimeric copper-containing amine oxidases (CuAOs). In the model organism of flowering plants *Arabidopsis thaliana*, ten putative genes annotated as *CuAOs* (*AtCuAO*) are present, of which only five have been characterized for substrate specificity, subcellular localization and regulation of gene expression. The apoplastic AtCuAOβ (formerly AtAO1; At4g14940) and AtCuAOγ1 (formerly AtCuAO1; At1g62810), the peroxisomal AtCuAOα2 (formerly AtCuAO8; At1g31690) and AtCuAOα3 (formerly AtCuAO2; At1g31710) and AtCuAOζ (formerly AtCuAO3; At2g42490) all

oxidize Spd at the primary amino group with an affinity comparable to that for Put (AtCuAOγ1, AtCuAOα2 and AtCuAOα3) or slightly lower (AtCuAOβ and AtCuAOζ). In addition to regulating the concentration of PAs in plant cells, AOs also contribute to important physiological processes through their reaction products, aminoaldehydes, DAP and H_2O_2, which is a shared compound of all the AO-catalyzed reactions and has a key role in both development and defense responses against biotic and abiotic stresses. In details, cell-wall localized AOs contribute to the constitutive and inducible defense responses against biotic stress inducing wall-stiffening events through H_2O_2 production in the apoplast and may play a key role as a mediator in the final events needed to accomplish full xylem differentiation, namely secondary wall deposition and developmental programmed cell death (PCD). Moreover, in responses to biotic and abiotic stresses, ABA induces the production of H_2O_2 in guard cells leading to stomatal closure. A well-known source of H_2O_2 in the cell-wall of guard cells is represented by plasma membrane NADPH oxidases, but recently it has been shown that the H_2O_2 produced by apoplastic catabolism of PAs can also be involved.

The aim of the present work is to highlight the physiological roles played by six Arabidopsis CuAOs (encoded by the respective genes *AtCuAOα2*, *AtCuAOα3*, *AtCuAOβ*, *AtCuAOγ1*, *AtCuAOγ2* and *AtCuAOδ*) during stress responses. To this purpose, transgenic Arabidopsis plants expressing *AtCuAO::green fluorescent protein-β-glucuronidase (GFP-GUS)* constructs, as well as both *AtCuAOβ* and *AtCuAOδ* insertional loss-of-function mutant plants have been exploited. Particularly, in order to lay the basis for future research on AtCuAO physiological roles, a comprehensive and extensive analysis of the expression patterns of the six *AtCuAO* under treatment with different stress related hormones (ABA, MeJA, SA) and IAA as well as after abiotic stress like wounding and dehydration were investigated by both quantitative analysis (RT-qPCR) and qualitative approaches (*AtCuAOs-promoter::GFP-GUS* transgenic plants). Concerning the physiological roles, the previously reported expression of *AtCuAOβ* in guard cells, together with its MeJA-inducible expression in xylem tissues, suggests a role of this gene in homeostatic mechanisms leading to a balance between xylem-dependent water-supply and stomata-dependent water-loss under stress conditions. Stomatal closure may represent a fast response to injury followed by remodeling of xylem tissue allowing plant acclimation to adverse conditions. Considering this, the involvement of AtCuAOβ in stomatal closure and xylem differentiation upon leaf or root wounding have been investigated, with particular attention to its possible involvement in systemic responses.

Additionally, the known role played by the vacuole in ABA-induced stomatal closure, along with the occurrence of an ABA-inducible *AtCuAOδ* expression in guard cells, led us to analyze the possible involvement of the vacuolar AtCuAOδ in the control of stomatal movement.

Regarding *AtCuAOβ*, data herein reported showed an increase in *AtCuAOβ* expression levels upon both leaf or root wounding and after treatment with the wound-signal-hormone MeJA, supporting its prominent role in mechanical damage responses. Moreover, histochemical assays showed that MeJA treatment, as well as cotyledonary leaf wounding and root wounding, induced *AtCuAOβ* expression in stomatal guard cells of the stressed *AtCuAOβ-promoter::GFP-GUS* plants, supporting its role in stomatal movement control. Coherently, herein reported results indicate the involvement of H_2O_2 delivered from AtCuAOβ-mediated PA catabolism in MeJA- and wound-induced stomatal closure. As concerns shorter time responses, interestingly WT plants respond to leaf or root wounding both with a local and systemic signalling, revealing the occurrence of a distal-tissues responses in AtCuAOβ-dependent way, as evidenced by the unresponsiveness of *Atcuaoβ* mutants to the same conditions of treatment. Overall, these results support the AtCuAOβ involvement in MeJA/wounding-induced stomatal closure with a dynamic implying extremely rapid long-distance root-to-leaf communication and could allow us to hypothesize a local and systemic action of AtCuAOβ related to water balance homeostasis regulating stomatal closure. As concerns the shoot-to-root long distal communication, analyses herein reported on root growth, protoxylem position and meristem size in cotyledonary leaf-wounded WT plants, show a DMTU-reversible early root-protoxylem differentiation occurring after the injury, with no observable changes in meristem size and root growth, confirming the involvement of AtCuAOβ in xylem differentiation which occurs under stress conditions, such as wounding. As a whole, the expression of *AtCuAOβ* in tissues or cell types regulating water supply and water loss such as xylem and stomata guard cells, with its role in protoxylem differentiation and in wound-induced stomatal closure suggests a role in water balance homeostasis by modulating coordinated adjustments in anatomical and functional features of xylem tissue and guard cells aperture levels in wounded plants.

As concerns *AtCuAOδ*, data show that is up-regulated by ABA and that two *Atcuaoδ* insertional mutants are less responsive to this hormone, showing reduced ABA-mediated stomatal closure and H_2O_2 accumulation in guard cells as compared to the WT plants. Furthermore, CuAO inhibitors, as well as the H_2O_2 scavenger *N,N*^{1}-dimethylthiourea, reversed most of the ABA-

induced stomatal closure in WT plants. Tacking together, data suggest that AtCuAOδ is involved in the H_2O_2 production related to ABA-induced stomatal closure.

Analysis herein reported of quantitative and tissue-specific gene expression performed by RT-qPCR and GUS-staining under stress conditions or after treatments with hormones or PAs, revealed that *AtCuAOα2, AtCuAOα3, AtCuAOγ1* and *AtCuAOγ2* expression was induced during dehydration recovery, wounding, treatment with IAA and Put. Moreover, the expression of these four genes in vascular tissues and hydathodes involved in water supply and/or loss, along with a dehydration-recovery dependent gene expression, would suggest a role in water balance homeostasis. In addition, occurrence in zones where an auxin maximum has been observed along with an IAA-induced alteration of expression profiles, support a role in tissue maturation and xylem differentiation events.

1. INTRODUCTON

1.1 Polyamines

Polyamines (PAs) are ubiquitous, low-molecular-weight aliphatic compounds, present in all living organisms and essential for cell growth and differentiation. PAs play a multitude of functions in cells and although their biological roles remain elusive, they interplay in basic cellular processes, including DNA replication and transcription, RNA modification, protein synthesis, regulation of ion-channel activities, free radical scavenging, cell cycle regulation as well as signal transduction pathways and programmed cell death (PCD). The fine regulation of their biosynthetic and catabolic pathways as well as conjugation and transport processes ensures an accurate homeostasis of PA cellular levels, supporting the biological relevance of these compounds. Furthermore, PAs may act as sources of biologically active compounds such as hydrogen peroxide (H_2O_2) and aldehydes, generated via PA catabolism/interconversion pathways. In mammalian cells, dysregulation of PA metabolism has been linked to cancer development and owing to their role as modulators of cell proliferation and apoptosis, PAs have been target of antineoplastic therapies (Tavladoraki *et al*., 2012; Murray-Stewart *et al*., 2016; Ohkubo *et al*., 2019).

In plants, the most common PAs are the triamine spermidine (Spd), the tetramine spermine (Spm) and their diamine precursor putrescine (Put). Additionally, thermospermine (T-Spm), an isomer of Spm which has not been detected in mammalian cells has been found at low levels in plants (Tavladoraki *et al*., 2012). PAs are positively charged at physiological pH values and interact with negatively charged macromolecules, such as DNA, RNA, proteins and phospholipids and, due to these interactions, the concentration of the freely available PAs is considered to be much lower than that of the total intracellular pool. PAs are essential for life and in plants this is supported by the evidence that Arabidopsis (*Arabidopsis thaliana*) loss-of-function mutants defective in Put and Spd biosynthetic pathways are embryo-lethal (Imai *et al*., 2004). Regarding their physiological role, it has been suggested that PAs play important roles in many developmental processes, including morphogenesis, growth, differentiation and senescence. Furthermore, H_2O_2 derived from PA catabolism participates in the complex network of reactive oxygen species (ROS) that act as signaling molecules involved in responses to biotic and abiotic stresses (Jiménez-Bremont *et al*., 2014; Minocha *et al*., 2014; Tiburcio *et al*., 2014; Cai *et al*., 2015).

1.2 Polyamines biosynthesis and catabolism

PA biosynthesis takes place according to a pattern conserved in different biological systems. The Put formation is the first step, followed by its conversion to Spd and Spm by the subsequent addition of an amino propyl group, transferred from decarboxylated *S*-adenosylmethionine, which in turn is synthesized from methionine (Fig. 1.1). In plants, Put biosynthesis occurs through two alternative metabolic pathways (Liu *et al.*, 2007), the direct pathway which involves the ornithine decarboxylation catalyzed by ornithine decarboxylase (ODC) and the indirect pathway which starts from the arginine decarboxylation catalyzed by arginine decarboxylase (ADC), which is absent in the animal PA catabolism. In addition, Spm is not present in bacteria, due to absence of Spm synthase, confirming the non-essentiality of Spm for life. Probably, the presence in plants of two independent biosynthetic pathways may be justified by their necessity to modulate PA concentration in response to developmental or pathological conditions (Medda *et al*., 2009). Furthermore, in plants T-Spm biosynthesis occurs via T-Spm synthase encoded by ACL5 (Hanzawa *et al*., 2000). In Arabidopsis, Put is produced exclusively through the ADC pathway since no genes or enzyme activities related to ODC have been detected (Alcázar *et al*., 2010).

PAs are catabolized through terminal or back-conversion metabolism giving rise to an amine moiety [ammonium, 1,3-diaminopropane (DAP) or the corresponding lower level PA], an amino-aldehyde and H_2O_2 by two different classes of enzymes belonging to the amine oxidase (AO) family, the monomeric FAD-containing polyamine oxidases (PAOs) and the homodimeric copper-containing amine oxidases (CuAOs), respectively oxidizing the carbon adjacent to the secondary or the primary amino group (Fig. 1.1). While PAOs include members that can catalyze either PA back-conversion metabolism (BC-PAOs) or terminal catabolism (TC-PAOs), CuAOs are exclusively responsible for terminal catabolism producing ammonium, an amino-aldehyde and H_2O_2 (Moschou et al., 2012, Tavladoraki *et al*., 2012, Tavladoraki *et al*., 2016). In most plant species, the preferred CuAO substrate is Put and these enzymes show mostly a lower affinity for Spd and Spm, with the exception of Arabidopsis CuAOs (Planas-Portell *et al*., 2013). Instead, PAOs catalyze the oxidation of Spm and Spd (Tavladoraki *et al*., 2016). The ability to catalyze the terminal oxidation of Put and, in some cases, the first higher PA Spd, positions CuAOs at an early key step in the PA oxidative metabolism allowing them to behave as important regulators of PA levels.

In the model organism of flowering plants Arabidopsis, ten putative genes annotated as *CuAOs* (*AtCuAO*) are present, of which only five have been characterized for substrate specificity, subcellular localization and regulation of gene expression. The apoplastic AtCuAOβ (formerly AtAO1; At4g14940) (Møller and McPherson, 1998) and AtCuAOγ1 (formerly AtCuAO1; At1g62810), the peroxisomal AtCuAOα2 (formerly AtCuAO8; At1g31690) and AtCuAOα3 (formerly AtCuAO2; At1g31710) and AtCuAOζ (formerly AtCuAO3; At2g42490) (Fukao *et al*., 2003; Groβ *et al*., 2017; Planas-Portell *et al*., 2013; Qu *et al*., 2014; Tavladoraki *et al*., 2016) all oxidize Spd at the primary amino group with an affinity comparable to that for Put (AtCuAOγ1, AtCuAOα2 and AtCuAOα3) or slightly lower (AtCuAOβ and AtCuAOζ).

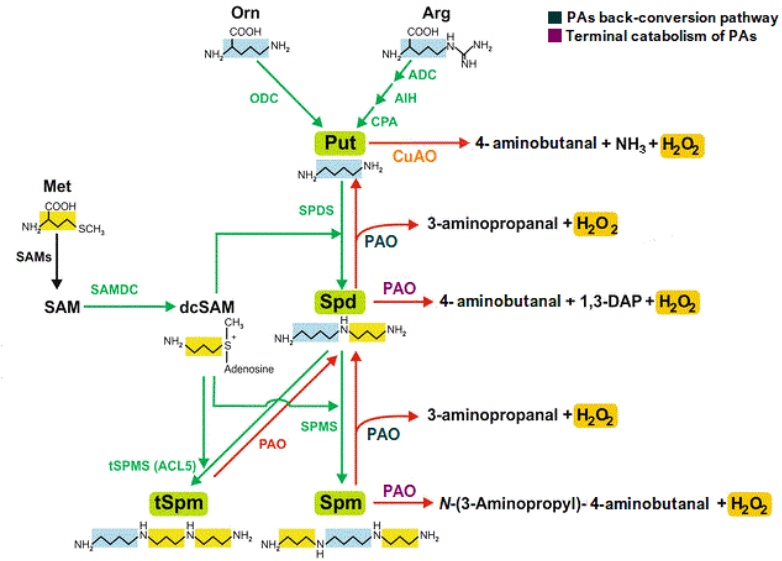

Figure 1.1 Polyamine metabolism in plants. Biosynthesis routes are colored in green and catabolism pathways in red. Modified from Marco *et al.* 2015.

1.3 Physiological roles of amine oxidases

Besides regulating the concentration of PAs in plant cells, AOs also contribute to important physiological processes through their reaction products, aminoaldehydes, DAP and H_2O_2. In particular, through the action of

an aldehyde dehydrogenase (ADH), 4-aminobutanal can be metabolized to γ-aminobutyric acid (GABA), which is rapidly produced in response to biotic and abiotic stresses and it is an important signaling-molecule associated with various physiological processes, such as regulation of cytosolic pH, carbon fluxes into the citric acid cycle, insect deterrence and protection against oxidative stress (Cona et al., 2006). Moreover, GABA can flow into the Krebs cycle after transformation into succinic acid, thus ensuring the recycling of carbon and nitrogen stored in Put (Moschou *et al*., 2012; Tavladoraki *et al.*, 2012). DAP is a precursor of β-alanine and of various uncommon PAs, and is associated in plants with stress tolerance (Cona *et al*., 2006). H_2O_2 is a shared compound of all the AO reaction and has a key role in both development and defense responses against biotic and abiotic stresses (Apel and Hirt, 2004; Mittler *et al*., 2004; Cona *et al*., 2006). H_2O_2 is a signaling-molecule produced by many different enzymatic systems (i.e. peroxidase, oxalate oxidase and NADPH oxidase; Fig. 1.2), and the redundancy of ROS-source reflects the necessity of specific ROS production in different stages of development and differentiation as well as in the course of defense responses. In this regard, both CuAOs and PAOs expression patterns are tissue-specific and spatially and temporally regulated, supporting their key role as ROS-regulators in essential events during plant life. Furthermore, AOs have different subcellular localizations both intracellular (vacuolar or peroxysomal) or apoplastic. In this regard, a prevalent role as modulator of PA levels is emerging for the intracellular AOs (Tavladoraki *et al*., 2016), although there are only few pieces of information about it. Conversely, the regulatory function of apoplastic AOs depends on substrate availability in the cell wall. Indeed, a previous study reports evidence for the limiting amount of freely available PAs in the extra-cellular space under control conditions (Rea *et al*., 2004). It has been proposed that controlled PA transport to the apoplast might occur during specific physiological or stress conditions (Yoda *et al*., 2003). In this context, the absence of detectable PA levels along with the lack of PA biosynthesis or interconversion pathway in the cell wall, suggest a prevalent role of apoplastic AOs in H_2O_2 production, following PA secretion in the apoplast upon biotic or abiotic stress (Ghuge *et al*., 2015a).

Regarding intracellular AOs, they have been shown to play an important role in the regulation of the level of T-Spm, that is implied in developmental processes such as the transition from vegetative to reproductive growth (Kim *et al*., 2014), as well as in xylem differentiation, interfering with auxin/cytokinin interplay (Alabdallah *et al*., 2017). Moreover, relevant roles

of intracellular AOs in stress tolerance, particularly in drought and salt stress, have been reported (Sagor *et al*., 2016).

Regarding apoplastic AOs, the H_2O_2 produced through PA oxidation has been shown to play a dual role in triggering peroxidase-mediated wall stiffening events during defense and development and in signaling the modulation of defense gene expression as well as of hypersensitive response (HR) and developmental cell death gene expression. In this regard, H_2O_2 behaves as the electron acceptor co-substrate of apoplastic peroxidase and indirectly plays an essential role in the wall stiffening process due to the increase in lignification and cross-linking events, followed by the inhibition of cell growth and cell wall strengthening as a structural barrier, preventing the entry of pathogenic microorganisms (Kärkönen and Kuchitsu, 2015; Fig. 1.2). Coherently with AO role in cross-linking events regulating growth, development and differentiation, a high levels of apoplastic AOs in tissues undergoing lignification or extensive wall-stiffening, such as xylem, xylem parenchima, rhizodermis, hypodermis, endodermis and epidermis, have been found, along with a positive spatial correlation between lignin, peroxidase and CuAO levels in chickpea (*Cicer arietinum*) and tobacco (*Nicotiana tabacum*) as well as a light- and indoleacetic acid (IAA)-regulation of their spatial and temporal expression in maize (*Zea mays*; Cona *et al.*, 2006). Finally, it has been suggested that AO-derived H_2O_2 may play a role in maturation of xylem cells by triggering the peroxidase-driven polymerisation of lignin and by signalling developmental PCD in differentiating xylem precursors, depending on developmentally-regulated PA secretion in the apoplast (Cona *et al.*, 2006).

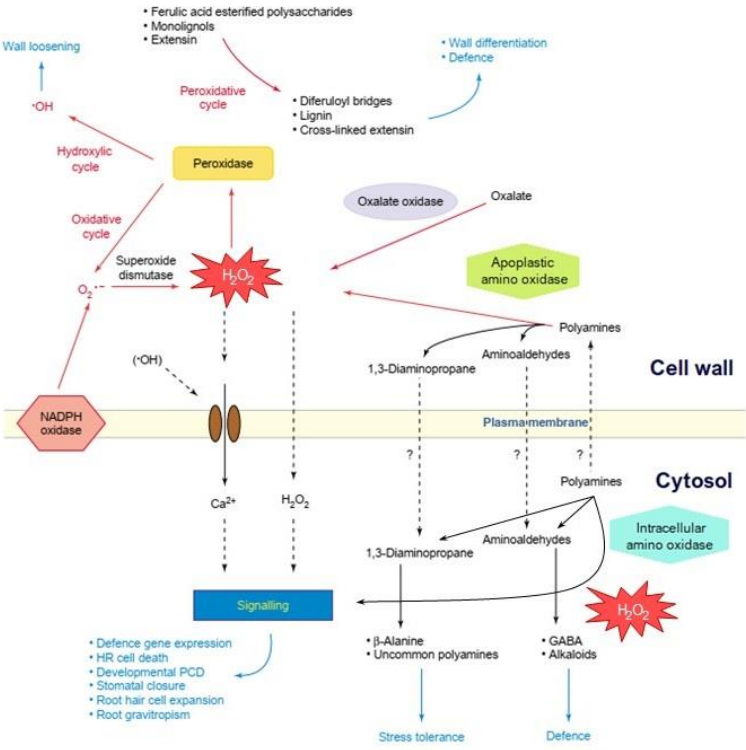

Figure 1.2 Contribution of apoplastic and intracellular amine oxidases in several physiological processes both through the control of polyamine homeostasis and as sources of biologically-active reaction products. Modified from Cona *et al.* 2006.

1.3.1 Amine oxidases in defense and stress responses

Cell-wall localized AOs contribute to the constitutive and inducible defense responses against biotic stress inducing wall-stiffening events through H_2O_2 production in the apoplast. In particular, in Arabidopsis the role of CuAOs in extra-cellular cross-linking of structural proteins or lignin precursors in defense against biotic stresses, has been demonstrated during interactions with nematode parasites. Indeed, it has been shown that the *AtCuAOβ* profile expression correlates with the re-differentiation process of root vascular tissues which occur to contrast the effects of mechanical pressure

caused by the nematode (Møller *et al.*, 1998). Furthermore, H_2O_2 derived from PA oxidation is involved in HR signaling. In this regard, it has been reported that in tobacco plants resistant to tobacco mosaic virus (TMV), PAO expression and PA levels increase in tissues displaying TMV-induced HR (Yoda *et al.*, 2003). In tobacco, infection by *Pseudomonas syringae* induces PAO expression and enzyme activity along with increased Spm secretion into the cell wall, resulting in an accumulation of H_2O_2 in the apoplast (Moschou *et al.*, 2009). Finally, PAO over-expressing plants showed an increase of tolerance against Pseudomonas, with the expression of resistance marker genes and increase of cell wall-based defense responses before the inoculation (Moschou *et al.*, 2009). These results highlight the key role played by AOs in plant-pathogen interaction, inducing defense responses to prevent pathogen colonization.

Likewise, AOs are involved in the complex network leading to wound- or herbivore-induced systemic protection. In this contest, it has been reported that in chickpea seedling, tissue damage results in a localized increase of CuAO expression and that this response also occurs in undamaged distal sites; moreover, CuAO inhibition by 2-bromoethylamine (2-BrEtA) reduces local and systemic wound-induced H_2O_2 accumulation (Rea *et al.*, 2002; Cona *et al*., 2006). In addition, it has been shown that tobacco plants over-expressing a fungal endopolygalacturonase (PG plants) showed an increase in CuAO activity and a decrease in PA levels in petioles and stems as compared with wild-type (WT) plants (Cona *et al.*, 2014). In details, PG plants show constitutively-activated defense responses, owing to excess of oligogalacturonide production, which are perceived as damage-associated molecular patterns. In this context, in wounded-PG plants a CuAO-induced intensification of the cell wall phenolic auto-fluorescence was observed in correspondence of wound surface, extending to epidermis and cortical parenchyma, phenomenon reversible when plants where treated with 2-BrEtA. Likewise, maize PAO (ZmPAO) enzyme activity, protein and mRNA levels increased in response to wounding as well as after jasmonate (JA) treatment in maize seedlings, especially in the epidermis and in the wounded zone (Angelini *et al.*, 2008). Additionally, *N*-prenilagmatine, a selective inhibitor of ZmPAO, inhibits wound-induced H_2O_2 production and strongly reduces lignin and suberin polyphenolic domain deposition along the wound site, evidence which supports the key role played by ZmPAO in wound healing (Angelini *et al.*, 2008).

Furthermore, *AtCuAO* expression is inducible by stress-related hormones and elicitors such as methyl jasmonate (MeJA; *AtCuAOα3,*

AtCuAOβ, *AtCuAOγ1* and *AtCuAOζ*), abscisic acid (ABA), salicylic acid (SA) and flagellin 22 (*AtCuAOγ1*, *AtCuAOζ*) and by wounding (*AtCuAOα3*) (Planas-Portell *et al*., 2013; Ghuge *et al*., 2015b) and it has been described that *AtCuAOγ1* and *AtCuAOζ* are involved in the ABA-mediated stress responses (Wimalasekera *et al*., 2011; Qu *et al*., 2014). Finally, AO-mediated PA-oxidation has been suggested to be involved in xylem differentiation and stomatal closure under stress conditions, as described in details below.

1.3.2 Amine oxidases in root xylem differentiation

In physiological condition, xylem differentiation is controlled by the auxin/citokinin/T-Spm loop (Cui *et al*., 2010; Baima *et al*., 2014; Ghuge et *al.*, 2015a). In Arabidopsis, it has been proposed that during xylem differentiation which occurs under stress conditions, ROS can act independently of the auxin/citokinin pathway (Tsukagoshi *et al.*, 2010). In this regard, the H_2O_2 delivered from AO-mediated-PA oxidation upon stress-induced PA secretion into apoplast, may play a key role as a mediator in the final events needed to accomplish full xylem differentiation, namely secondary wall deposition and developmental PCD. In support of this, in maize it is known that treatment with Spd, simulating stress conditions, induces nuclear condensation and DNA fragmentation as well as early differentiation and cell death in both early metaxylem and late metaxylem precursors due to the H_2O_2 produced from ZmPAO-mediated PA oxidation (Tisi *et al.*, 2011a). Moreover, ZmPAO over-expression in cell wall of tobacco promoted vascular cell differentiation and induced PCD in root cap cells. (Tisi *et al*., 2011a). Whereas, under stress conditions an increase of the apoplastic catabolism of PAs occurs (Cona *et al.*, 2006), it has been proposed that the high rate of apoplastic Spd oxidation due to Spd supply in maize as well as PAO over-expression in tobacco, simulate a stress-like conditions under which the AO-driven H_2O_2 production act as a xylem differentiation induction signaling (Tisi *et al*., 2011b). Consistently, it has been reported that *AtCuAOβ* is expressed in developing xylem tissues in Arabidopsis root and that its expression profile overlaps with lignin biosynthesis (Møller and McPherson, 1998). In particular, it has been shown that *AtCuAOβ* is expressed in protoxylem at the transition, elongation and maturation zones and its expression is strongly induced by the phytohormone MeJA (Ghuge *et al*., 2015b). Furthermore, MeJA treatment induces an early root protoxylem differentiation within H_2O_2 accumulation in the position where the first cell with fully developed cell wall thickening is detected (defined as protoxylem position), while it does not occur in *Atcuaoβ* loss-of-

function mutants, suggesting a role of *AtCuAOβ* in the root protoxylem differentiation under stress conditions (Ghuge *et al*., 2015b, Ghuge *et al*., 2015a). Additionally, higher CuAO activity, lower Put level, local H_2O_2 accumulation and an earlier xylem differentiation were found in roots of tobacco PG plants. In this plants, treatment with 2-BrEtA, a specific CuAO inhibitor, partially induces a recovery of protoxylem position and inhibits the H_2O_2 accumulation (Cona *et al*., 2014).

As a whole, these data suggest a key role of the H_2O_2 delivered from apoplastic PA-oxidation mediated by the cell-wall localized AOs in stress induced xylem differentiation.

1.3.3 Amine oxidases in stomatal movement

The stomatal movement consists of a complex physiological event, mediated by changes in osmotic pressure in the guard cells and consequent entry or exit of water, which causes structural modifications and therefore the opening or closing of the stomatal pore, respectively. This physiological process has evolved to regulate gas exchanges and thermoregulation in plants, essential processes for survival and growth during the conquest of emerged lands, which is why several signaling systems that control it coexist. This phenomenon is in fact influenced by different exogenous factors, such as light, temperature, drought and pathogens. These stimuli are detected and signaled to the guard cells by specific phytohormones and other molecules or ions involved in the signal transduction (i.e. H_2O_2, NO, Ca^{2+}). In this context, in guard cells ROS, calcium and the ion transport from the apoplast for storage in the vacuole through passage in the cytosol, are fundamental components of the complex network regulating stomatal movements (Kollist *et al*., 2014; Murata *et al*., 2015). In responses to biotic and abiotic stresses, ABA induces the production of H_2O_2 in guard cells, which in turn induces the increase of intracellular NO and Ca^{2+} levels leading to stomatal closure (Mittler and Blumwald, 2015). A well-known source of H_2O_2 in the cell-wall of guard cells is represented by plasma membrane NADPH oxidases, but recently it has been shown that the H_2O_2 produced by apoplastic catabolism of PAs can also be involved (Tavladoraki *et al*., 2016).

Supporting this hypothesis, it has been shown that in fava bean (*Vicia faba*) ABA-mediated stomatal closure implies the production of H_2O_2 delivered from an apoplastic CuAO, needed to increase the level of cytosolic Ca^{2+} in response to ABA (An *et al.*, 2008). In addition, it has been described that, in grapevine (*Vitis vinifera*) and Arabidopsis, PAOs contribute to the

control of stomatal movement (Paschalidis *et al*., 2010; Hou *et al*., 2013). Coherently, evidence of the AO involvement in the regulation of stomatal movement has been reported. The apoplastic AtCuAOβ was shown to be expressed in stomatal guard cells of leaves and flowers (Ghuge *et al.*, 2015c), and the peroxisomal AtCuAOζ, also expressed in guard cells, was shown to be involved in the ABA-mediated control of stomatal closure (Qu *et al.,* 2014).

1.4 Aim of the thesis

The aim of the present work is to highlight the physiological roles played by six Arabidopsis CuAOs (encoded by the respective genes *AtCuAOα2*, *AtCuAOα3*, *AtCuAOβ*, *AtCuAOγ1*, *AtCuAOγ2* and *AtCuAOδ*) during stress responses. To this purpose, transgenic Arabidopsis plants expressing *AtCuAO::green fluorescent protein-β-glucuronidase (GFP-GUS)* constructs, as well as both *AtCuAOβ* and *AtCuAOδ* insertional loss-of-function mutant plants have been exploited.

The previously reported expression of *AtCuAOβ* in guard cells, together with its MeJA-inducible expression in xylem tissues, suggests a role of this gene in homeostatic mechanisms leading to a balance between xylem-dependent water-supply and stomata-dependent water-loss under stress conditions. Stomatal closure may represent a fast response to injury followed by remodeling of xylem tissue allowing plant acclimation to adverse conditions. Considering this, the involvement of *AtCuAOβ* in stomatal closure and xylem differentiation upon leaf or root wounding was investigated, with particular attention to the involvement of this gene in systemic responses. Additionally, the known role played by the vacuole in ABA-induced stomatal closure, along with the occurrence of an ABA-inducible *AtCuAOδ* expression in guard cells, led us to analyze the possible involvement of the vacuolar AtCuAOδ in the control of stomatal movement.

Moreover, in order to lay the basis for future investigation focused to unravel the physiological roles of other members of AtCuAO family, a comprehensive and extensive analysis of the expression patterns of the other four *AtCuAOs* (*AtCuAOα2*, *AtCuAOα3*, *AtCuAOγ1*, *AtCuAOγ2*) under treatment with different stress related hormones (ABA, MeJA, SA) and IAA as well as after abiotic stress like wounding and dehydration was carried out by both quantitative analysis (RT-qPCR) and qualitative approaches (*AtCuAOs-promoter::GFP-GUS* transgenic plants).

2. MATERIALS AND METHODS

2.1 Plant materials, growth conditions and treatments

The Columbia-0 (Col-0) ecotype of Arabidopsis (*Arabidopsis thaliana*) was used as the wild type (WT). The Arabidopsis Col-0 T-DNA insertion lines *Atcuaoβ.1* (SALK_145639.55.25.x; TAIR accession number 1005841762; previously *Atao1.1* Ghuge *et al.*, 2015b) and *Atcuaoβ.2* (SALK_077391.40.85.x; TAIR accession number 4284859; previously *Atao1.2* Ghuge *et al*., 2015b) of the *CuAO* gene At4g14940 (*AtCuAOβ*, formerly *AtAO1*; TAIR accession number 2129519) used were obtained and characterized as described by Ghuge *et al*., 2015b, while the T-DNA insertion line *Atcuaoβ.3* (SALK_082394.32.30.x, TAIR accession number 1005822711; previously *Atao1.3*, Carucci 2017) was characterized by Ghuge SA during his PhD thesis, as described by Carucci 2017.

The Arabidopsis Col-0 T-DNA insertion lines *Atcuaoδ.1* (SALK_072954.55.00.x line, TAIR accession number 4122972) and *Atcuaoδ.2* (GK-011C04-013046 line, TAIR accession number 4242275) of the *CuAO* gene At4g12290 (*AtCuAOδ*, TAIR accession number 2139069) used were obtained and characterized as described by Fraudentali *et al*., 2019. Transgenic plants *prom-AtCuAO::GFP-GUS* of *AtCuAOα2* (*At1g31690*; TAIR accession number 2028636), *AtCuAOα3* (*At1g31710*; TAIR accession number 2028606), *AtCuAOγ1* (*At1g62810*; TAIR accession number 2026267) and *AtCuAOγ2* (*At3g43670*; TAIR accession number 2080173) were prepared by Ghuge SA during his PhD thesis using Gateway technology (Ghuge 2014). The homozygous Arabidopsis Col-0 T-DNA insertion lines *glr3.3-1* and *glr3.3-2* have been originally reported in Qi *et al*., 2006 and kindly provided by Costa A. laboratory (University of Milano, Department of Bioscience).

Plants were grown in vitro in a growth chamber at a temperature of 23 °C under long-day conditions (16/8 h photoperiod; 50 μmol m^{-2} s^{-1} and 55% relative humidity). For *in vitro* growth, seeds were surface sterilized as described by Valvekens *et al*., 1988. In details, seeds were surface-sterilized by treating them with 70% (v/v) ethanol for 2 min and then with 10% sodium hypochlorite containing 0.2% (v/v) Triton X-100 for 5-10 min. After extensive washing with sterile water, seeds were stratified at 4°C for 2 days in the dark and then sown in ½ Murashige and Skoog (MS) salt mixture (pH 5.7) supplemented with 0.5 (w/v) sucrose, 0.8% (w/v) agar (solid medium) and 50 μg/mL kanamycin (when antibiotic selection was necessary). Plates were placed vertically in the growth chamber.

Hormone and PA treatments as well as abiotic stress (wounding and dehydration) for RT-quantitative PCR (RT-qPCR) analysis of *AtCuAO* genes were performed on 7-day-old (for *AtCuAOα2*, *AtCuAOα3*, *AtCuAOβ*, *AtCuAOγ1* and *AtCuAOγ2*) /12-day-old (for *AtCuAOδ*) WT seedlings grown for 6/11 days in solid medium and then transferred to ½ MS salt mixture (pH 5.7) supplemented with 0.5 (w/v) sucrose (liquid medium) for one more day, as acclimation. After this period, for hormone/PA treatments liquid medium was replaced by fresh liquid medium containing the analyzed hormone or PA as follows: 1, 10 or 100 μM ABA (Duchefa), 50 μM methyl jasmonate (MeJA; Duchefa), 2 mM salicylic acid (SA; Sigma-Aldrich), 10 μM 3-indolacetic acid (IAA), 500 μM putrescine (Put), 500 μM spermidine (Spd). Fresh liquid medium alone was used for control. For leaf-wounding analysis, cotyledons from acclimated seedlings were cut with scissors soon after liquid medium exchange, and then incubated in a growth chamber prior to be sampled at the time indicated below. For root-wounding analysis, acclimated seedlings were injured by using tweezers exerting pressure below the hypocotyl, soon after liquid medium exchange, and then incubated in a growth chamber prior to be sampled at the time indicated below. For dehydration/recovery stress analysis, acclimated seedlings were left "drying" for 30 minutes on an open plate under a ventilated hood. Material was collected before treatment (dehydration time 0) and immediately after this treatment (30 min dehydration). Fresh liquid medium was added to the plates and material was collected after the times indicated below for recovery time course (30 min dehydration represents 0 h recovery). Plant samples for gene expression studies were harvested at the described times, frozen in liquid nitrogen and then kept at -80° C until RNA extraction.

To perform histochemical GUS analysis, seedlings were grown on solid medium supplemented with kanamycin and then used as hereafter described. In detail, for the analysis of inducible tissue-specific gene expression upon hormone/PA treatments or abiotic stress, *AtCuAOs-promoter::GFP-GUS* 6-day-old seedlings were transferred to 12-well tissue culture clusters containing liquid medium for 1 day. Then, the later was replaced with fresh liquid medium supplemented or not with the specific hormone/PA. For leaf-wounding and drought-stress GUS analysis, acclimated seedlings were treated as described for RT-qPCR analysis and sampled at relative mRNA-induction time. Samples were analyzed under light microscope (LM).

Stomatal aperture measurements were performed on 7- or 12-day-old WT plants, *Atcuaoβ*, *Atcuaoδ* and *glr3.3* mutants, grown on agar medium

under control conditions or after treatment with ABA (1, 10, and 100 μM), MeJA (50 μM), 2-bromoethylamine (2-BrEtA; 0.5, 5 mM), aminoguanidine (AG; 0.1, 1 mM), *N,N*^{1}-dimethylthiourea (DMTU; 100 μM) or after leaf/root wounding, any treatment/stress done alone or in combination with another treatment, as described below.

Analysis under Laser Scanning Confocal Microscope (LSCM) of root protoxylem position and meristem size by propidium iodide (PI) staining as well as H_2O_2 accumulation by Amplex Ultra Red (AUR) staining were carried out on WT and *Atcuaoβ* mutant seedlings as described by Fraudentali *et al*., 2018. Briefly, 7-day-old seedlings were selected for homogeneity in root length and then transferred onto fresh medium with or without 100 μM DMTU or 100 μM Put. After the transfer, seedlings were injured by cutting the cotyledonary leaf with scissors and after 6 h (AUR staining) or 3 days (PI staining) unwounded control and leaf-wounded plants were collected for analysis under LSCM of AUR and PI staining respectively. The effect of leaf wounding on root growth was evaluated as the difference between the length measured at the onset of the wounding and that measured after 3 days, accordingly to Fraudentali *et al*., 2018.

2.2 RNA extraction, RT-PCR and RT-quantitative PCR (RT-qPCR) analysis

Total RNA was isolated from WT seedlings (100 mg) by using TRIzol® Reagent (Invitrogen) following the manufacture's instruction with slight modifications. To eliminate traces of genomic DNA, RNA samples were treated with RNase-Free DNase Set (QIAGEN).

Quantitative expression profiles of *AtCuAO* genes were determined by RT-quantitative PCR (RT-qPCR) on 7-day-old or 12-day-old whole seedlings after different treatments. In detail, RT-qPCR analysis was performed on DNase-treated RNA (4 μg) as follows. cDNA synthesis and PCR amplification were carried out using *GoTaq® 2-Step RT-qPCR System200* (Promega) following manufacturer's protocol. The first cDNA strand was synthesized using random and oligo *dT* primers in an *iCycler ™ Thermal Cycler* (Bio-Rad) with the following parameters: 25°C for 5 min, 42°C for 60 min and 70°C for 15 min. The PCRs were run in a Corbett RG6000 (Corbett Life Science, QIAGEN) utilizing the following program: 95°C for 2 min then 40 cycles of 95°C for 7 s and 60°C for 40 s. The melting program ramps from 60°C to 95°C rising by 1°C each step. *AtCuAO* specific primers were *AtCuAO-qPCR-for/rev* (Table 2.1). Ubiquitin-conjugating enzyme 21 (UBC21,

At5g25760) was used as reference gene and specific primers were prepared (Czechowski et al., 2005; *UBC21-for* and *UBC21-rev*; Table 2.1). The software used to control the thermocycler and to analyze data was the Corbett Rotor-Gene 6000 Application Software (version 1.7, Build 87; Corbett Life Science, QIAGEN). Fold change in the expression of the *AtCuAO* genes were calculated according to the $\Delta\Delta C_q$ method as previously described (Livak and Schmittgen 2001; Fraudentali *et al*., 2019).

Name of primer	Sequence of primer
UBC21-for	5′- CTGCGACTCAGGGAATCTTCTAA -3′
UBC21-rev	5′- TTGTGCCATTGAATTGAACCC -3′
AtCuAOα2-qPCR-for1	5′- GACGACACATTAGCCGTATGGTC -3′
AtCuAOα2-qPCR-rev1	5′- AAGCCGCCAAACATAGTAGGCA -3′
AtCuAOα3-qPCR-for1	5′- ATTACGGAGGTTAGACCGGACG -3′
AtCuAOα3-qPCR-rev1	5′- CCGTGTATGTCTTCCCCTAGTT -3′
AtCuAOβ-qPCR-for	5′- CAAGTGGGGAAGCTGAAATAAGTTTAGTG -3′
AtCuAOβ-qPCR-rev	5′- TCCTCCGAGAAGACGTTTTGTTAACTTC -3′
AtCuAOγ1-qPCR-for1	5′- GCTGGCGACATTCTGAGATCC -3′
AtCuAOγ1-qPCR-rev1	5′- CACCATTAACATTCCCGAAGCC -3′
AtCuAOγ2-qPCR-for1	5′- CACAAACAATCAGATATGGGTGA -3′
AtCuAOγ2-qPCR-rev1	5′- CACTATGTCCTTGTTCTCAATGG -3′
AtCuAOδ-qPCR-for	5′- GATGACACTCTTGCAGTTTGG -3′
AtCuAOδ-qPCR-rev	5′- GGAATGTGATGGAAACCAAGTG -3′

Table 2.1 Primers used for RT-qPCR analysis on whole Arabidopsis seedlings after different treatments.

2.3 Histochemical analysis of GUS assay

GUS staining was performed as described by Jefferson, 1987. Samples were gently soaked in 90% (v/v) cold acetone for 30 min at -20°C for prefixation and rinsed 3 times with 50 mM sodium phosphate buffer pH 7.0. After that, plant material was immersed in the staining solution [1 mM 5-bromo-4-chloro-3-indolyl-β-D-glucuronide, 2.5 mM potassium ferrocyanide, 2.5 mM potassium ferricyanide, 0.1% (v/v) Triton X-100, 10 mM EDTA, 50 mM sodium phosphate buffer, pH 7.0] under *vacuum*. Histochemical GUS staining following hormone/abiotic stress treatments was allowed to proceed until differences in the intensity between treated and untreated plants were detected under the microscope. Chlorophyll was extracted by several washings: first with ethanol/acetic acid ratio 1:3 (v/v) for 30 min, then with ethanol/acetic acid ratio 1:1 (v/v) for 30 min and finally with 70% ethanol. Samples were stored in 70% ethanol at 4°C, prior to being observed under LM. Images were acquired by a Leica DFC450C digital camera applied to a Zeiss Axiophot 2 microscope. Shown images of whole plants were reconstructed aligning overlapping micrographs of the same seedling.

2.4 Measurement of stomatal aperture

Measurement of stomatal aperture was performed as described by Jung *et al*., 2008, with modifications. In detail, seedlings from 7-day-old (WT, *Atcuaoβ* and *glr3.3* mutants) or 12-day-old (WT and *Atcuaoδ* mutants) plants grown on solid medium were incubated in opening solution (30 mM KCl, 10 mM MES-Tris, pH 6.15) for 3 h under light to allow stomatal opening. Then, seedlings from WT plants and *Atcuao/glr3.3* mutants were incubated for 2 h under light in liquid medium in the absence or presence of treatment performed as follows: ABA 1, 10, and 100 μM, DMTU 100 μM, and ABA 1, 10, and 100 μM/DMTU 100 μM for seedling from WT and *Atcuaoδ* mutants; MeJA 50 μM, DMTU 100 μM, MeJA 50 μM + DMTU 100 μM, leaf/root-wounding, leaf/root-wounding + DMTU 100 μM for seedling from WT and *Atcuaoβ* mutants; leaf/root-wounding for seedling from *glr3.3* mutants. Treatments with CuAOs inhibitors 2-BrEtA and AG were performed as follows: after 3 h incubation with opening solution, seedlings from WT plants and *Atcuaoδ* mutants were incubated in liquid medium supplemented or not with 2-BrEtA (0.5, 5 mM) or AG (0.1, 1 mM) for 30 min under light, after which ABA at the final concentration of 100 μM was added and further incubated for 2 h under light. Unlike Jung *et al*, treatments were done in fresh liquid medium instead

of directly in the opening solution and the variation of the method was validated with a series of pilot experiments to confirm the stable maintenance in different solutions of the stomatal aperture induced by the opening solution (liquid medium, liquid medium without sucrose, distilled water; Fig. 2.1). Following the various treatments, seedlings were treated with a fixing solution (1% glutaraldehyde, 10 mM NaPi pH 7.0, 5 mM $MgCl_2$, and 5 mM EDTA) and incubated for 30 min under light. Images of stomata with the outline of stomatal pores in the focal plane were acquired by a Leica DFC 450C digital camera applied to a Zeiss Axiophot 2 microscope at the magnification of 20×, and stomatal apertures (width/length) were measured using a digital ruler (ImageJ 1.44). Width and length of stomata pores were measured, and stomatal apertures were expressed as the width/length ratio.

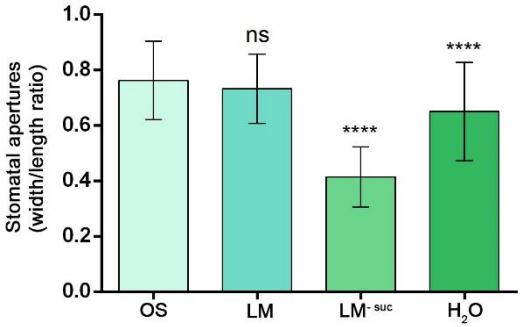

Figure 2.1 Validation of treatment in liquid medium method to confirm the stable maintenance in different solutions (liquid medium, LM; liquid medium without sucrose, LM^{-suc}; distilled water, H_2O) of the stomatal aperture induced by the opening solution (OS). 7-day-old WT seedlings grown on solid medium were incubated in opening solution for 3 h under light to allow stomatal opening. Then, seedlings were incubated for 24 h under light in fresh OS, LM, LM^{-suc} and H_2O to analyzes di difference in variation of stomatal apertures (width/length ratio). Mean values ± SD (n = 15) are reported. The significance levels between control plants in OS and plants in the other solutions are reported. *P* levels have been calculated with one-way ANOVA analysis; *P* levels > 0.05; **** *P* levels are equal to or less than 0.0001; ns, not significant.

2.5 Protoxylem position and meristem size analysis under LSCM by cell wall PI staining and bright-field examination of root tissues

Root apices from 10-day-old WT and *Atcuaoβ* unwounded control and leaf-wounded seedlings treated or not with 100 µM DMTU or with 100

μM Put for the last 3 days, were incubated for 5/10 min in PI (10 μg/ml) to highlight cell wall and protoxylem (Mähönen *et al*., 2014) and then observed under LSCM using a 488 nm argon laser, with a 600–680 nm band-pass filter and a 40× oil immersion objective. The PI staining was allowed to proceed until protoxylem was completely highlighted. Roots were concurrently analyzed by bright-field microscopy, using the same laser beam as described above. To analyze protoxylem maturation, the distance from the root apical meristem of the first protoxylem cell with fully developed secondary wall thickenings was measured following the method described by Ghuge *et al*., 2015b. The length of the meristematic zone was determined by measuring the distance between the quiescent center and the first elongating cell in the cortex cell file (Chen *et al*., 2011; Casamitjana-Martínez *et al*., 2003; Dello Ioio *et al*., 2008; Fraudentali *et al*., 2018). Images were obtained by serial aligning of overlapping micrographs of the same root by Photoshop Software (Adobe, San Jose CA, USA). Protoxylem position (defined by the position of the first protoxylem cell with fully developed secondary cell wall thickenings; Fraudentali *et al*., 2018) and meristem size were estimated exploiting the Leica Application Suite Advanced Fluorescence software.

2.6 Hydrogen peroxide *in situ* detection

To reveal the *in situ* extracellular H_2O_2 accumulation, the fluorogenic peroxidase substrate AUR (Molecular Probes, Invitrogen, Carlsbad, CA, USA) was exploited (Ashtamker *et al.*, 2007) and the fluorescence of the peroxidase reaction-product was detected under LSCM in root apices from 7-day-old WT and *Atcuaoβ* unwounded control and leaf-wounded seedlings 6 h after the injury as described by Fraudentali *et al*., 2018.

2.7 Statistics

For RT-qPCR analysis of three biological replicates each with three technical replicates were performed ($n = 3$). The analysis by GUS staining of inducible tissue-specific gene expression was performed on a minimum of thirty plants from five independent experiments. Images from single representative experiments are shown. The analysis under LSCM of protoxylem position, meristem size and H_2O_2 accumulation after PI and AUR staining as well as root growth analysis were performed on five independent experiments on a minimum of ten plants per treatment and per genotype ($n = 50$), yielding reproducible results. Images from single representative

experiments are shown. For the stomatal aperture measurements, three independent experiments were performed for each treatment on the different genotypes. For each time-point, five similarly-sized leaves were harvested from different seedlings for each genotype and treatment. In this case, each of the five leaves from the three experiments was considered a biological replicate for a total of fifteen biological replicates for each genotype and treatment (n = 15). For each leaf, four random chosen fields (430 μm × 325 μm) were acquired and approximately 60 stomata were measured, and the mean values were used in the statistical analysis.

Statistical tests of RT-qPCR, protoxylem position, meristem size, root growth and stomatal aperture were performed using GraphPad Prism (GraphPad Software) with One-way ANOVA analysis followed by Sidak's multiple comparison tests. Statistical significance of differences was evaluated by *P* levels. *ns*, not significant *P* levels > 0.05; *, **, *** and **** *P* levels ≤ 0.05, 0.01, 0.001 and 0.0001 respectively.

3. RESULTS

Phylogenetic analysis based on amino acid sequence identity revealed that members of the AtCuAO family are represented in each of the three plant CuAO family clades (Tavladoraki *et al.*, 2016) as followes: AtCuAOβ, AtCuAOα1, AtCuAOα2 and AtCuAOα3 being included in clade I, AtCuAOδ, AtCuAOε1, AtCuAOε2, AtCuAOγ1 and AtCuAOγ2 in clade II and AtCuAOζ in clade III. The alignment of the aminoacid sequences of the AtCuAO putative proteins encoded by the ten genes annotated as *AtCuAOs* with that of *Pisum sativum* CuAO (referred as PSAO), revealed that eight of them include all the active site residues crucial for the catalytic activity, except for AtCuAOε1 and AtCuAOε2 which, being located upstream of *AtCuAOδ* on chromosome 4, could be fragments arisen from a copy of the latter generated by a duplication event (Tavladoraki *et al.*, 2016), followed by the insertion of the transposable element *At4g12275* (The Arabidopsis Information Resource; https://www.arabidopsis.org).

Considering that except for the already characterized (Planas-Portell *et al.*, 2013; Qu *et al.*, 2014) clade III-belonging AtCuAOζ, most of the AtCuAOs are clustered in clade I and II, we have chosen to focus on members included in the latter major branches of the phylogenetic tree. Concerning clade I, as several studies have been already carried out about AtCuAOβ tissue-specific expression and physiological roles (Ghuge *et al.*, 2015a, Ghuge *et al.*, 2015b, Ghuge *et al.*, 2015c), the attention has been focused on deepening its roles in both root protoxylem differentiation and stomatal closure in response to wounding. Moreover, efforts have been made in unravelling the inducible-gene expression profile under both stress or hormone treatments of other two clade I-belonging genes, that is the peroxisomal α members AtCuAOα2 and AtCuAOα3. Concerning clade II, considering that the δ/ε sub-branch includes only one-member encoding for a putative functional enzyme, that is the vacuolar AtCuAOδ, attention has been paid on its physiological role in the ABA-induced stomatal closure. Furthermore, investigation have been carried out to unravel the inducible-gene expression profile under both stress or hormone treatments of other two members of the γ sub-branch, the apoplastic *AtCuAOγ1* and *AtCuAOγ2*.

3.1 Physiological role of *AtCuAOβ* in the early root protoxylem maturation and stomatal closure induce by leaf wounding

As previously described, *AtCuAOβ* encodes an apoplastic CuAO expressed at the early stages of vascular tissue differentiation in roots and in stomatal guard cells (Ghuge *et al*., 2015b, Ghuge *et al*., 2015c). Moreover, it has been demonstrated that the expression of this gene is strongly induced by the wound-signal hormone MeJA after 1 h of treatment, especially in the root vascular tissues (Ghuge *et al*., 2015b). It has also been shown that the H_2O_2 derived by the *AtCuAOβ*-driven oxidation of Put mediates the early protoxylem differentiation occurring in the primary root apex upon treatment with MeJA in Arabidopsis roots (Ghuge *et al*., 2015b). Here, the *AtCuAOβ* roles in root protoxylem differentiation and stomatal closure after wound triggered long-distance signaling or MeJA treatments have been analyzed.

3.1.1 Expression profile of AtCuAOβ after MeJA treatment or under leaf/root wounding

To integrate information from previous reported data (Ghuge *et al*., 2015b), a 24 h time-course analysis of the modulation of *AtCuAOβ* expression by 50 µM MeJA treatment was carried out by RT-qPCR analysis. Moreover, to correlate the MeJA-modulated *AtCuAOβ* gene expression with *AtCuAOβ* responses to the MeJA-signaled abiotic stress, the variations of *AtCuAOβ* gene expression profile upon wounding of either cotyledonary leaf or root were also investigated (Fig. 3.1). All treatments induced the *AtCuAOβ* expression although with different dynamics. In particular, MeJA induced *AtCuAOβ* expression of 2-fold after 30 min, strongly peaked at 4-fold from 1 to 3 h, followed by a progressive reduction towards the last time point in this study (24 h), where a 2.7-fold induction was still observed (Fig. 3.1, upper panel); cotyledonary leaf wounding presented a profiles where a strong progressive inductions from 1 to 24 h, with 3-, 5-, 6.5- and 7-fold increases respectively, was observed (Fig. 3.1, middle panel); after root wounding *AtCuAOβ* expression strongly peaked after 1 h (8-fold), followed by a maintained induced level at 3, 6 and 24 h (6-, 5.5- and 5-fold, respectively) compared to T0 levels.

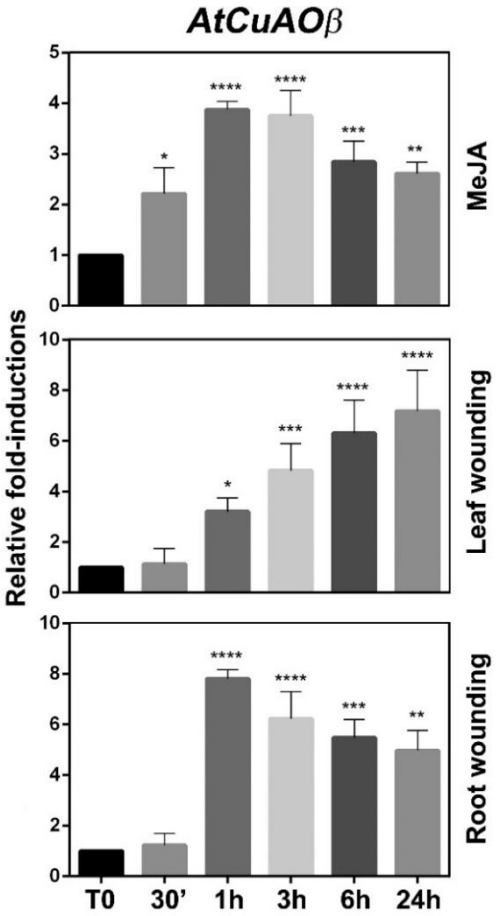

Figure 3.1 Time-course analysis of *AtCuAOβ* gene expression by RT-qPCR after 50 μM MeJA treatment and upon leaf or root wounding. Gene expression was analyzed in 7-day-old WT seedlings untreated or treated/wouded for 0h (T0), 5, 15, 30 min 1, 3, 6 and 24 h. The reported values of expression fold-inductions after treatment are relative to the corresponding expression values of non-treated plants for each time point, with the value for time zero assumed to be one. Data is the result of three biological replicates, each with three technical replicates (mean values ± SD; n = 3). The significance levels between relative mRNA levels at each time point and time 0 are reported only when $P \leq 0.05$. **, ***, **** P levels ≤ 0.01, 0.001 and 0.0001 respectively.

It has been demonstrated that *AtCuAOβ* expression is strongly induced by the wound-signal hormone MeJA in the root vascular tissues (Ghuge *et al*., 2015b). Herein, considering data from RT-qPCR, the analysis of the tissue specific expression pattern of *AtCuAOβ* after MeJA treatment and after leaf/root wounding were carried out using *promoter::GFP-GUS* plants. MeJA induced *AtCuAOβ* expression also in stomata of the cotyledons, as revealed by the presence of an intense GUS staining at the stomatal guard cells of leaves form treated-seedling (Fig. 3.2, right upper panel) as compared to control untreated plants (Fig. 3.2, left upper panel). Likewise, both cotyledonary leaf wounding (Fig. 3.2, left lower panel) and root wounding (Fig. 3.2, right lower panel) induced *AtCuAOβ* expression in stomatal guard cells of stressed *AtCuAOβ-promoter::GFP-GUS* plants as compared to control untreated plants (Fig. 3.2, left middle/lower panel respectively).

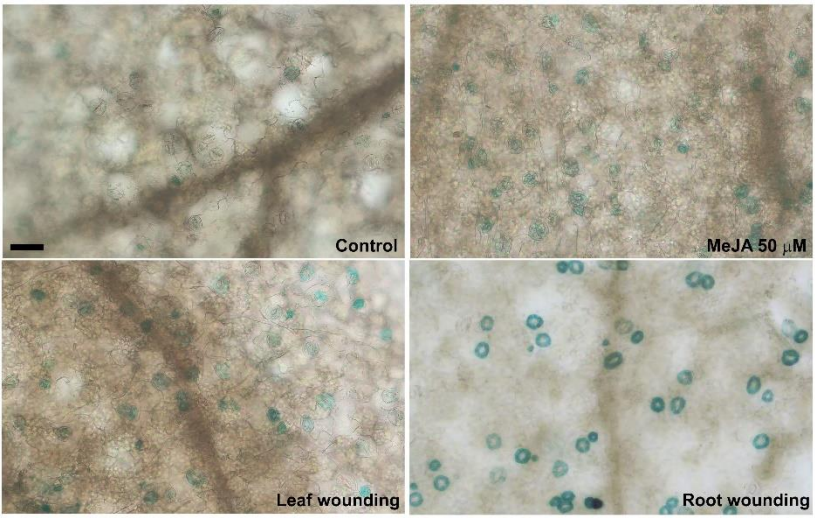

Figure 3.2 Analysis of *AtCuAOβ* tissue specific expression pattern upon treatment with MeJA or after leaf/root wounding. Light microscopy analysis by GUS staining of 7-day-old *AtCuAOβ*::*GFP-GUS* transgenic seedlings untreated (left upper panel) or treated with 50 μM MeJA for 3h (right upper panel), subjected to cotyledonary leaf wounding for 3h (left lower panel), and subjected to root wounding for 3h (right lower panel). The staining reaction proceeded for 2 h for all the treatment. Micrographs are representative of those obtained from 25 leaves from five independent experiments. Bar = 50 μm.

Moreover, cotyledonary leaf wounding induced *AtCuAOβ* expression in the vascular tissues at the transition, elongation and maturation root zone, as well as in root cap cells, as revealed by the presence of an intense GUS staining in root tissues of stressed *AtCuAOβ-promoter::GFP-GUS* plants (Fig. 3.3, right) as compared to control untreated plants (Fig. 3.3, left).

Figure 3.3 Analysis of *AtCuAOβ* tissue-specific expression pattern upon leaf wounding. Light microscopy analysis by GUS staining of 7-day-old *AtCuAOβ-promoter::GFP-GUS* transgenic seedlings untreated (left) or treated (right) with cotyledonary leaf wounding for 3 h. The staining reaction proceeded for 2 h. Shown images were obtained aligning serial overlapping micrographs of the same root by Photoshop Software (Adobe) and are representative of those obtained from 25 roots from five independent experiments. Bar: 200 μm.

3.1.2 Physiological role of AtCuAOβ in the early root protoxylem maturation induced by leaf wounding

Xylem maturation depends on coordinated events of cell wall lignification and developmental PCD, which can both be triggered by developmental- and/or stress-driven H_2O_2 production. Considering that, the AtCuAOβ-driven H_2O_2 production has been previously involved in the MeJA-induced early root protoxylem (Ghuge *et al*., 2015b), here, the role of *AtCuAOβ* in root protoxylem maturation induced by leaf wounding was explored.

In order to unravel the occurrence of phenotypic plasticity induced by long-distance communication triggered by biotic/abiotic stresses imposed at a specific distal site, we first analyzed the effect of leaf wounding on root growth and protoxylem differentiation by analysis under LSCM. After that, the role played in these events by the *AtCuAOβ*-mediated H_2O_2 production has been investigated.

3.1.2.1 Effect of leaf wounding on root growth and xylem differentiation in Arabidopsis

To explore the effect of leaf wounding on root xylem phenotypic plasticity, 7-day-old Arabidopsis seedlings were injured by cutting a cotyledonary leaf, and then roots were observed under LSCM 3 days after the injury, for the investigation of the distance from the root apical meristem of the first protoxylem cell with fully developed secondary wall thickenings (whose location is here referred as "protoxylem position") and meristem size. Fig. 3.4 shows images acquired under LSCM after PI staining and relative bright-field images of root apexes from unwounded control and leaf-wounded seedlings. Plantlets in which a cotyledonary leaf was cut present an anticipation of the maturation of protoxylem, as shown by the earlier presence of cells with fully developed secondary wall thickenings that appear closer to the apical meristem as compared to unwounded control plants.

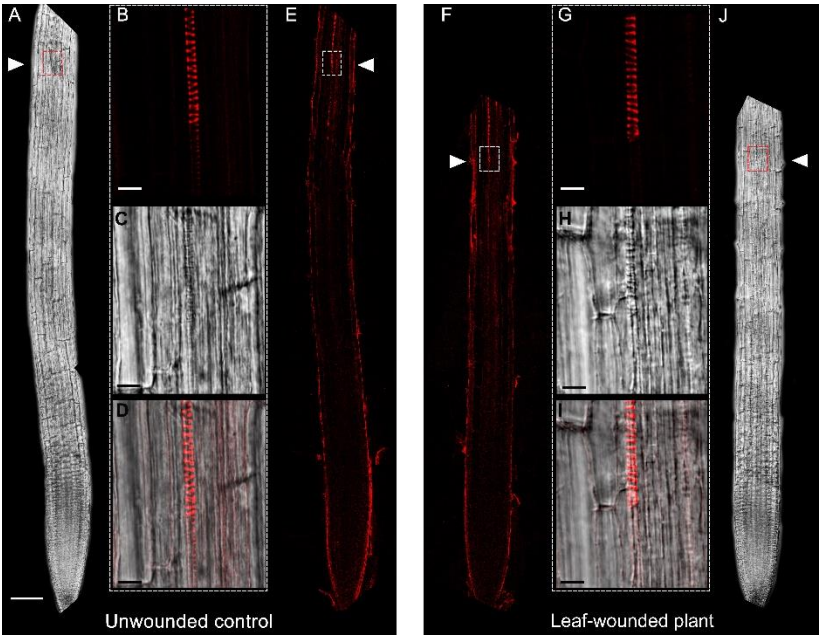

Figure 3.4 Analysis under LSCM after PI staining of root apexes and respective bright-field images from 10-day-old unwounded control (**A**–**E**) and leaf-wounded (**F**–**J**) seedlings. (**A**–**E**) bright-field of the root from unwounded control seedlings (**A**), PI staining (**B**) bright-field (**C**) and overlay image (**D**) of the magnified zone of the root from unwounded control seedlings, in which protoxylem position (defined by the position of the first protoxylem cell with fully developed secondary cell wall thickenings) is located, PI staining of the root shown in A (**E**); (**F**–**J**) PI staining of the root from leaf wounded seedling injured at the age of 7 days by cutting the cotyledonary leaf, analyzed 3 days after injury (**F**), PI staining (**G**) bright-field (**H**) and overlay image (**I**) of the magnified zone of the root from leaf-wounded seedlings, in which protoxylem position is located, bright-field of the root shown in F (**J**). The images presented are representative of experiments repeated at least five times with ten seedlings analyzed each time. Shown images were obtained aligning serial overlapping micrographs of the same root by Photoshop Software (Adobe). Bars: 100 μm (**A**, **E**, **F**, **J**) and 10 μm (**B**-**D**, **G**-**I**). Data published in Fraudentali *et al*., 2018.

Fig. 3.5 demonstrates that these qualitative data were confirmed by statistically significant quantitative analysis. In fact, the mean distance of the first protoxylem cell with fully developed secondary wall thickenings from the root apical meristem was approximately 1620 μm in leaf-wounded plants as

compared to unwounded control plants, showing a distance of approximately 2060 µm. Furthermore, 100 µM DMTU opposes the effect of leaf wounding on early protoxylem maturation, consistently with what previously demonstrated for the MeJA-mediated induction of protoxylem differentiation (Ghuge *et al*., 2015b).

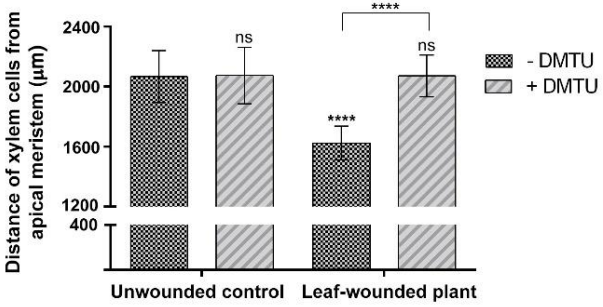

Figure 3.5 Analysis of differences in protoxylem maturation in leaf-wounded seedlings grown in medium with or without the H_2O_2-scavenger DMTU. Distances from the apical meristem of the protoxylem position (defined by the position of the first protoxylem cell with fully developed secondary cell wall thickenings) are reported. These experiments were repeated at least five times with ten seedlings analyzed each time (mean values ± SD; $n = 50$). The statistical significance levels between unwounded control DMTU-untreated plants and DMTU-treated and/or wounded plants were evaluated by P levels as follows: ****, $P \leq 0.0001$; ns, not significant. The significance levels between wounded DMTU-untreated and DMTU-treated plants are reported above the horizontal square bracket. Data published in Fraudentali *et al*., 2018.

The effect of leaf wounding on protoxylem position was specific and not dependent upon variation in root growth or meristem size, which were unchanged in leaf-wounded plants compared to unwounded control plants (Fig. 3.6, Table 3.1).

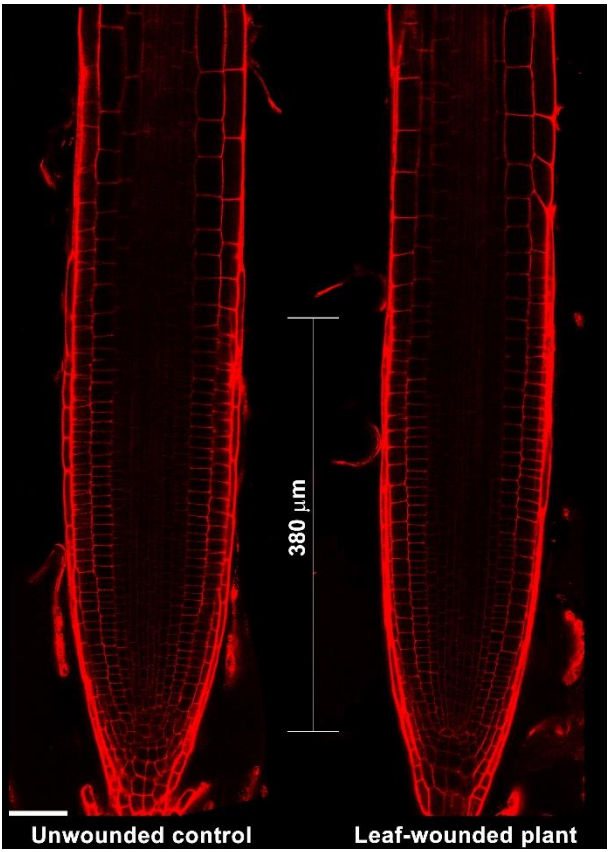

Figure 3.6 Analysis under LSCM after PI staining of the leaf wounding effect on the length of the meristematic zone, determined by measuring the distance between the quiescent center and the first elongating cell in the cortex cell file. The images presented show roots from 10-day-old unwounded control and leaf-wounded seedlings, injured at the age of 7 days by cutting the cotyledonary leaf with scissors and analyzed 3 days after the injury; roots presented are representative of experiments repeated at least five times with ten seedlings analyzed each time. Shown images were obtained aligning serial overlapping micrographs of the same root by Photoshop Software (Adobe). Bar: 50 µm. Data published in Fraudentali *et al*., 2018.

	Root growth (cm)		Meristem size (µm)	
	Unwounded control	Leaf-wounded plant	Unwounded control	Leaf-wounded plant
- DMTU	2.55 ± 0.20	2.39 ± 0.15 ns	374.0 ± 28.4	372.3 ± 34.6 ns
+ DMTU	2.54 ± 0.25	2.39 ± 0.24 ns	373.3 ± 15.9	370.1 ± 17.3 ns

Table 3.1. Analysis of differences in root growth and meristem size in leaf-wounded seedlings grown in medium with or without the H_2O_2-scavenger DMTU. The effect of leaf wounding on root growth was evaluated as the difference between the length measured at the onset of the wounding and that measured after 3 days. The length of the meristematic zone was determined by measuring the distance between the quiescent center and the first elongating cell in the cortex cell file. These experiments were repeated at least five times with ten seedlings analyzed each time (mean values ± SD; *n* = 50). The statistical significance levels between unwounded control and wounded plants were evaluated by *P* values as follows: ns, not significant. Data published in Fraudentali *et al*., 2018.

To confirm that the effect of the wound-induced signalling on the early maturation of protoxylem cells require H_2O_2, this compound was *in situ* detected in Arabidopsis roots following leaf wounding by exploiting the fluorogenic peroxidase substrate AUR. Fig. 3.7 shows that 6 hours after leaf wounding, a strong AUR signal was revealed in the root zone where the first protoxylem cell with fully developed secondary cell wall thickenings is found, which was not detectable in unwounded control roots, suggestive of a tissue-specific H_2O_2 production triggered by a long-distance leaf-to-root communication and leading to early protoxylem differentiation.

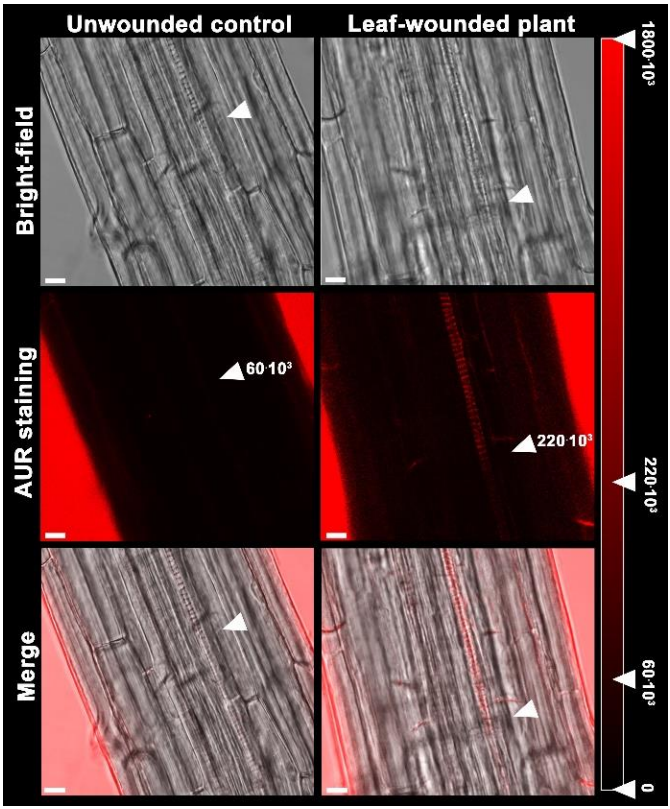

Figure 3.7 *In situ* H_2O_2 detection by analysis under LSCM after AUR staining, of roots from 7-day-old unwounded control and leaf-wounded seedlings 6 hours after injury. The corresponding bright-field and overlay images are shown. Micrographs show the root zone corresponding to the site of appearance of the first protoxylem cell with fully developed secondary cell wall thickenings (arrows) and have been taken at the level of the central root section. Images are representative of those obtained from ten seedlings from five independent experiments. In the red degrading scale are indicated the average values of fluorescence intensity measured as the sum of the pixels of each 65 µm^2 rectangle, for unwounded control and leaf-wounded plants that were $60\times10^3 \pm 19\times10^3$ and $220\times10^3 \pm 38\times10^3$ respectively (mean values ± SD; $n = 25$). The maximum pixel sum for a completely saturated square was approximately 1800×10^3. Bars: 10 µm. Data published in Fraudentali *et al.*, 2018.

3.1.2.2 Involvement AtCuAOβ-derived H_2O_2 in the early root protoxylem maturation induced by leaf wounding

Here, to explore the role played by *AtCuAOβ* in leaf wounding-triggered alteration of root phenotypic plasticity, 7-day-old Arabidopsis WT and loss-of-function *Atcuaoβ* mutant (*Atcuaoβ.1* and *Atcuaoβ.2*) seedlings were treated or not with DMTU or Put and then injured by cutting a cotyledonary leaf. After 3 days from the injury roots were observed under LSCM, for the investigation of the protoxylem position and meristem size.

Fig. 3.8 shows that, in control conditions, roots of both *Atcuaoβ* mutants present no apparent altered phenotype in xylem tissues in comparison with WT roots. Interestingly, cotyledonary leaf wounding induced early protoxylem differentiation in roots of WT plants (1600 μm) without affecting protoxylem differentiation in *Atcuaoβ* mutants (2000 and 2100 μm respectively). Moreover, DMTU reversed the leaf wounding-induced early protoxylem differentiation in WT plants, while having no effect in wounded-*Atcuaoβ* mutants. In fact, in WT plants, the protoxylem position recovered to approximately 2000 μm upon 100 μM DMTU treatment. Treatment with DMTU alone did not affect the protoxylem differentiation (Fig. 3.8).

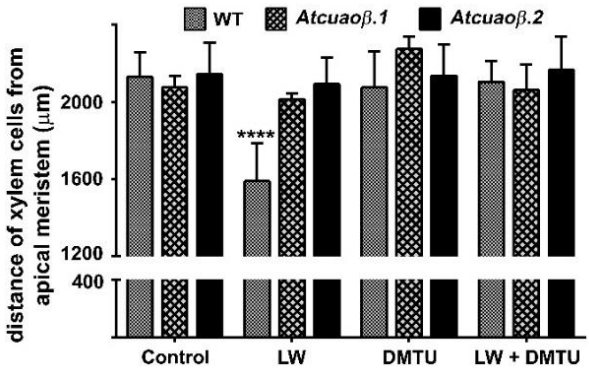

Figure 3.8 Analysis of differences in protoxylem maturation in 10-day-old leaf-wounded WT and mutant (*Atcuaoβ.1* and *Atcuaoβ.2*) seedlings, grown in medium with or without the H_2O_2-scavenger DMTU at the final concentration of 100 μM. Distances from the apical meristem of the protoxylem position (defined by the position of the first protoxylem cell with fully developed secondary cell wall thickenings) are reported. These experiments were repeated at least five times with ten seedlings analyzed each

time (mean values ± SD; $n = 50$). The statistical significance levels were evaluated by P values. P values between WT unwounded control and leaf-wounded plants and between WT leaf-wounded and DMTU treated leaf-wounded plants are reported (****, $P \leq 0.0001$). No significant differences are not represented in the graph.

In order to obtain further evidence of the involvement of AtCuAOβ activity in xylem differentiation, the AtCuAOβ substrate Put (Møller *et al.*, 1998) was provided at the concentration of 100 μM to unwounded and wounded WT and *Atcuaoβ* mutant seedlings. Fig. 3.9 shows that treatment with 100 μM Put induced early protoxylem differentiation in WT plants (protoxylem position at 1800 μm from the apical meristem) but not in *Atcuaoβ* mutants as compared with the corresponding untreated plants. Leaf-wounded Put-treated WT plants (protoxylem position at 1600 μm from the apical meristem) apparently do not present any additive/synergic effect in respect to either leaf-wounded or Put-treated plants, suggesting a plateau effect on protoxylem position induced by leaf wounding.

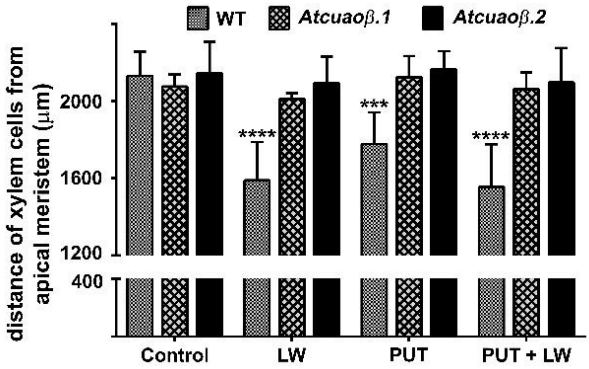

Figure 3.9 Analysis of differences in protoxylem maturation in 10-day-old leaf-wounded WT and mutant (*Atcuaoβ.1* and *Atcuaoβ.2*) seedlings, grown in medium with or without 100 μM Put. Distances from the apical meristem of the protoxylem position (defined by the position of the first protoxylem cell with fully developed secondary cell wall thickenings) are reported. These experiments were repeated at least five times with ten seedlings analyzed each time (mean values ± SD; $n = 50$). The statistical significance levels were evaluated by P values. P values between unwounded Put-untreated WT control plants and Put-treated and/or wounded WT plants and between leaf-wounded WT and mutant plants for each condition are reported (****, $P \leq 0.0001$; ***, $P \leq 0.001$). No significant differences are not represented in the graph.

The effect of leaf wounding and Put on protoxylem position was specific and not dependent upon variation in root growth (Table 3.2) or meristem size (Table 3.3), that were unchanged in leaf-wounded/treated plants as compared to unwounded/untreated control plants.

	Root Growth (cm)		
	WT	***Atcuaoβ.1***	***Atcuaoβ.2***
Control	2.34 ± 0.23	2.34 ± 0.22 ns	2.33 ± 0.21 ns
LW	2.26 ± 0.35	2.38 ± 0.25 ns	2.22 ± 0.25 ns
DMTU 100 µM	2.31 ± 0.22	2.35 ± 0.26 ns	2.32 ± 0.34 ns
LW + DMTU 100 µM	2.37 ± 0.22	2.31 ± 0.28 ns	2.24 ± 0.25 ns
Put 100 µM	2.32 ± 0.25	2.24 ± 0.35 ns	2.35 ± 0.28 ns
LW + Put 100 µM	2.31 ± 0.26	2.31 ± 0.21 ns	2.37 ± 0.28 ns

Table 3.2 Analysis of differences in root growth in leaf-wounded 10-days-old WT and mutant (*Atcuaoβ.1* and *Atcuaoβ.2*) seedlings grown in medium with or without 100 µM Put or 100 µM DMTU. The effect of leaf wounding/treatments on root growth was evaluated as the difference between the length measured at the onset of the wounding/treatment and that measured after 3 days. These experiments were repeated at least five times with ten seedlings analyzed each time (mean values ± SD; $n = 50$). The statistical significance levels between unwounded/untreated control and wounded/treated plants were evaluated by *P* values as follows: ns, not significant.

	Meristem size (µm)		
	WT	***Atcuaoβ.1***	***Atcuaoβ.2***
Control	350,7 ± 16,7	339,9 ± 14,4 ns	355,7 ± 8,4 ns
LW	335,6 ± 13,4	331,7 ± 16,0 ns	345,0 ± 20,9 ns
DMTU 100 µM	353,4 ± 23,7	341,4 ± 7,5 ns	350,8 ± 11,6 ns
LW + DMTU 100 µM	346,8 ± 28,2	345,0 ± 17,0 ns	341,3 ± 17,5 ns
Put 100 µM	337,3 ± 17,5	336,1 ± 17,1 ns	345,0 ± 10,0 ns
LW + Put 100 µM	351,6 ± 35,3	338,3 ± 12,5 ns	350,0 ± 10,8 ns

Table 3.3 Analysis of differences in meristem size in leaf-wounded 10-days-old WT and mutant (*Atcuaoβ.1* and *Atcuaoβ.2*) seedlings grown in medium with or without 100 µM Put or 100 µM DMTU. The length of the meristematic zone was determined by measuring the distance between the quiescent center and the first elongating cell in the cortex cell file. These experiments were repeated at least five times with ten seedlings analyzed each time (mean values ± SD; $n = 50$). The statistical significance levels between unwounded/untreated control and wounded/treated plants were evaluated by *P* values as follows: ns, not significant.

Furthermore, to verify the involvement of H_2O_2 produced via *AtCuAOβ*-driven PA oxidation in the wound-induced-signaling pathways leading to an early protoxylem differentiation, an AUR assay was performed in 7 day-old roots of *Atcuaoβ* mutants wounded or not on the cotyledonary leaf (Fig. 3.10) and in 7 day-old roots of WT and *Atcuaoβ* mutants cotyledonary leaf-wounded treated or not with exogenous Put (Fig. 3.11).

In roots of untreated mutants, H_2O_2-dependent AUR fluorescence was not detectable at the site of differentiating protoxylem elements. Interestingly, in roots of leaf-wounded *Atcuaoβ* mutants the AUR fluorescence was not detectable, as compared to WT wounded plants in which a clearly visible fluorescence is reported (Fig. 3.7, red degrading scale of Fig. 3.10).

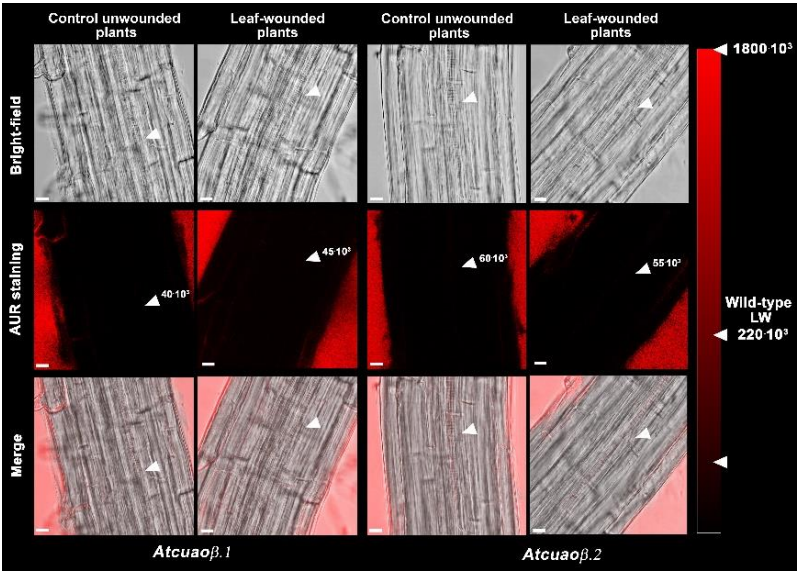

Figure 3.10 *In situ* H_2O_2 detection by analysis under LSCM after AUR staining, of roots from 7-day-old unwounded control and leaf-wounded mutant (*Atcuaoβ.1* and *Atcuaoβ.2*) seedlings 6 hours after the injury. The corresponding bright-field and overlay images are shown. Micrographs show the root zone corresponding to the site of appearance of the first protoxylem cell with fully developed secondary cell wall thickenings (arrows) and have been taken at the level of the central root section. Images are representative of those obtained from ten seedlings from five independent experiments. The average values of fluorescence intensity measured as the sum of the pixels of each of five 65 μm^2 rectangle are reported for each condition (mean values ±

SD; *n* = 25). The maximum pixel sum for a completely saturated square was approximately 1800×10^3. In the red degrading scale are reported for comparison the average values of fluorescence intensity for unwounded control and leaf-wounded WT plants that respectively were $60\times10^3 \pm 19\times10^3$ and $220\times10^3 \pm 38\times10^3$ (data from Fraudentali *et al*., 2018). Bars: 10 μm.

Figure 3.11 shows that 6 h after treatment with 100 μM Put, a strong AUR signal was revealed in the root zone where the first protoxylem cell with fully developed secondary cell wall thickenings is found, which was not detectable in roots of untreated control and Put-treated *Atcuaoβ* mutant seedlings. Moreover, the combination of cotyledonary leaf wounding and Put treatment, did not seem to increase the H_2O_2 accumulation in the site of differentiating protoxylem elements compared to wounding or Put-treatment alone, suggesting a plateau effect on H_2O_2 production induced by leaf wounding (Fig. 3.11). The above-reported results confirmed that AtCuAOβ is the source of a tissue-specific H_2O_2 production triggered by a long-distance leaf-to-root communication and leading to early protoxylem differentiation.

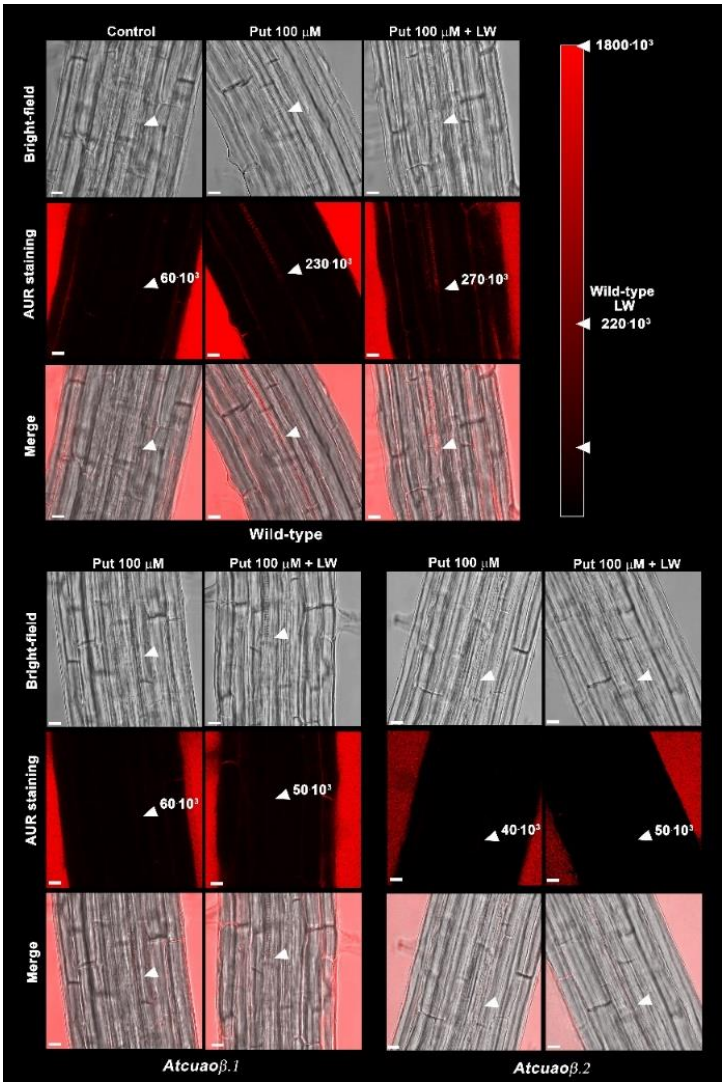

Figure 3.11 *In situ* H_2O_2 detection by analysis under LSCM after AUR staining, of roots from 7-day-old unwounded untreated control (WT) and unwounded control and leaf-wounded WT and mutant (*Atcuaoβ.1* and *Atcuaoβ.2*) seedlings treated with 100

μM Put 6 hours after the injury. The corresponding bright-field and overlay images are shown. Micrographs show the root zone corresponding to the site of appearance of the first protoxylem cell with fully developed secondary cell wall thickenings (arrows) and have been taken at the level of the central root section. Images are representative of those obtained from ten seedlings from five independent experiments. The average values of fluorescence intensity measured as the sum of the pixels of each of five 65 μm^2 rectangle are reported for each condition (mean values ± SD; n = 25). The maximum pixel sum for a completely saturated square was approximately 1800×10^3. In the red degrading scale are reported for comparison the average values of fluorescence intensity for leaf-wounded (Put-untreated) WT plants that was respectively were $60\times10^3 \pm 19\times10^3$ and $220\times10^3 \pm 38\times10^3$ (data from Fraudentali *et al*., 2018). Bars: 10 μm.

3.1.3 AtCuAOβ involvement in MeJA/wounding-induced stomatal closure

The constitutive expression of *AtCuAOβ* in guard cells of leaves and flowers together with its induction in the same organs upon wounding or treatment with the stress-related hormone MeJA, would suggest a role of *AtCuAOβ* in the regulation of stomatal aperture levels under stress conditions. Considering this hypothesis, studies on the involvement of *AtCuAOβ* in the regulation of stomatal movement under MeJA treatment or after wounding, with particular attention to the involvement of this gene in systemic responses, were performed, using WT plants and two different *Atcuaoβ* loss-of-function mutants, *Atcuaoβ.1* and *Atcuaoβ.3*.

WT, *Atcuaoβ.1* and *Atcuaoβ.3* seedlings were treated for 15, 30 min, 1, 3 and 24 h with 50 μM MeJA or injured by alternatively wounding the leaf or the root and then incubated for 5, 15, 30 min, 1, 3 and 24 h to analyze stomatal aperture by measuring the width/length ratio of the stomatal pore. In control conditions, no significant differences in stomatal aperture levels were found between 7-day-old WT and *Atcuaoβ* mutants.

Stomata guard cells of WT MeJA-treated plants displayed a peak of closure of 65% in respect to control untreated plants after 1 h (Fig. 3.12, second left panel). Instead, *Atcuaoβ* loss-of-function mutants did not show any differences in stomatal aperture levels upon MeJA-treatment, displaying the same value of width/length ratio in comparison to both WT and mutant untreated plants. Furthermore, the H_2O_2 scavenger, *N-N*^{1}-dimethylthiourea (DMTU), at the concentration of 100 μM, reversed the MeJA-induced stomatal closure in WT plants restoring the pore width/length ratio at the level of untreated plants, whereas it did not significantly affect stomatal aperture under control conditions in WT plants, or in MeJA-treated and untreated mutants (Fig. 3.12).

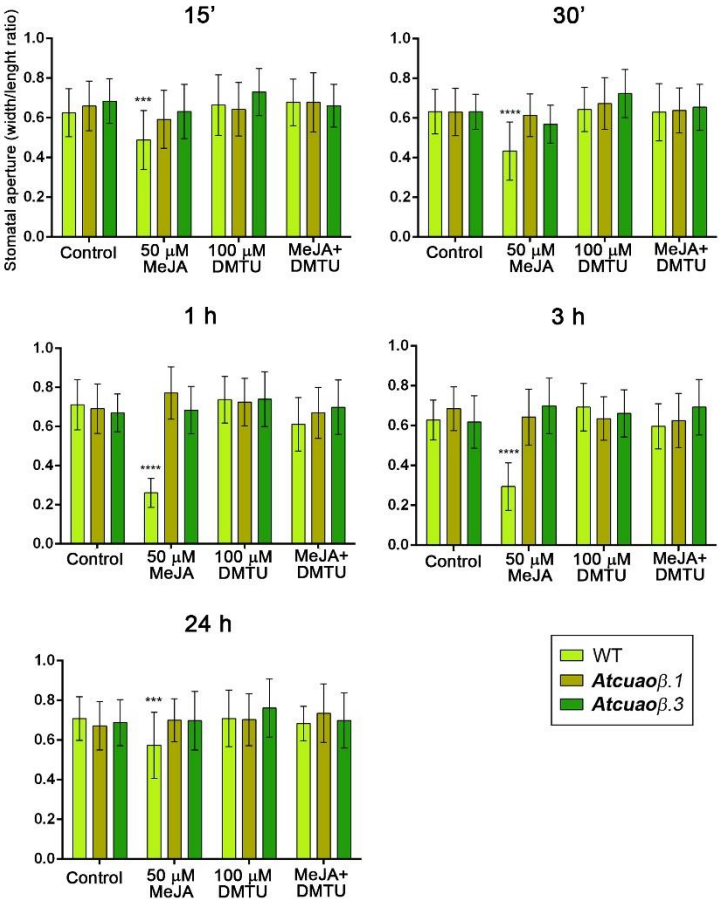

Figure 3.12 Effect of MeJA and *N,N'*-dimethylthiourea (DMTU) on stomatal pore width/length ratio of 7-day-old seedlings from WT, *Atcuaoβ.1* and *Atcuaoβ.3*. Seedlings were treated for 15, 30 min, 1, 3 and 24 h with 50 µM MeJA and 100 µM DMTU, either alone or in combination with the hormone. Mean values ± SD (n = 15) are reported. The significance levels between WT control plants and WT treated plants are reported. *P* levels have been calculated with one-way ANOVA analysis; *P* levels > 0.05; ***, and **** *P* levels are equal to or less than 0.001, and 0.0001, respectively.

Stomata guard cells of WT leaf-wounded plants started to close after 5 min and displayed a peak of closure of 75% after 1 h in the wounded cotyledon consequent to a local effect of wounding (Fig. 3.13, left panels), while they started to close after 30 min displaying a peak of closure between 3 and 24 h (70%, as compared to WT unwounded plants) in the unwounded cotyledon possibly due to a systemic wounding effect (Fig. 3.13, right panels). However, *Atcuaoβ* loss-of-function mutants did not show any differences in stomatal aperture levels upon cotyledonary-leaf wounding, displaying the same value of width/length ratio in comparison to both WT and mutant unwounded plants. Furthermore, 100 μM DMTU reversed the leaf wounding-induced stomatal closure in WT plants restoring the width/length ratio at the level of unwounded plants, whereas it did not significantly affect stomatal aperture under control conditions in WT plants, or in leaf-wounded and unwounded mutants (Fig. 3.13).

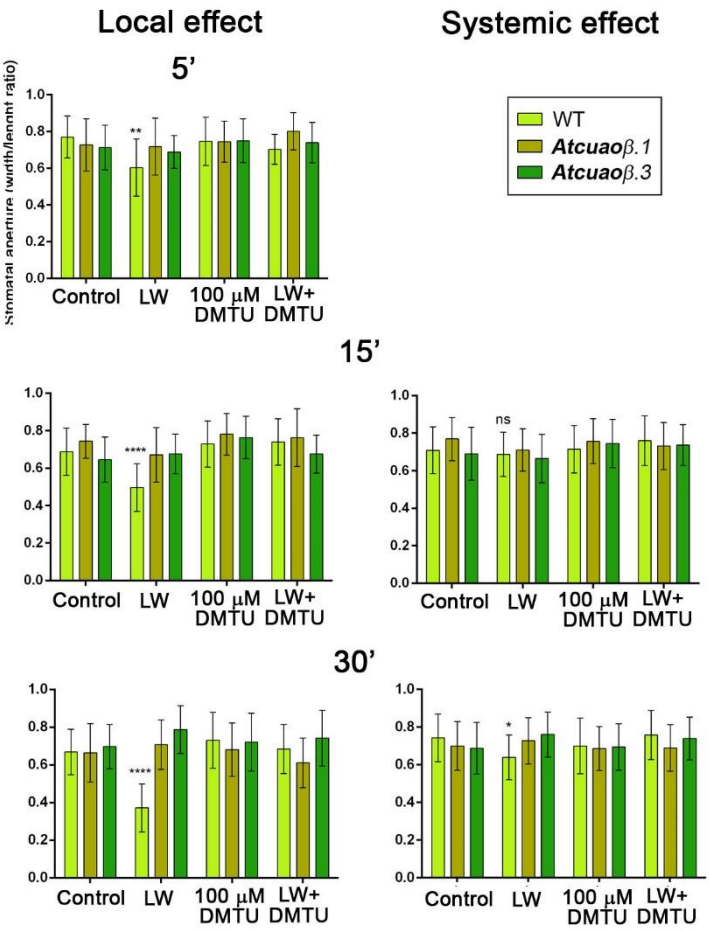
Local effect
Systemic effect
5'
15'
30'
WT
Atcuaoβ.1
Atcuaoβ.3
Stomatal aperture (width/lenght ratio)
1.0
0.8
0.6
0.4
0.2
0.0
**
****
ns
*
Control
LW
100 µM DMTU
LW+ DMTU

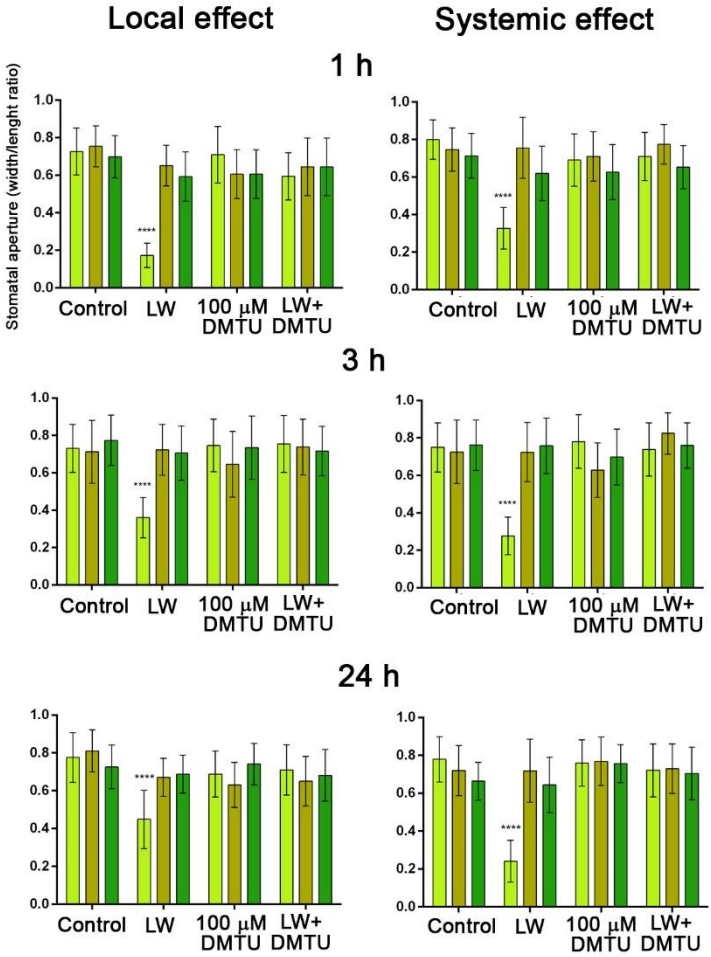

Figure 3.13 Effect of cotyledonary-leaf wounding and *N,N′*-dimethylthiourea (DMTU) on stomatal pore width/length ratio of 7-day-old seedlings from WT, *Atcuaoβ.1* and *Atcuaoβ.3*. Seedlings were leaf-wounded or treated with 100 μM DMTU and incubated for 5, 15, 30 min, 1, 3 and 24 h, both alone or in combination. The stomatal pore analysis was made by distinguishing between the stomata measured from the wounded leaf (local effect, left panels) and those from the distal unwounded leaf (systemic effect, right panels). Mean values ± SD (n = 15) are reported. The significance levels between

WT control plants and WT treated plants are reported. *P* levels have been calculated with one-way ANOVA analysis; *P* levels > 0.05; *, ** and **** *P* levels ≤ 0.05, 0.01 and 0,0001 respectively; ns, not significant.

Stomata guard cells of WT root-wounded plants started to close after 5 min showing a peak of closure between 1 and 3 h (75%), in respect to WT unwounded plants, suggesting a systemic communication from the root to the shoot (Fig. 3.14). As observed in the case of leaf-to-leaf analysis, *Atcuaoβ* loss-of-function mutants did not show any differences in stomatal aperture levels upon root wounding, displaying the same value of width/length ratio in comparison to both WT and mutant unwounded plants. Furthermore, 100 μM DMTU reversed the root wounding-induced stomatal closure in WT plants restoring the width/length ratio at the level of unwounded plants, whereas it did not significantly alter stomatal aperture under control conditions in WT plants, or in both root-wounded and -unwounded mutants (Fig. 3.14).

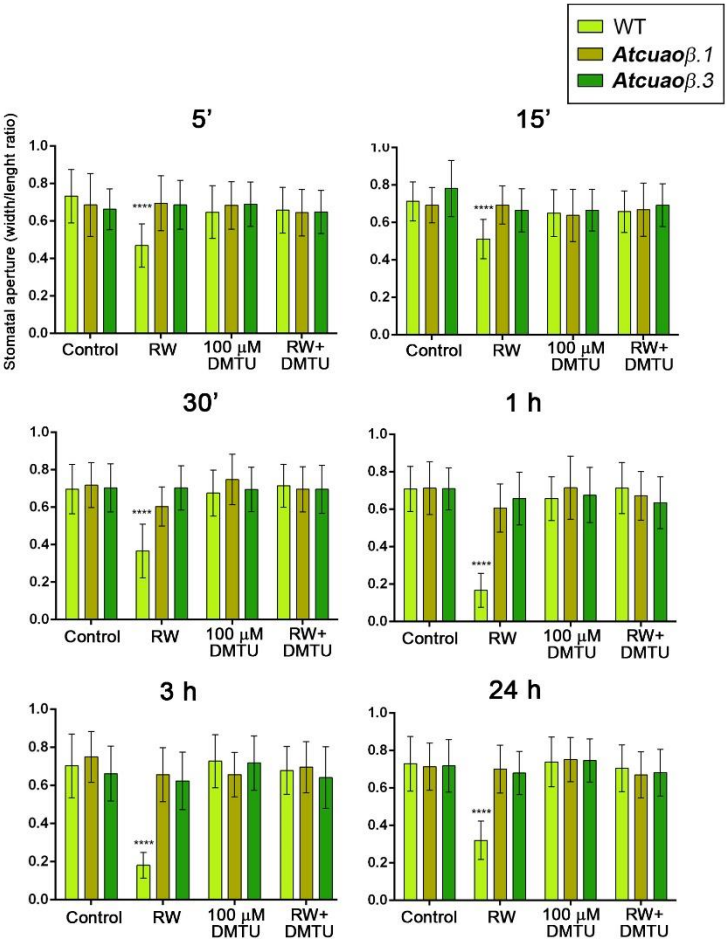

Figure 3.14 Effect of root wounding and *N,N′*-dimethylthiourea (DMTU) on stomatal pore width/length ratio of 7-day-old seedlings from WT, *Atcuaoβ.1* and *Atcuaoβ.3*. Seedlings were root-injured or treated with 100 µM DMTU and incubated for 5, 15, 30 min, 1, 3 and 24 h, both alone or in combination. Mean values ± SD (n = 15) are reported. The significance levels between WT control plants and WT treated plants are reported. *P* levels have been calculated with one-way ANOVA analysis; *P* levels > 0.05; **** *P* levels are equal to or less than 0.0001.

3.1.4 Involvement of GLRs on wounding-induced stomatal closure

The evidence of the MeJA-regulated AtCuAOβ involvement in response to wounding and the occurrence of leaf-to-leaf and root-to-leaf systemic responses observed concerning the regulation of stomatal closure, led us to analyze the involvement of glutamate receptors-like (GLRs) in the wounding-induced stomatal closure, considering that these receptors have been described as involved in systemic responses. The identity of the cell files necessary for the long distance transmission of wound signals in plants has been debated for decades. In Arabidopsis, wounding initiates the GLR-dependent propagation of membrane depolarization that lead to defense genes activation, through the synthesis of the defense hormone JA in distal sites to wounds (Nguyen *et al*., 2018).

In this context, considering the GLR essential role in cell to cell communication, and to clarify the nature of the rapid response to wounding observed in data reported above, GLR involvement on wounding-induced stomatal movement was analyzed using *glr3.3* loss-of-function mutants, *glr3.3-1* and *glr3.3-2*. WT, *glr3.3-1* and *glr3.3-2* seedlings were injured by alternatively wounding the cotyledonary-leaf or the root and then incubated for 5, 30 min, 1, 3 and 24 h. The stomatal aperture was analyzed by measuring the width/length ratio of the stomatal pore. In control conditions, no significant differences in stomatal aperture levels were found between 7-day-old WT and *glr3.3* mutants.

Consistently with the data shown in Fig. 3.13, stomata guard cells of WT leaf-wounded seedlings displayed a closure of 65% after 30 min and a peak of closure of 75 % after 1 h in the wounded leaf, as a consequence of local wounding effect (Fig. 3.15, upper panel), while a closure of 15% after 30 min with a peak of 70% up to 24 h in the unwounded leaf due to a systemic wounding effect (Fig. 3.15, lower panel), as compared to WT unwounded plants. Interestingly, the stomata of both *glr3.3* mutants also show the same pattern of stomatal pore closure as those observed in WT seedlings in the wounded leaf, while in the unwounded leaf they displaying a much reduced closure extent, of around 15% width/length ratio in comparison to both WT and mutant unwounded plants.

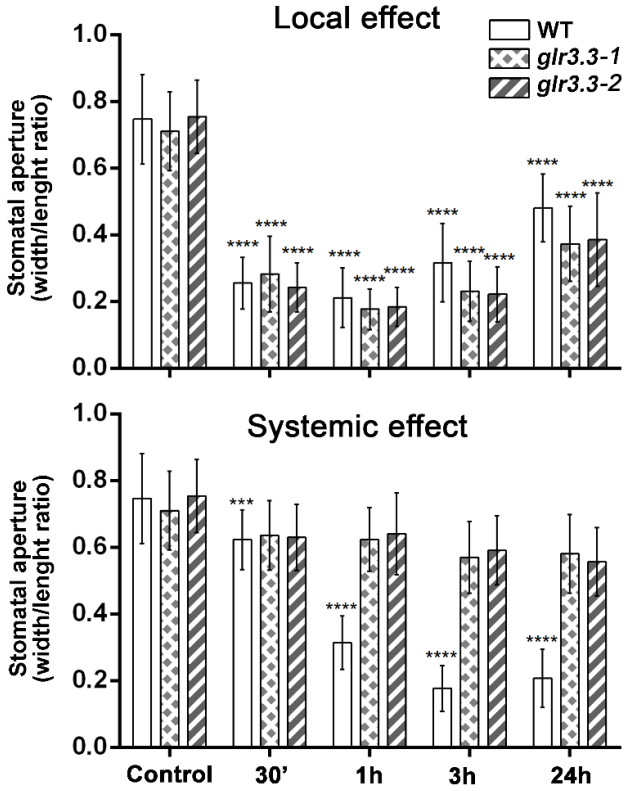

Figure 3.15 Effect of cotyledonary-leaf wounding on stomatal pore width/length ratio of 7-day-old seedlings from WT, *glr3.3-1* and *glr3.3-2*. Seedlings were leaf-wounded and incubated for 30 min, 1, 3 and 24 h. The mean of the values of unwounded control plants for each genotype and time point is reported as Control. Mean values ± SD (n = 15) are reported. The significance levels between control plants and leaf-wounded plants are reported. P levels have been calculated with one-way ANOVA analysis; P levels > 0.05; ***, and **** P levels are equal to or less than 0.001, and 0.0001, respectively.

Guard cells of WT root-wounded plants showed the same pattern of stomatal pore closure described in Fig. 3.14, displaying a closure of 50% after 5 min peaking at 75% between 1 and 3 h, consequent to the observed systemic communication from the root to the leaf (Fig. 3.16). Interestingly, *glr3.3* loss-

of-function mutants showed a much reduced closure extent, of around 15%, after each time analyzed upon root wounding compared to both WT and mutant unwounded plants.

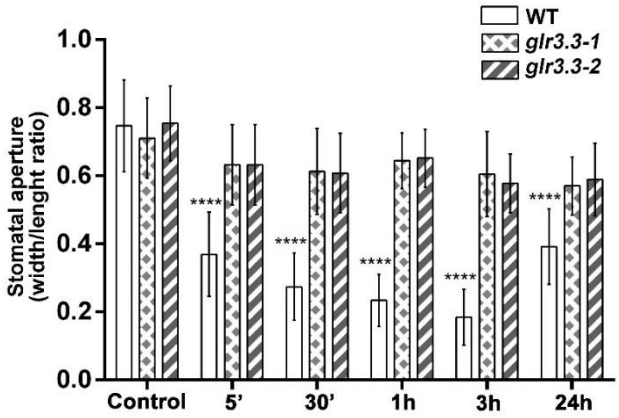

Figure 3.16 Effect of root wounding on stomatal pore width/length ratio of 7-day-old seedlings from WT, *glr3.3-1* and *glr3.3-2*. Seedlings were root-injured and incubated for 5, 30 min, 1, 3 and 24 h. The mean of the values of unwounded control plants for each genotype and time point is reported as Control. Mean values ± SD (n = 15) are reported. The significance levels between WT control plants and WT root-wounded plants are reported. *P* levels have been calculated with one-way ANOVA analysis; *P* levels > 0.05; **** *P* levels are equal to or less than 0.0001.

3.2 Physiological role of *AtCuAOδ* in stomatal closure induced by ABA treatment

The gene product of *AtCuAOδ* (At4g12290) has been identified among proteins purified from the central vacuoles of rosette leaf tissues by means of complementary proteomic methodologies (Carter *et al*., 2004). The occurrence of an ABA-inducible *AtCuAOδ* expression in guard cells, as reported by the Arabidopsis eFP Browser (http://bar.utoronto.ca/efp/cgi-bin/efpWeb.cgi; Winter *et al*., 2007), along with the role played by the vacuole in ABA-induced stomatal closure (Bak *et al*., 2013), led us to analyze the possible involvement of AtCuAOδ in the control of stomatal movement.

3.2.1 Expression profile of AtCuAOδ after ABA treatment

A promoter region of approximately 2.7 kb upstream of the *AtCuAOδ* start codon has been analyzed *in silico* for the presence of cis-acting elements by the Arabidopsis eFP Browser (http://bar.utoronto.ca/cistome/cgi-bin/BAR_Cistome.cgi). On the basis of this analysis, two recognition sequences (CATGTG) for the ABA-inducible MYC factor (MYCATERD1) necessary for the expression of *erd1* (early responsive to dehydration) in dehydrated Arabidopsis plants, have been identified. Moreover, the analysis of microarray data retrieved from the Arabidopsis eFP Browser revealed the occurrence of *AtCuAOδ* mRNA in guard cells, whose level increased upon ABA-treatment. These data are supported by RT-qPCR studies which showed a 2- to 3-fold increase of *AtCuAOδ* expression levels depending on ABA concentration as soon as 3 h from the onset of treatment (Fig. 3.17). This induction peaked at 6 h with a 4-fold increase at 100 µM ABA, and returned to almost control levels at 24 h for the two lower concentrations while it was still 2-fold higher at 100 µM ABA.

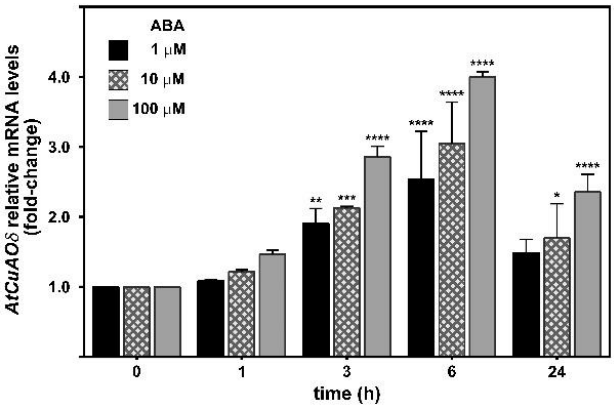

Figure 3.17 Analysis of *AtCuAOδ* gene expression upon ABA treatment by RT-qPCR. The expression of *AtCuAOδ* gene was analyzed in 12-day-old WT seedlings untreated or treated with 1, 10, 100 µM ABA for 0, 1, 3, 6 and 24 h. Five biological replicates each with three technical replicates were performed (mean values ± SD; n=5). *AtCuAOδ* mRNA level after ABA treatment is relative to that of the corresponding untreated plant for each time point. The significance levels between the relative mRNA level at each time and the mRNA level of control untreated plant at time 0, which is assumed to be one, is reported. *P* levels have been calculated with one-way ANOVA analysis. *, **,

*** and **** *P* levels equal or less than 0.05, 0.01, 0.001 and 0.0001 respectively. Data published in Fraudentali *et al*., 2019.

3.2.2 AtCuAOδ involvement in ABA-induced stomatal closure

Here, the involvement of H_2O_2 delivered by PA oxidation mediated by *AtCuAOδ* in the ABA-induced stomatal closure was investigated using WT plants and two different *Atcuaoδ* loss-of-function mutants, *Atcuaoδ.1* and *Atcuaoδ.2*.

WT, *Atcuaoδ.1* and *Atcuaoδ.2* 12-day-old seedlings were treated with 1, 10, and 100 µM ABA or with 100 µM DMTU, either alone or in combination with the different hormone concentrations, and incubated for 2 h to induce stomata closure and the stomatal aperture was analyzed by measuring the width and the length of the stomatal pore (width/length ratio). Fig. 3.18 shows that while between control untreated WT (Control WT) and control untreated insertional mutants (Control *Atcuaoδ.1* or Control *Atcuaoδ.2)* no differences at the pore width/length ratio were detected, a significant reduction of the ABA-mediated stomatal closure was observed in the *Atcuaoδ* mutants as compared to WT plants. Indeed, stomatal closure was induced in WT by ABA treatments from 50,7% at 1 µM to a maximum of 77% at 100 µM, as compared to untreated WT, while the ABA-mediated stomatal closure ranged from ~9-12% to a maximum of ~15-17% in *Atcuaoδ.1* and in *Atcuaoδ.2* as compared to the respective Control mutant plants (Fig. 3.18A). Furthermore, DMTU reversed the ABA-induced stomatal closure in WT plants (91, 80 and 78% respectively) while it did not significantly affect stomatal aperture under control conditions in WT plants as well as in 1 and 10 µM ABA-treated and untreated mutants (Fig. 3.18A). At the highest ABA concentration used, DMTU reversion was not complete in the mutant genotypes where a significant closure effect of 8% and 11% was observed in *Atcuaoδ.1* and *Atcuaoδ.2*, respectively.

Consistently with these data, the action of the CuAO-specific inhibitors, 2-bromoethylamine (2-BrEtA) and aminoguanidine (AG), on stomatal apertures of *Atcuaoδ* mutants was also studied. (Fig. 3.18B). At the two different inhibitor concentrations used, in the presence of 100 µM ABA (the highest hormone concentration used), diverse antagonistic effects were observed. At the 2-BrEtA highest concentration, a considerable reduction of stomatal closure was observed in WT (from 77% to 10%) while the mutant genotypes were further unresponsive to ABA (5% from 15% in *Atcuaoδ.1* and 9% from 17% in *Atcuaoδ.2*). The other CuAO inhibitor, AG, prevented

partially, the stomatal closure effects induced by ABA in WT (35% and 24% at 0.1 mM and 1 mM respectively). However, by itself this inhibitor presented a similar effect on stomatal aperture in all the studied genotypes (10% closure in respect to the untreated control WT and mutant; Fig. 3.18B).

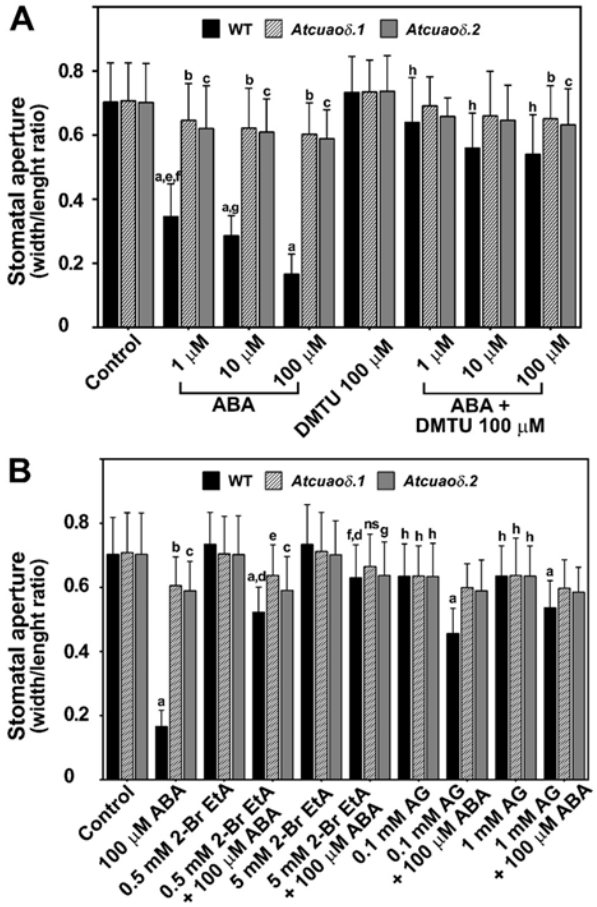

Figure 3.18 Effect of ABA, DMTU (**A**) and CuAO inhibitors, 2-BrEtA and AG (**B**), on stomatal pore width/length ratio of 12-day-old seedlings from WT, *Atcuaoδ.1* and *Atcuaoδ.2*. Results from three independent experiments are reported (mean values ± SD). *P* levels have been calculated with one-way ANOVA analysis; non-significant (ns)

differences: *P* levels > 0.05; *, **, *** and **** *P* levels are equal to or less than 0.05, 0.01, 0.001 and 0.0001, respectively. **(A)** Seedlings were treated for 2 h with ABA (1, 10, 100 µM) and DMTU (100 µM) either alone or in combination with the hormone. The significance levels are described with letters where appropriate, non-significant differences are not indicated. **a** = ****, ABA 1, 10, 100 µM WT vs Control WT; **b** = **, ABA 1 µM / ABA100 µM + DMTU *Atcuaoδ.1* vs Control *Atcuaoδ.1*; **c** = ****, ABA 1, 10, 100 µM *Atcuaoδ.2* /ABA 100 µM + DMTU *Atcuaoδ.2* vs Control *Atcuaoδ.2*; **d**= ****, ABA 10, 100 µM *Atcuaoδ.1* vs Control *Atcuaoδ.1*; **e** = *, ABA 1 µM WT vs ABA 10 µM WT; **f** = ****, ABA 1 µM WT vs ABA 100 µM WT; **g** = ****, ABA 10 µM WT vs ABA 100 µM WT; **h** = ****, ABA 1, 10, 100 µM WT vs ABA 1, 10, 100 µM + DMTU WT. **(B)** Seedlings were treated with 2-BrEtA (0.5, 5 mM) or AG (0.1, 1 mM) for 30 min. ABA was added (100 µM) and further incubated for 2 h. The significance levels are described with letters where appropriate.; **ns:** ABA 100 µM + 5 mM 2-BrEtA *Atcuaoδ.1* vs Control *Atcuaoδ.1*; **a**: ****, ABA 100 µM, ABA 100 µM + 0.5 mM 2-BrEtA, ABA 100 µM + AG 0.1 or 1 mM WT vs Control WT; **b**: ****, ABA 100 µM *Atcuaoδ.1* vs Control *Atcuaoδ.1*; **c**: ****, ABA 100 µM/ABA 100 µM + 0.5mM 2-BrEtA *Atcuaoδ.2* vs CNT *Atcuaoδ.2*; **d**: ****, ABA 100 µM + 2-BrEtA 0.5 or 5 mM WT vs ABA 100 µM WT; **e**: ** ABA 100 µM + 0.5mM 2-BrEtA *Atcuaoδ.1* vs Control *Atcuaoδ.1*; **f**: ** ABA 100 µM + 2-BrEtA 5 mM WT vs Control WT; **g**: * ABA 100 µM + 2-BrEtA 5 mM *Atcuaoδ.2* vs Control *Atcuaoδ.2*; **h**: *, AG 0.1 or 1 mM, WT, *Atcuaoδ.1* e *Atcuaoδ.2* vs Control WT, Control *Atcuaoδ.1* or Control *Atcuaoδ.2*. Data published in Fraudentali *et al*., 2019.

3.3 Analysis of the inducible expression profile of of the AtCuAOs α and γ phylogenetic branches

Herein, to lay the basis for future investigations on the roles played by other members of the AtCuAO family under physiological or pathological conditions, a comprehensive and extensive analysis of the stress-, hormone- and PA treatment-induced gene expression pattern of four *AtCuAOs* from the *α* (clade I) and *γ* (clade II) phylogenetic subfamilies, namely *AtCuAOα2*, *AtCuAOα3*, *AtCuAOγ1* and *AtCuAOγ2* (Tavladoraki *et al.*, 2016), encoding for the two peroxisomal AtCuAOα2/α3 (α2, Fukao *et al.*, 2003; α3, Planas-Portell *et al.*, 2013) and the two apoplastic AtCuAOγ1/γ2 (γ1, Planas-Portell *et al.*, 2013; γ2, http://suba.plantenergy.uwa.edu.au/flatfile.php?id=At3g43670), has been carried out. To this purpose, tissue-specific analysis of *AtCuAO*s expression patterns, exploiting *promoter::GFP-GUS* fusion transgenic plants, was integrated with quantitative investigation of gene expression by RT-qPCR analysis.

The analysis of the tissue specific expression of *AtCuAOα2, AtCuAOα3, AtCuAOγ1* and *AtCuAOγ2* previously performed in our laboratory exploiting *AtCuAO::GFP-GUS* transgenic plants (Ghuge 2014), revealed a tissue specific expression of these genes in hydathodes of new emerging leaves

(*AtCuAOγ1* and *AtCuAOγ2*) and/or cotyledons (*AtCuAOα2*, *AtCuAOγ1* and *AtCuAOγ2*), in vascular tissues of new emerging leaves (*AtCuAOγ1*) or hypocotyl and root (*AtCuAOα3*), in cotyledon and young leaf epidermis (*AtCuAOα2*), in cortical root cells at the division/elongation transition zone (*AtCuAOγ1*) as well as in cotyledon margins and columella cells (*AtCuAOγ2*) (Ghuge 2014; Carucci 2017). Moreover, preliminary data about these genes expression profile by RT-qPCR analysis upon treatment with three different stress-related hormones revealed an induction by ABA (*AtCuAOγ1*), MeJA (*AtCuAOα2*, *AtCuAOα3*) and SA (*AtCuAOγ1, AtCuAOγ2*) (Carucci 2017).

In order to provide valuable information on the role that these *AtCuAO* genes play in physiological and pathological processes, here a comprehensive and extensive investigation of the stress-, hormone- and PA treatment-induced gene expression pattern of *AtCuAOα2*, *AtCuAOα3*, *AtCuAOγ1* and *AtCuAOγ2* has been carried out in Arabidopsis seedlings by promoter-driven GUS activity and GFP fluorescence analysis and RT-qPCR.

3.3.1 Expression profile of AtCuAOα2 and AtCuAOα3 under stress conditions or after treatments with hormones or PAs

The modulation of *AtCuAOα2* and *AtCuAOα3* expression profiles by auxin (IAA), MeJA, ABA and SA were investigated by RT-qPCR analysis. IAA (10 µM) induced an initial peak followed by a repression, MeJA induced expression of both genes while ABA and SA showed a down-regulating effect (Fig. 3.19). In particular, IAA induced the expression of *AtCuAOα2* of 3.6- and 3.2-fold at 1 and 3 h respectively. A strong repression effect, 20% of control untreated plants (T0), was visible only at the 24 h time-point (Fig. 3.19 first left panel). The effect of IAA induction on *AtCuAOα3* expression was significant albeit at a lower level (2- and 1.4-fold at the same time points) than for *AtCuAOα2*. The observed repression effect was visible earlier, but at a reduced level (40% of T0) than for *AtCuAOα2*, at 6 and 24 h time-point (Fig. 3.19 first right panel). On the other hand, 50 µM MeJA induced *AtCuAOα2* expression by 2.7- and 2.4- fold respectively after 6 and 24 h from the treatment onset, while no significant changes were observed after 1 and 3 h in comparison with T0 (Fig. 3.19 second left panel). Similarly, a strong induction of *AtCuAOα3* expression was observed after the same treatment. In detail, we observed an induction after 3 h (4-fold), peaking at 6 h (5-fold) followed by a reduction (4-fold) after 24 h, from the treatment onset in comparison with T0 (Fig. 3.19 second right panel). Upon 100 µM ABA treatment, *AtCuAOα2* and *AtCuAOα3* expression rapidly decreased during the period of the time course

analysis. In particular, we observed 40%, 67% and 90% decrease of *AtCuAOα2* gene expression after 3, 6 and 24 h from the treatment onset in respect to T0 (Fig. 3.19 third left panel). Furthermore, a similar profile was observed for *AtCuAOα3* gene expression, with 80% and 90% decrease after 6 and 24 h from the treatment onset in respect to T0 (Fig. 3.19 third right panel). A decrease in *AtCuAOα2* and *AtCuAOα3* expression was also observed upon 2 mM SA treatment. Specifically, no significant differences in *AtCuAOα2* expression profile were observed until 3 h from the treatment onset as followed by a decrease of 50% and 80% at 6 and 24 h respectively, compared with T0 (Fig. 3.19 fourth left panel). *AtCuAOα3* expression level presented a similar profile with no difference from T0 up to 6 h from the treatment onset and a significant 72% decrease in expression at 24 h compared with T0 (Fig. 3.19 fourth right panel).

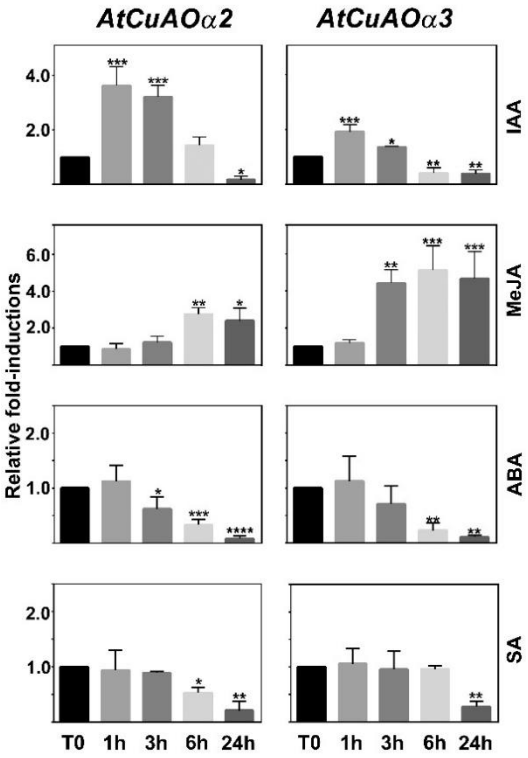

Figure 3.19 Time-course analysis of *AtCuAOα2* and *AtCuAOα3* gene expression by RT-qPCR upon treatment with IAA, MeJA, ABA and SA. Gene expression was analyzed in 7-day-old WT seedlings untreated or treated with 10 µM IAA, 50 µM MeJA, 100 µM ABA or 2 mM SA for 0 (T0), 1, 3, 6 and 24 h. The reported values of expression fold-inductions after treatment are relative to the corresponding expression values of non-treated plants for each time point, with the value for time zero assumed to be one. Data is the result of three biological replicates, each with three technical replicates (mean values ± SD; n = 3). The significance levels between relative mRNA levels at each time point and time 0 are reported only when $P \leq 0.05$. *, **, ***, **** *P* levels ≤ 0.05, 0.01, 0.001 and 0.0001 respectively.

Considering data from RT-qPCR, the analysis of the tissue specific expression pattern of *AtCuAOα2* and *AtCuAOα3* after IAA and MeJA treatments were carried out using *promoter::GFP-GUS* plants. IAA induced *AtCuAOα2* expression in cotyledons and newly formed expanding leaves, especially in hydathodes and epidermis (Fig. 3.20a-d), as revealed by the presence of an intense GUS staining at the external border of cotyledons (Fig. 3.20b) as well as at the hydathodes of new emerging leaves (Fig. 3.20d), as compared to control untreated plants (Fig. 3.20a, c). Furthermore, IAA induced *AtCuAOα3* expression (Fig. 3.20k-n) in stipules, in the petiole/apex junction (Fig. 3.20l) and remarkably in the stele of root mature zone (Fig. 3.20n), as compared to control untreated plants (Fig. 3.20k, m). MeJA induced *AtCuAOα2* expression in cotyledons and newly formed expanding leaves, especially in hydathodes and epidermis (Fig. 3.20e-j), as revealed by the presence of a more intense GUS staining at the apical hydathode (Fig. 3.20f) and at the external border of cotyledons (Fig. 3.20h) as well as at the hydathodes of new emerging leaves (Fig. 5j), as compared to control untreated plants (Fig. 3.20e, g, i). Furthermore, MeJA induced *AtCuAOα3* expression (Fig. 3.20o-t) in stipules (Fig. 3.20p), in the hypocotyl stele and in hypocotyl/root junction (Fig. 3.20r), and principally in the stele of root mature zone (Fig. 3.20r). Particularly, analysis of GFP fluorescence (Fig. 3.20s-t) revealed that in root mature zone of MeJA treated plants, gene expression was induced in the vascular tissue (Fig. 3.20t) as compared to untreated plants, in which fluorescence was barely detectable (Fig. 3.20s).

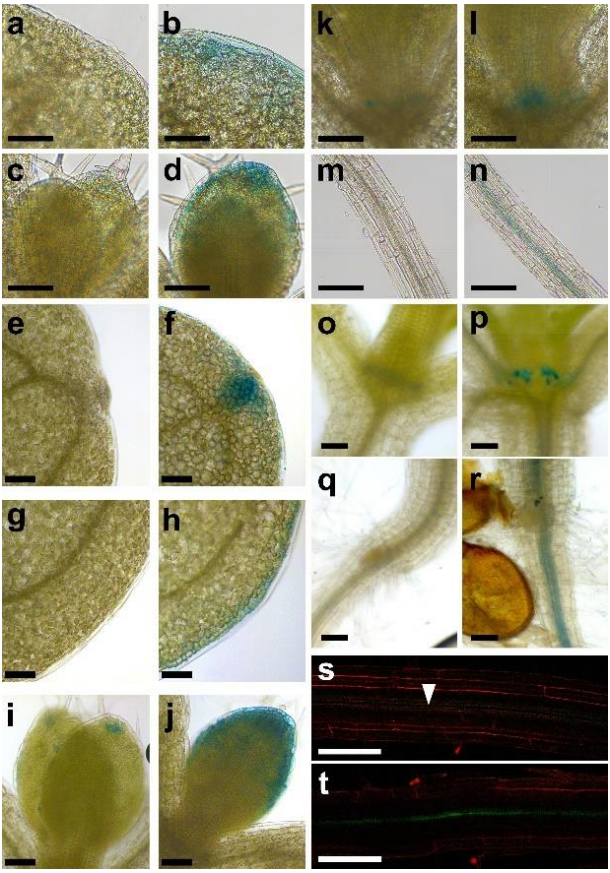

Figure 3.20 Analysis of *AtCuAOα2* and *AtCuAOα3* tissue specific expression pattern upon IAA and MeJA treatments. **a**-**j** Light microscopy analysis by GUS staining of 7-day-old *AtCuAOα2*::*GFP-GUS* transgenic seedlings untreated (a, c, e, g, i) or treated with 10 µM IAA for 3 h (b, d) or with 50 µM MeJA for 24 h, (f, h, j). The staining reaction proceeded for 2 h. **a** and **b** Cotyledon apical zone showing a slight increase of GUS staining at the apical hydathode (b). **c** and **d** Shoot apex with newly formed expanding leaves showing an increase of promoter activity in the apical hydathode (d). **e** and **f** Cotyledon apical zone showing a strong increase of GUS staining at apical hydathode (f). **g** and **h** Cotyledon lateral zone showing increase of GUS staining at the external border (h). **i** and **j** Shoot apex with newly formed expanding leaves showing an increased promoter activity in the apical hydathode and leaflet margins (j). **k**-**r** Light microscopy analysis by GUS staining of 7-day-old *AtCuAOα3-promoter::GFP-GUS*

transgenic seedlings untreated (k, m, o, q) or treated with 10 μM IAA for 3 h (l, n) or with 50 μM MeJA for 6 h (p, r). The staining reaction proceeded 2 h and 1 h for IAA and MeJA treatments, respectively. **k** and **l** Shoot apex showing an increase of GUS staining, particularly in stipules (l). **m** and **n** Mature root showing a clear increase of promoter activity in the vascular tissues (n). **o** and **p** Shoot apex showing an increase of GUS staining in stipules (p). **q** and **r** Hypocotyl/root junction showing a clear increase of promoter activity in the hypocotyl, and the mature root zone (r). **s** and **t** LSCM analysis of GFP signal and PI staining of 5-day-old *AtCuAOα3*::*GFP-GUS* transgenic seedlings untreated (s) or treated (t) with 50 μM MeJA for 2 h showing a stronger signal in the vascular tissue of treated plants. a-d, k-n bar = 200 μm; e-j, o-t, bar = 100 μm.

To correlate the *AtCuAOα2* and *AtCuAOα3* gene expression profiles after ABA and MeJA treatments with the responses of the same genes to the main ABA and MeJA-signaled abiotic stresses, the variations of *AtCuAOα2* and *AtCuAOα3* gene expression profiles under dehydration and successive recovery, and upon leaf wounding (Fig. 3.21) were analyzed. As shown in Fig. 3.21, after 30 min. dehydration (T1) no apparent changes in the expression levels were observed for both genes (Fig. 3.21, inset in both upper panels) while significant changes were observed during the successive dehydration recovery (DR). In particular, *AtCuAOα2* presented peaks of expression at T3 and T4 (3 and 6 h DR) with 4-fold inductions, that returned to T0 levels at T5 (24 h DR), while *AtCuAOα3*, presented a peak from T2 to T3 (2-fold induction at 1 and 3 h DR) that were no longer significantly different from T0 levels at T4 and T5 (6 and 24 h DR) (Fig. 3.21, upper right and left panels). Upon leaf-wounding *AtCuAOα2* expression presented a small but significant peak (1.6-fold) of induction at 1 h time point, followed by a quick return to T0 levels (Fig. 3.21, lower left panel), while *AtCuAOα3* expression presented an induction from 1 to 6 h time points with a strong induction peak at 3 h (2-fold for 1 and 6 h, 4-fold at 3 h) returning to T0 levels at 24 h (Fig. 3.21, lower right panel).

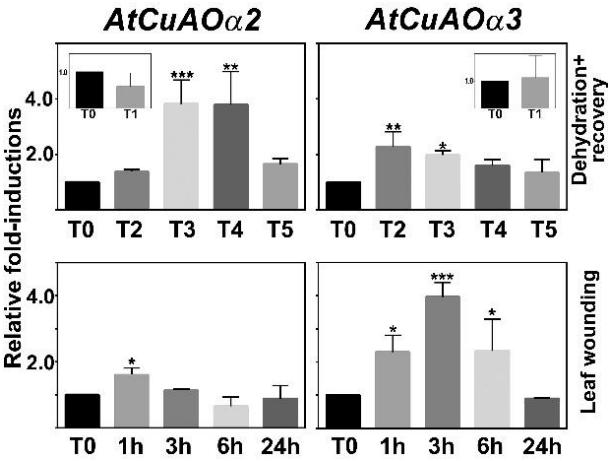

Figure 3.21 Time-course analysis of *AtCuAOα2* and *AtCuAOα3* gene expression by RT-qPCR upon abiotic stress treatments (dehydration, dehydration recovery and leaf wounding). Gene expression was analyzed in 7-day-old WT seedlings untreated or treated for 0h (T0), 30 min. dehydration (T1) (see inset graph) followed by 1 (T2), 3 (T3), 6 (T4) and 24 h (T5) recovery, or 0 (T0), 1, 3, 6 and 24 h after leaf wounding. The reported values of expression fold-inductions after treatment are relative to the corresponding expression values of non-treated plants for each time point, with the value for time zero assumed to be one. Data is the result of three biological replicates, each with three technical replicates (mean values ± SD; n = 3). The significance levels between relative mRNA levels at each time point and time 0 are reported only when $P \leq 0.05$. *, **, ***, **** *P* levels ≤ 0.05, 0.01, 0.001 and 0.0001 respectively.

Considering data from RT-qPCR, the analysis of the tissue-specific expression pattern of *AtCuAOα2* and *AtCuAOα3* after these stress treatments have been carried out. Both DR and leaf wounding stresses induced *AtCuAOα2* expression in cotyledon margins and newly formed expanding leaves, especially in hydathodes and epidermis (Fig. 3.22a-f), as revealed by the presence of an intense GUS staining at the external border of cotyledons (Fig. 3.22d, f) as well as in the hydathodes and in leaf margins of new emerging leaves (Fig. 3.22c, e) of stressed *AtCuAOα2-promoter::GFP-GUS* plants as compared to control untreated plants (Fig. 3.22a, b). Furthermore, both stresses induced *AtCuAOα3* expression (Fig. 3.22g-l) in stipules (Fig. 3.22i, k), and in the stele of root mature zone (Fig. 3.22j, l) as compared to control untreated plants (Fig. 3.22g, h).

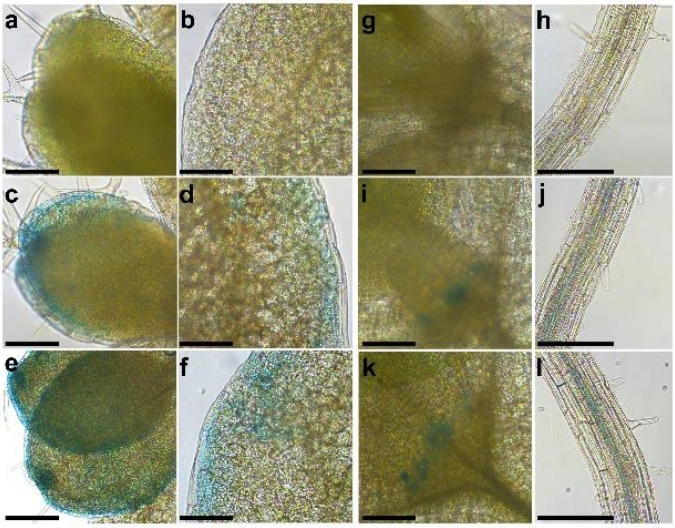

Figure 3.22 Analysis of *AtCuAOα2* and *AtCuAOα3* tissue-specific expression pattern upon abiotic stress (leaf wounding and dehydration recovery) treatments. **a-f** Light microscopy analysis by GUS staining of 7-day-old *AtCuAOα2*::*GFP-GUS* transgenic seedlings untreated (a, b) or subjected to dehydration 30 min plus 3 h recovery (c, d), or to cotyledonary leaf wounding for 3 h (e, f). The staining reaction proceeded for 2 h in both treatments. **a, c, and e** Young leaves of untreated (a), subjected to dehydration recovery (c) or to cotyledonary leaf wounding (e). **b, d, and f** Cotyledon of untreated (b) subjected to dehydration recovery (d) or to wounding (f). **g-l** Light microscopy analysis by GUS staining of 7-day-old *AtCuAOα3-promoter::GFP-GUS* transgenic seedlings untreated (g, h) or treated with dehydration 30 min plus 3 h recovery (i, j), or with cotyledonary leaf wounding for 3 h (k, l). The staining reaction proceeded for 2 h in both treatments. **g, i** and **k** Petiole/apex junction of untreated (g), submitted to dehydration recovery (i) or to cotyledonary leaf wounding (k). **h, j and l** Root mature zone of untreated (h), submitted to dehydration recovery (j) or to cotyledonary leaf wounding (l). a-l, bar = 200 µm.

To verify the occurrence of a direct effect of exogenous Put and Spd on the *AtCuAOα2* and *AtCuAOα3* gene expression profiles, RT-qPCR analysis was carried out on plants treated with Put or Spd at the final concentration of 500 µM. As shown in Fig. 3.23, treatments with Put and Spd had different effects on the expression of these genes. Treatment with 500 µM Put induced *AtCuAOα2* only at the last time point studied (2-fold at 24 h; Fig. 3.23, upper left panel). Instead, Put strongly induced *AtCuAOα3* after 1 h (2-fold) and up

to 6 h (3-fold), returning to T0 levels at the last time point (Fig. 3.23, upper right panel). Responses to 500 µM Spd treatment presented opposite time course profiles for *AtCuAOα2* and *AtCuAOα3* with induction peaks of 4- and 2-fold at 3- and 24 h for the former (Fig. 3.23, lower left panel), and a strong repression at 6 h (20%) which returned approximately to T0 levels at 24 h (1.4-fold) for the latter (Fig. 3.23, lower right panel).

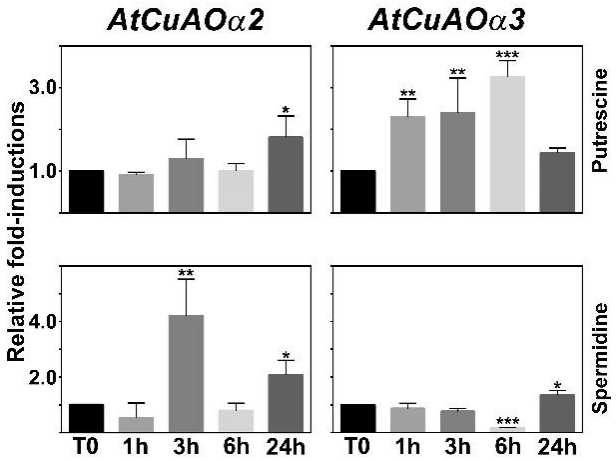

Figure 3.23 Time-course analysis of *AtCuAOα2* and *AtCuAOα3* gene expression by RT-qPCR upon treatment with the polyamines putrescine e spermidine. Gene expression was analyzed in 7-day-old WT seedlings untreated or treated with 500 µM putrescine or 500 µM spermidine for 0 (T0), 1, 3, 6 and 24 h. The reported values of expression fold-inductions after treatment are relative to the corresponding expression values of non-treated plants for each time point, with the value for time zero assumed to be one. Data is the result of three biological replicates, each with three technical replicates (mean values ± SD; n = 3). The significance levels between relative mRNA levels at each time point and time 0 are reported only when $P \leq 0.05$. *, **, ***, **** *P* levels ≤ 0.05, 0.01, 0.001 and 0,0001 respectively.

Considering data from RT-qPCR, an analysis of the tissue specific expression pattern of *AtCuAOα2* and *AtCuAOα3* after Put and Spd treatments were carried out. Both PAs induced *AtCuAOα2* expression in cotyledon margins and newly formed expanding leaves, especially in hydathodes and epidermis (Fig. 3.24a-f), as revealed by the presence of an intense GUS staining in the hydathodes and in leaf margins of new emerging leaves (Fig. 3.24c, e) as well as in the hydathodes of cotyledons (Fig. 3.24d, f) of Put- and

Spd-treated *AtCuAOα2-promoter::GFP-GUS* plants as compared to control untreated plants (Fig. 3.24a, b). Furthermore, Put induced *AtCuAOα3* expression (Fig. 3.24g-j) in the stele of root mature zone (Fig. 3.24h), and in stipules (Fig. 3.24j), as compared to control untreated plants (Fig. 3.24g, i).

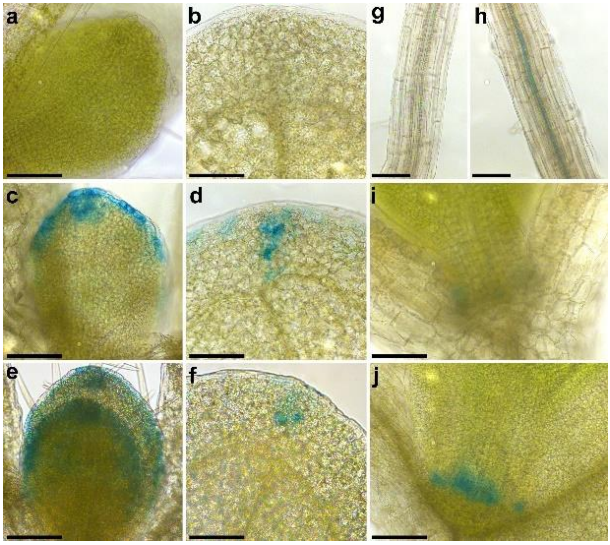

Figure 3.24 Analysis of *AtCuAOα2* and *AtCuAOα3* tissue specific expression pattern upon putrescine or spermidine treatment.**a-f** Light microscopy analysis by GUS staining of 7-day-old *AtCuAOα2*::*GFP-GUS* transgenic seedlings untreated (a, b) or treated with 500 µM Put (c, d), or with 500 µM Spd (e, f), for 3 h. The staining reaction proceeded for 2 h. **a, c, e** Shoot apex with newly formed expanding leaves showing an increase of promoter activity in the apical hydathode and leaf margins with Put (c) and Spd (e) treatment. Cotyledonary leaf apical zone showing an increase of GUS staining at the apical hydathode with Put (d) and Spd (f) treatment. **g-j** Light microscopy analysis by GUS staining of 7-day-old *AtCuAOα3-promoter::GFP-GUS* transgenic seedlings untreated (g, i) or treated with 500 µM Put for 1 h (h, j). The staining reaction proceeded for 2 h. **g** and **h** Root mature zone showing an increase of GUS staining in the vascular tissue after Put treatment (h). **i** and **j** Stipules showing an increased promoter activity after Put treatment (j). a-f, i, j, bar = 200 µm; g, h bar = 100 µm.

3.3.2 Expression profile of AtCuAOγ1 and AtCuAOγ2 under stress conditions, after treatments with hormones or PAs

The quantitative analysis of *AtCuAOγ1* and *AtCuAOγ2* expression by RT-qPCR upon treatment with IAA showed similar profiles with an initial induction (2-fold) followed by return to T0 levels or a repression (40%) at the last time point studied (24 h). Instead of the three stress-related hormones analyzed, induction effects were observed on *AtCuAOγ1* expression upon ABA and SA treatments, while repressive or no effect was observed for all the other treatments (Fig. 3.25). In particular, IAA (10 µM) induced *AtCuAOγ1* expression of approximately 2-fold from 1 to 6 h. This effect was no longer visible at the 24 h time point (Fig. 3.25 first left panel). A significant 2-fold induction of *AtCuAOγ2* expression was observed at the 3 h time point, while a repression effect was clear at the last time point studied (40%) when compared to T0 (Fig. 3.25 first right panel). After treatment with 50 µM MeJA, no significant changes in *AtCuAOγ1* expression profile occurred at each analyzed time point as compared with T0 (Fig. 3.25 second left panel), while a 40% and 50% decrease of *AtCuAOγ2* expression was revealed respectively at 1 and 3 h (Fig. 3.25 second right panel). Treatment with 100 µM ABA induced *AtCuAOγ1* expression by 2-fold after 3 h from the treatment onset (Fig. 3.25 middle left panel) while a 60 % decrease of *AtCuAOγ2* expression was detected at 24 h (Fig. 3.25 middle right panel). On the other hand, 2 mM SA-treated plants showed a 50% decrease of *AtCuAOγ1* (Fig. 3.25 third lower left panel) and *AtCuAOγ2* (Fig. 3.25 third right panel) expression respectively at 1 h of treatment in respect to T0 while only *AtCuAOγ1* was induced after 6 h of treatment (1.8-fold).

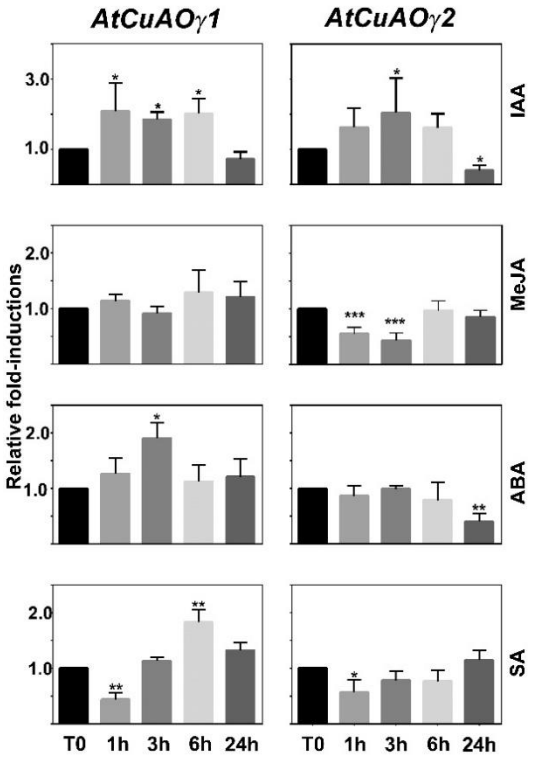

Figure 3.25 Time-course analysis of *AtCuAOγ1* and *AtCuAOγ2* gene expression by RT-qPCR upon treatment with IAA, MeJA, ABA and SA. Gene expression was analyzed in 7-day-old WT seedlings untreated or treated with 10 µM IAA, 50 µM MeJA, 100 µM ABA or 2 mM SA for 0 (T0), 1, 3, 6 and 24 h. The reported values of expression fold-inductions after treatment are relative to the corresponding expression values of non-treated plants for each time point, with the value for time zero assumed to be one. Data are the result of three biological replicates, each with three technical replicates (mean values ± SD; n =3). The significance levels between relative mRNA levels at each time point and time 0 are reported only when $P \leq 0.05$. *, **, ***, **** *P* levels ≤ 0.05, 0.01, 0.001 and 0,0001 respectively.

Considering data from RT-qPCR, a GUS staining analysis was carried out to investigate the IAA-induced tissue specific expression pattern for both *AtCuAOγ1* and *AtCuAOγ2* while the ABA- and SA-induced tissue specific expression pattern was explored only for *AtCuAOγ1* (Fig. 3.26). Consistently,

IAA-treated *AtCuAOγ1-promoter::GFP-GUS* plants displayed a stronger blue staining in the root elongation zone (Fig. 3.26a) as compared to control untreated plants (Fig. 3.26b). ABA-treated *AtCuAOγ1-promoter::GFP-GUS* plants displayed a more intense promoter driven GUS-staining in root transition/elongation zone as compared with control untreated plants (Fig. 3.26c, d). Moreover, while SA induced *AtCuAOγ1* expression in the same root zone (Fig. 3.26e, f) the tissue specific expression pattern revealed that the promoter activity detectable in the ground tissues of the root elongation zone in control untreated plants (Fig. 3.26e) spread towards the ground tissues of the root maturation zone upon SA treatment (Fig. 3.26f). IAA induced *AtCuAOγ2* expression in the columella (Fig 11h) and the stipules of young emerging leaves (Fig. 3.26j) as revealed by the presence of a more intense GUS staining in IAA-treated *AtCuAOγ2-promoter::GFP-GUS* plants when compared with control untreated plants (Fig. 3.26g, i).

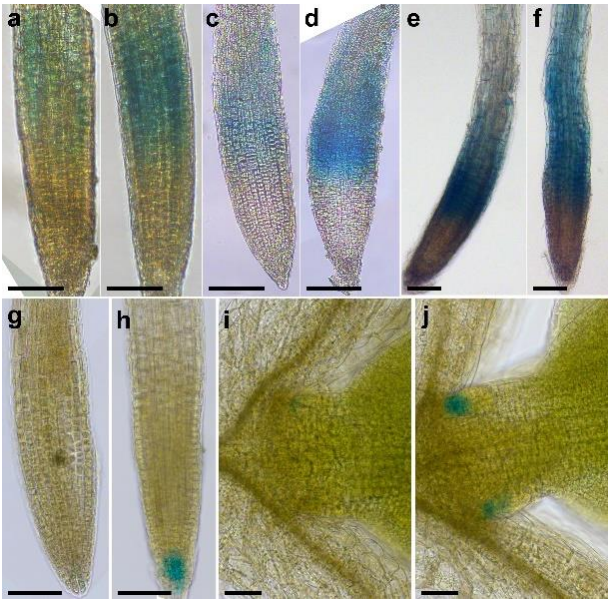

Figure 3.26 Analysis of *AtCuAOγ1* and *AtCuAOγ2* tissue specific expression pattern upon IAA, ABA and SA treatments. **a** and **b** Light microscopy analysis by GUS staining of 7-day-old *AtCuAOγ1*::*GFP-GUS* transgenic seedlings untreated (a) or treated (b) with 10 µM IAA for 3 h, showing an increase of GUS staining in the root

transition/elongation zone (b). The staining reaction was allowed to proceed for 30 min. **c** and **d** Light microscopy analysis by GUS staining of 5-day-old *AtCuAOγ1*::*GFP-GUS* transgenic seedlings untreated (c) or treated (d) with 100 µM ABA for 24 h showing an increase of GUS staining in the root transition/elongation zone (d). The staining reaction proceeded for 2 h. **e** and **f** Light microscopy analysis by GUS staining of 7-day-old *AtCuAOγ1*::*GFP-GUS* transgenic seedlings untreated (e) or treated (f) with 2 mM SA for 3 h, showing a slight increase of GUS staining towards the ground tissues of the maturation root zone (f). The staining reaction proceeded for 5 min. **g-j** Light microscopy analysis by GUS staining of 7-day-old *AtCuAOγ2*::*GFP-GUS* transgenic seedlings untreated (g, i) or treated (h, j) with 10 µM IAA for 3 h, showing an increase of GUS staining in the root cap (columella) (h) and the stipules associated with the first emerging leaves (j). The staining reaction proceeded for 2 h. a-j, bar = 100 µm.

To investigate the possible correlation between the *AtCuAOγ1* and *AtCuAOγ2* gene expression profiles after ABA and MeJA treatments with the expression profile of these genes after the abiotic stresses signaled by the same hormones, the variations of *AtCuAOγ1* and *AtCuAOγ2* gene expression profiles under dehydration and successive recovery, and upon leaf wounding were analyzed (Fig. 3.27). The applied dehydration stress caused no relevant change in expression levels for *AtCuAOγ1* (Fig. 3.27, inset in left upper panel) while it strongly repressed *AtCuAOγ2* (40% of T0; Fig. 3.27, inset in right upper panel). The effects of DR caused significant changes in the expression profiles of both genes. In the case of *AtCuAOγ1*, a peak of 2-fold was observed at T3 time point (3 h DR) followed by a gradual return to T0 levels (Fig. 3.27, left panel), while for *AtCuAOγ2*, a peak of 1.6 fold was observed at T2 that was followed by a steady reduction towards the last time point (T5, 24 h DR) at which a 50% repression was observed. Leaf wounding presented regulation profiles of both *AtCuAOγ1* and *AtCuAOγ2* where stronger inductions than in the case of dehydration and recovery stress were observed. In fact, *AtCuAOγ1* expression was induced stably from 3 to 24 h, with 2.7-, 1.7- and 2-fold increases, respectively (Fig. 3.27, lower left panel) and *AtCuAOγ2* presented induced expression at 1 and 3 h (2-fold) returning at 6 h to T0 levels (Fig. 3.27, lower right panel).

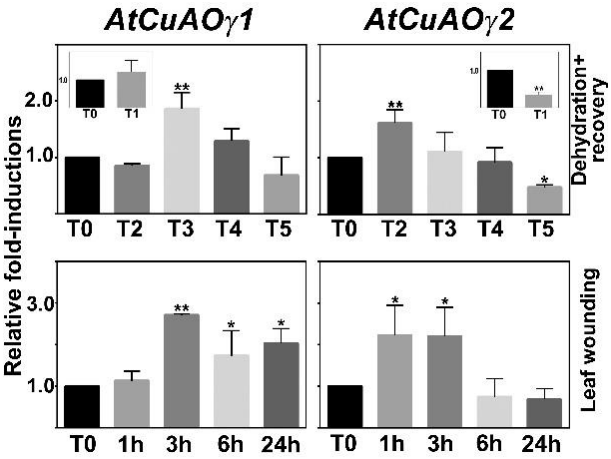

Figure 3.27 Time-course analysis of *AtCuAOγ1* and *AtCuAOγ2* gene expression by RT-qPCR upon abiotic stress treatments (dehydration and recovery and leaf wounding). Gene expression was analyzed in 7-day-old WT seedlings untreated or treated for 0h (T0), 30 min. dehydration (T1) (see inset graph) followed by 1 (T2), 3 (T3), 6 (T4) and 24 h (T5) recovery, or 0 (T0), 1, 3, 6 and 24 h after leaf wounding. The reported values of expression fold-inductions after treatment are relative to the corresponding expression values of non-treated plants for each time point, with the value for time zero assumed to be one. Data is the result of three biological replicates, each with three technical replicates (mean values ± SD; n = 3). The significance levels between relative mRNA levels at each time point and time 0 are reported only when $P \leq 0.05$. *, **, ***, **** *P* levels ≤ 0.05, 0.01, 0.001 and 0,0001 respectively.

Considering the data from RT-qPCR, the analysis of the tissue-specific expression pattern of *AtCuAOγ1* and *AtCuAOγ2* after these stress treatments, were carried out (Fig. 3.28a-l). Both DR and wounding induced *AtCuAOγ1* expression in the apex/petiole junction after 3 h (Fig. 3.28b, DR and 13c, leaf wounding) and in the root elongation zone after 6 h (Fig. 3.28e, DR) and 3 h (Fig. 3.28f, leaf wounding) when compared to the respective zones of control untreated plants (Fig. 3.28a, d). *AtCuAOγ2* expression was only induced upon wounding stress (Fig. 3.28g-l). Expression in the cotyledon apical hydathode (Fig. 3.28j), stipules of young leaves (Fig. 3.28k) and the root cap (Fig. 3.28l) was increased as compared to control untreated plants (Fig. 3.28g-i).

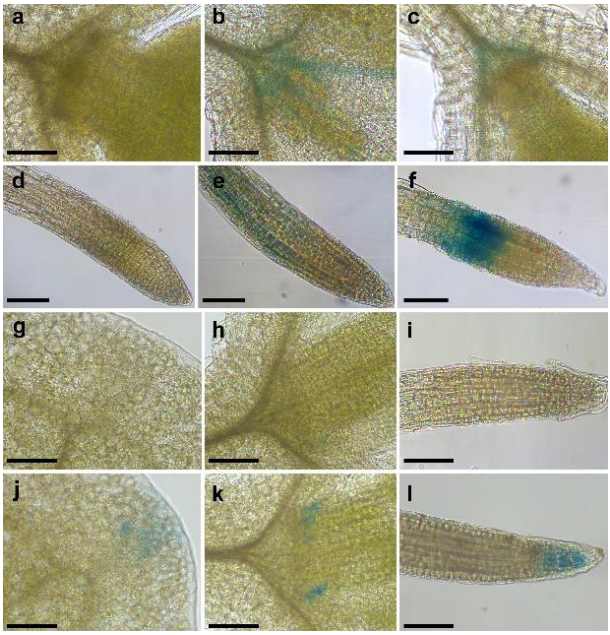

Figure 3.28 Analysis of *AtCuAOγ1* and *AtCuAOγ2* tissue specific expression pattern upon abiotic stress (cotyledonary leaf wounding and dehydration recovery) treatments. **a-f** Light microscopy analysis by GUS staining of 7-day-old *AtCuAOγ1*::*GFP-GUS* transgenic seedlings untreated (a, d), subjected to dehydration 30 min plus 3 h recovery (b) or 6 h recovery (e), or to cotyledonary leaf wounding for 3 h (c, f). The staining reaction proceeded for 2 h in both treatments. **a, b, and c** Petiole/apex junction of untreated seedlings (a), subjected to dehydration recovery (b) or to cotyledonary leaf wounding (c). **d, e, and f** Root apex of untreated (d) subjected to dehydration recovery (e) or to cotyledonary leaf wounding (f). **g-l** Light microscopy analysis by GUS staining of 7-day-old *AtCuAOγ2-promoter::GFP-GUS* transgenic seedlings untreated (g-i) or subjected to cotyledon wounding for 3 h (j-l). The staining reaction proceeded for 2 h. **g, h** and **i** Cotyledon (g), Petiole/apex junction (h) and root apex (i) of untreated seedlings. **j, k and l** Cotyledon (h), Petiole/apex junction (k) and root apex (l) subjected to cotyledon wounding. a-l, bar = 100 µm.

To verify the occurrence of a direct effect of exogenous Put and Spd on the *AtCuAOγ1* and *AtCuAOγ2* gene expression profiles, RT-qPCR analysis were carried out on plants treated with Put or Spd at the final concentration of 500 µM. These two PAs had diverse effects on the expression of these genes (Fig. 3.29). Treatment with Put induced both *AtCuAOγ1* and *AtCuAOγ2*

expression at similar levels from 1 h up to 3 h (2- to 3-fold). From this time point onward, expression of *AtCuAOγ1* was maintained at an induced level (3- and 2-fold, respectively at 6 and 24 h) compared to T0 levels (Fig. 3.29, upper left panel) while at the same time points *AtCuAOγ2* expression returned to T0 levels (Fig. 3.29, upper right panel). The Spd treatment responses presented an opposite pattern with visible repression of *AtCuAOγ1* expression at 1 and 3 h (approximately 40% and 50% of T0 respectively; Fig. 3.29, lower left panel) and no observed significant differences as compared to T0 in the case of *AtCuAOγ2* (Fig. 3.29, lower right panel).

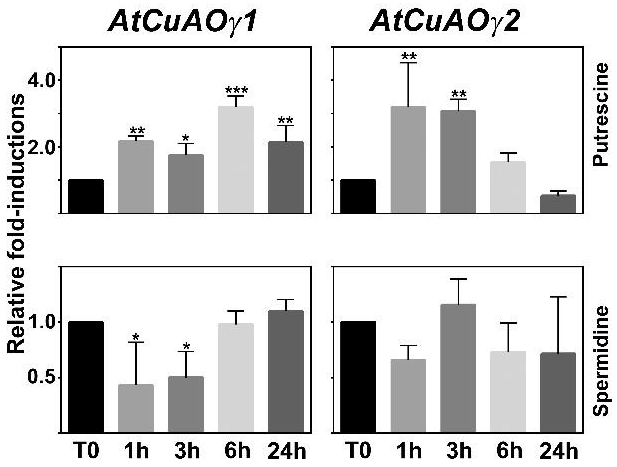

Figure 3.29 Time-course analysis of *AtCuAOγ1* and *AtCuAOγ2* gene expression by RT-qPCR upon treatment with the polyamines putrescine e spermidine. Gene expression was analyzed in 7-day-old WT seedlings untreated or treated with 500 µM putrescine or 500 µM spermidine for 0 (T0), 1, 3, 6 and 24 h. The reported values of expression fold-inductions after treatment are relative to the corresponding expression values of non-treated plants for each time point, with the value for time zero assumed to be one. Data are the result of three biological replicates, each with three technical replicates (mean values ± SD; n = 3). The significance levels between relative mRNA levels at each time point and time 0 are reported only when $P \leq 0.05$. *, **, ***, **** *P* levels ≤ 0.05, 0.01, 0.001 and 0,0001 respectively.

Considering data from RT-qPCR, the analysis of the tissue-specific expression pattern of *AtCuAOγ1* and *AtCuAOγ2* after Put treatments were carried out (Fig. 3.30). In detail, Put induced *AtCuAOγ1* expression in the stipules, hydathodes of new emerging leaves and root elongation zone (Fig.

3.30a-d), as revealed by the presence of an intense GUS staining in these tissues (Fig. 3.30b, d) in comparison to control untreated plants (Fig. 3.30a, c). Furthermore, Put induced *AtCuAOγ2* expression (Fig. 3.30e-h) in the cotyledon apical hydathodes and root columella (Fig. 3.30f, h), as shown by the tissue-specific increase of the promoter-driven GUS expression in Put-treated *AtCuAOγ2-promoter::GFP-GUS* plants as compared to control untreated plants (Fig. 3.30e, g).

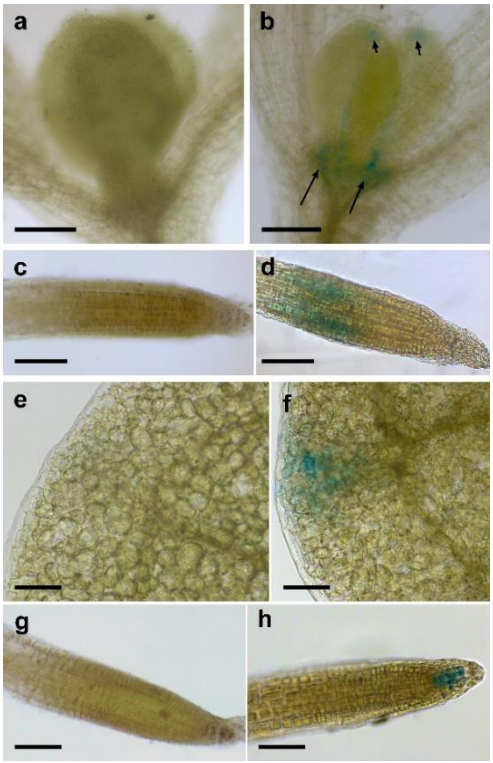

Figure 3.30 Analysis of *AtCuAOγ1* and *AtCuAOγ2* tissue specific expression pattern upon putrescine treatment. **a-d** Light microscopy analysis by GUS staining of 7-day-old *AtCuAOγ1*::*GFP-GUS* transgenic seedlings untreated (a, c) or treated (b, d) with 500 µM putrescine for 1 h showing GUS staining in the apex/petiole junction and apical hydathodes (arrows) (b) and the root transition/elongation zone (d). The staining reaction was allowed to proceed for 2 h. **e-h** Light microscopy analysis by GUS staining

of 7-day-old *AtCuAOγ2*::*GFP-GUS* transgenic seedlings untreated (e, g) or treated (f, h) with 500 µM putrescine for 3 h, showing GUS staining in the cotyledon apical hydathode (f) and in the root cap (columella) (h). The staining reaction proceeded for 2 h. a-h, bar = 100 µm.

4. DISCUSSION

In the last years, significant progress in the study of the physiological regulation and molecular features of AOs in plants allowed to have a more comprehensive picture on the biological role of these enzymes. Recent updates focused particularly on the role played by the H_2O_2 delivered by AO-mediated PA oxidation as an important signaling molecule in the life of plant cells, such as in wall structural reinforcement, HR and defense responses to pathogen attack. The research work herein presented aims to improve the knowledge about the function and regulation of different members of AtCuAO family during stress responses. For this purpose, Arabidopsis plants expressing *AtCuAO::GFP-GUS* constructs, as well as both *AtCuAOβ* and *AtCuAOδ* insertional loss-of-function mutants have been analysed.

4.1 *AtCuAOβ* plays a role in the control of stomatal closure in response to MeJA or wounding and mediate the early root protoxylem differentiation induced by wounding

Plant-pathogen interaction has been the subject of in-depth studies due to its huge economic and agricultural implication. In order for the infection to occur, pathogens must first enter the plant tissues. Fungal pathogens have the ability to directly penetrate epidermis, a feature that bacteria cannot do. Indeed, they must enter internal tissues exclusively from openings that are already present, natural, such as stomata, or accidentally created, such as wounds (Zeng *et al*., 2010). Stomata are physiological pores present in plant epidermis and have long been recognized as a major point of entry for plant pathogenic bacteria (Huang 1986). Historically, these surface openings have been considered as passive portals of entry for plant pathogenic bacteria. However, some studies have shown that stomata can play an active role in limiting bacterial invasion as part of the plant innate immune system (Melotto *et al.*, 2008). Pathogens/microbe-associated molecular patterns (PAMPs/MAMPs) together with hormonal signals, such as SA, could be involved in stomatal closure in response to pathogens attack (Zeng *et al*., 2010). In this context, H_2O_2 delivered from AO-mediated PA catabolism could play a role as an important mediator in stress-induced stomata closure. Indeed,

the production of H_2O_2 could result in an increase of intracellular Ca^{2+} concentration, which, in turn, would lead to an increase in pH and in reduction of K^+ and Cl^- content in guard cells. These changes lead, as final effect, to stomatal closure.

The data herein reported confirm a role for AtCuAOβ in wounding-/MeJA-induced stomatal closure. Indeed, results showed an increase in *AtCuAOβ* expression levels upon both leaf or root wounding and after treatment with the wound-signal-hormone MeJA, supporting the prominent role of this gene in mechanical damage responses. Moreover, histochemical assays showed that MeJA treatment, as well as cotyledonary leaf wounding and root wounding, induced *AtCuAOβ* expression in stomatal guard cells of the stressed *AtCuAOβ-promoter::GFP-GUS* plants, supporting its role in stomatal movement control. Coherently, these results indicate the involvement of H_2O_2 delivered from AtCuAOβ-mediated PA catabolism in MeJA- and wounding-induced stomatal closure. Indeed, WT MeJA-treated plants displayed a peak of closure of 65% after 1 h and likewise leaf-wounded WT plants displayed a peak of closure of 75% after 1 h in the wounded cotyledon. A similar response in the unwounded cotyledon was observed in both leaf- and root-wounded plants showing a stomatal closure respectively 65% and 75% at 1h, as compared to WT untreated/unwounded plants. Interestingly, *Atcuaoβ* loss-of-function mutants were not affected by both leaf/root wounding nor MeJA treatment, confirming the AtCuAOβ-involvement in this event. Furthermore, treatment with the H_2O_2-scavenger DMTU reversed both MeJA- or wounding-induced stomatal closure in WT plants, supporting the role of AtCuAOβ-delivered H_2O_2 in this stress-induced response. Consistently, AtCuAOβ expression was induced of 4-, 3.5- and 8- fold respectively after MeJA treatment and upon both leaf and root wounding.

As concern shorter time responses, it is interesting to underline that WT plants respond to leaf or root wounding both with a local and systemic signalling, revealing the occurrence of a systemic responses in AtCuAOβ-dependent way, as evidenced by the unresponsiveness of *Atcuaoβ* mutants to the same conditions of treatment. In detail, the effect of leaf wounding in stomatal closure was detected after 5 min in the wounded cotyledon, while after 30 min in the unwounded distal cotyledon. Even more remarkably, effects due to root-wounding were observable quite rapidly as stomata guard cells started to close after 5 min, suggesting a quick signal transmission from root to leaf. As a whole, these results support the AtCuAOβ involvement in MeJA/wounding-induced stomatal closure with a dynamic implying extremely rapid long-distance root-to-leaf communication and could allow us to

hypothesize a local and systemic action of AtCuAOβ related to water balance homeostasis regulating stomatal closure.

The involvement of AtCuAOβ in quick local and systemic stress-induced stomatal closure could be due to an early gene induction picking before 30 min and/or to a stress-induced secretion of PAs in the apoplast. Moreover, to clarify the complex mechanism occurring in the fast long-distance root to leaf communication, leading to AtCuAOβ dependent stomatal closure, further analyses need to be carried out on the potential interaction between this gene and other key components of the long-distance signaling pathway, such as GLRs (see below).

Leaf-to-root long-distance communication is crucial in coordinating biochemical and physiological events between aerial and underground organs, especially in response to changes in environmental conditions (Huber and Bauerle 2016; Katz and Chamovitz 2017; Chen *et al*., 2018; Hilleary and Gilroy 2018). Moreover, leaf damage is a frequent injury during plant lifespan, which may be caused by both herbivores, such as chewing insects, or weather conditions. As previously indicated, the wound site is an easy way for both pathogen entry and water loss and the presence of a leaf mechanical damage triggers several local responses devoted to wound healing (Angelini *et al*., 2008; Cona *et al*., 2014; Savatin *et al*., 2014; Heyman *et al*., 2018). Furthermore, complex signaling networks propagate information from the wound site through the whole plant body allowing systemic responses (Hilleary *et al*., 2018) among which xylem root remodeling could represent a strategy to enhance water uptake and counteract the excessive water loss caused by the wound.

In this regard, analyses herein reported on root growth, protoxylem position and meristem size in cotyledonary leaf-wounded WT plants, show a DMTU-reversible early root-protoxylem differentiation occurring 3 days after the injury, with no observable changes in meristem size and root growth. A root-protoxylem specific accumulation of H_2O_2 was detectable 6 h after the injury, supporting its involvement in the variation of protoxylem position. This response is consistent with previous data where roots of MeJA-treated plants, showed a H_2O_2-dependent remodeling of the protoxylem that appeared to be closer to the root tip independently from root growth or meristem size (Ghuge *et al*., 2015b). The effects of MeJA treatment on protoxylem differentiation led to hypothesize that, under stress conditions, an extracellular H_2O_2 production may drive early xylem differentiation independently from the auxin/cytokinin/T-Spm loop (Ghuge *et al*., 2015a). In particular, in differentiating protoxylem precursors the H_2O_2 production driven by cell wall-

localized oxidation of PAs was suggested to be involved in both PCD and peroxidase-mediated lignin polymerization (Tisi *et al.*, 2011b; Ghuge *et al*., 2015a; Ghuge *et al*., 2015b), which represent key steps in the terminal phase of the xylem differentiation process. Considering the involvement of H_2O_2 delivered from AO-mediated PA oxidation, among the cell-wall sources of ROS, in wound healing responses (Angelini *et al*., 2008; Tavladoraki *et al*., 2016) and in root xylem differentiation (Cona *et al*., 2014), together with the strong induction of *AtCuAOβ* expression in the vascular tissues at the transition, elongation and maturation root zone in leaf wounded *AtCuAOβ-promoter::GFP-GUS* plants (here reported), led us to hypothesize a role of AtCuAOβ in the early root protoxylem differentiation which occurs after leaf wounding, providing a link via systemic signaling between a abiotic stress such as leaf wounding and a distal root phenotypic plasticity such as variation in protoxylem position. In this regard, data reported herein reveals that leaf wounding results in early protoxylem differentiation in Arabidopsis WT seedlings, without affecting it in *Atcuaoβ* mutants. These data, together with the reversion effect exerted by DMTU on wounding-induced early protoxylem differentiation in WT roots, and the increased accumulation of H_2O_2 after the leaf injury at the site of protoxylem position, support the hypothesis that wounding effect on protoxylem differentiation could be mediated by the H_2O_2 produced via AtCuAOβ -driven Put oxidation. This possibility is consistent with the previously suggested hypothesis in which both apoplastic AO levels and PA secretion in the cell wall increase under stress growth conditions, with a consequent decrease of the PA/H_2O_2 ratio and the activation of defence responses (Moschou *et al*., 2008; Tisi *et al*., 2011). Interestingly, treatment with DMTU alone did not affect xylem differentiation in both WT and *Atcuaoβ* mutants. Taking together, these results confirm the involvement of AtCuAOβ in xylem differentiation which occurs under stress conditions, such as wounding.

PAs are well known to affect root development and xylem differentiation (Couée *et al*., 2004; Vera-Sirera *et al*., 2010). In particular, H_2O_2-derived from CuAO- or PAO-mediated PA oxidation has been revealed to be involved in the Put/Spd-induced root early xylem differentiation respectively in Arabidopsis and maize (Tisi *et al*., 2011b; Ghuge *et al*., 2015b). However, data herein reported revealed that Put and wounding didn't show a synergic effect as exogenous Put supply to leaf-wounded plants didn't result in earlier protoxylem differentiation as compared to leaf wounded or Put-treated plants. These results confirm the occurrence of a specific role of AtCuAOβ-mediated Put oxidation in root protoxylem differentiation.

Considering that wound stress, such as tip removal and leaf wounding (de Agazio *et al*., 1992; this work), or stress-simulating conditions, such as exogenous PA or MeJA treatments (Tisi *et al*., 2011b; Ghuge *et al*., 2015b), result in early root protoxylem differentiation, the hypothesis that PAs may behave as a stress signalling compounds during root vascular differentiation can be considered plausible.

As a whole, the expression of *AtCuAOβ* in tissues or cell types regulating water supply and water loss such as xylem and stomata guard cells, with its role in protoxylem differentiation and in wound-induced stomatal closure suggest a role in water balance homeostasis by modulating coordinated adjustments in anatomical and functional features of xylem tissue and guard cells aperture levels in wounded plants.

4.2 GLRs are involved in wound-induced distal communication leading to stomatal closure

With the aim to unravel the signalling pathway leading to fast root-to-shoot long distance communication, stomatal closure in both leaf- and root-wounded *glr3.3* insertional mutants was investigated. Analysis of stomatal closure in *glr3.3* mutants showed similar behaviour as compared to WT plants upon local injury, and a partial overlapping stomatal behaviour with respect to *Atcuaoβ* mutants upon root or distal leaf wounding. Indeed, in wounded leaf stomata close at the same extent of WT plants, while in unwounded leaf *glr3.3* mutants showed a much reduced closure extent, of around 15%, upon distal-leaf wounding or root wounding after each time analyzed compared to both WT and mutant unwounded plants. Overall, analysis of WT, *Atucaoβ* and *glr3.3* mutants suggest that AtCuAOβ may be a component of different signalling pathway in local and distal responses, likely involving MeJA and/or other unknown components in local and systemic responses, and GLR as a component of long distance communication leading to stomatal closure upon root or distal leaf wounding.

4.3 *AtCuAOδ* plays a role in the control of stomatal closure in response to ABA

Data herein reported show that *AtCuAOδ* is regulated by ABA, consistently with the ABA regulated recognition sites identified in its promoter region. In this regard, it is known that ABA, the water-deficit hormonal signal, is involved in defence responses against abiotic stresses, such as drought

and/or high soil saline levels (Davies and Zhang 1991; Tardieu and Davies 1992). In line with this, several results have suggested that the ABA-responsive AOs (An *et al.*, 2008; Qu *et al.*, 2014) are likely involved in salt stress responses (Yang *et al*., 2016) and in water balance regulation (Ghuge *et al.*, 2015a). Another important role of this phytohormone is regulating stomatal movement in response to variations in water potential (Gémes *et al*., 2016; Brodribb *et al*., 2017). Concerning this, our results demonstrate that alterations in *AtCuAOδ* expression levels by reverse genetics approaches, or inhibition of AtCuAO enzyme activity by pharmacological treatments with the two known CuAO activity inhibitors, 2-BrEtA or AG (Biegański *et al*., 1982; Medda *et al*., 1997; Todaka *et al*., 2017), caused alterations of the hormonal control of guard cells responses. In fact, a complete to partial unresponsiveness to ABA in stomatal closure was observed in *Atcuaoδ* mutants, compared to WT, and the lack of ABA responsiveness in WT in combination treatments involving the two inhibitors. It must be pointed out that this effect was also evident in the case of AG, even if this inhibitor caused by itself a similar stomatal closure effect on all the three studied genotypes. This unspecific effect could be attributed to AG-induced alterations of the plasma membrane potential (Padiglia *et al*., 1998) which could influence stomatal movements.

Noteworthy, vacuoles have an important role in the regulation of stomatal pore aperture associated with different environmental or hormonal factors signalling water stress (Peiter *et al*., 2005; Andrés *et al*., 2014; Murata *et al*., 2015). Moreover, ROS can regulate several channel activities located in the tonoplast, which influence ion fluxes, cytosolic pH and the uptake/release of calcium (Carter *et al*., 2004), all of which are involved in modulation of stomatal aperture. It is thus not surprising that a vacuolar AtCuAO protein can influence stomatal closure as an element in the ABA transduction pathway regulating this phenomenon. No clear contribution of vacuoles in guard cells to ROS signalling network has been identified (Song *et al*., 2014). Nevertheless, reports in the literature indicate that vacuoles can be sites of H_2O_2 production (Pradedova *et al*., 2013; Leshem *et al*., 2010; Wang *et al*., 2015). Thus, our data might represent a first indication that ROS such as H_2O_2 produced by a vacuolar AtCuAO may have a causal role in ABA regulation of stomatal movement.

The complexity of the ABA signal transduction in guard cells is also highlighted by evidence showing that multiple pathways involving several components and compartments are required in the control of stomatal movements in Arabidopsis. In this context, plasma membrane-located NADPH oxidases, regulated by the ABA-induced phospholipase D (PLDα1;

Qu *et al*., 2014) and ABA-activated OST1 (Kwak *et al*., 2003), peroxisomal AtCuAOζ (Qu *et al*., 2014) and possibily vacuolar AtCuAOδ represent multiple ROS sources. These different ROS sources are active in different cellular compartments, targeted by ABA, and necessary for this response, suggesting that a strongly coordinated network is needed for the hormonal control of stomatal closure. Indeed, coordination of ROS signalling from different organelles has been reported for ABA-induced stomatal closure (Sirichandra *et al*., 2009). Furthermore, some evidence shows that ABA presents an apparently minor ROS-independent effect on stomatal closure as its effects could not be entirely counter-balanced by either ROS scavengers or ROS-biosynthesis inhibitors. This data revealed that another player is necessary in ABA-mediated regulation of stomatal closure and points out the necessity to understand the hierarchy of action or eventual synergy of actors involved.

4.4 *AtCuAOα2/α3* and *AtCuAOγ1/γ2*: possible relevance in development and water balance

AOs have been involved in growth and developmental processes in several plant species. In this regard, previously performed GUS analysis (Ghuge 2014; Carucci 2017) revealed gene expression in the epidermis and hydathodes of cotyledon and young leaf (*AtCuAOα2*), in root vascular tissues (*AtCuAOα3*), in the root cortex at the division/elongation transition zone (*AtCuAOγ1*) as well as in cotyledon margins and columella cells (*AtCuAOγ2*) (Table 4.1). It is worth mentioning that analysis of *AtCuAOα2, α3, γ1 and γ2* expression pattern reveals overlapping profiles both to each other and in relation to the tissue distribution pattern of free-auxin production sites (Aloni *et al*., 2003; Jacobs and Roe, 2005). This evidence supports a role for CuAO in tissue maturation events and xylem differentiation, by H_2O_2 production and PA homeostasis and transport regulation, consequent to the modulation of *AtCuAO* gene expression. Indeed, the positive regulation of CuAO expression by Put with respect to genes under study (Table 4.1) may represent the necessity of a fine PA homeostasis and/or a mechanism for H_2O_2 production. Specifically, apoplastic AOs have been implicated in the cell wall maturation during developmental-regulated or light-induced tissue differentiation in tobacco as well as in species belonging to Fabaceae and Poaceae (Cona *et al.*, 2006; Kärkönen and Kuchitsu, 2015; Tavladoraki *et al*., 2016). In these processes, H_2O_2 derived from AO-mediated PA-oxidation behaves as a co-substrate in the peroxidase-mediated cross-linking of cell wall polymers and/or

lignin/suberin biosynthesis (Angelini *et al*., 2010). On the other hand, since the simultaneous production of H_2O_2 and superoxide anion (O_2^-) leads to the enzymatic or chemical formation of the wall-loosening agent hydroxyl radical (·OH), the H_2O_2 derived from AO-mediated PA oxidation could thus participate in the ROS-mediated cell-wall expansion (Gupta *et al*. 2016; Schmidt *et al*., 2016). ROS have also been involved in meristem size specification by controlling the transition between cell proliferation and differentiation, with H_2O_2 and $O_2^{-}\cdot$ respectively promoting cell differentiation and cell division (Tsukagoshi *et al*., 2010). Interestingly, results herein reported show that the cell-wall resident AtCuAOγ2 is specifically expressed in columella cells and is positively regulated by IAA, suggesting a possible link with gravitropic response through an AO-mediated H_2O_2-dependent negative regulatory loop (Su *et al.*, 2017; Zhou *et al.*, 2018). Moreover, *AtCuAOγ1*, encoding an apoplastic CuAO, is positively regulated by IAA in fast expanding tissues of root elongation zone, the encoded enzyme possibly contributing to H_2O_2 biosynthesis needed for wall expansion. As concerning peroxisomal AtCuAOα members, the vascular IAA-induced *AtCuAOα3* is likely involved in IAA-induced root xylem differentiation, although this latter phenomenon may be further regulated by T-Spm and its metabolism by other AOs (Yoshimoto *et al.*, 2016; Alabdallah *et al.*, 2017).

The expression pattern of *AtCuAOα2*, *α3*, *γ1* and *γ2* revealed by GUS staining shows an association with tissues and cells involved in water supply and water loss such as vascular tissues and hydathodes (Ghuge 2014; Carucci 2017). In this regard, the occurrence of AOs in tissues involved in water balance homeostasis has been revealed in several plant species. In detail, some AO members have been shown to be expressed in vascular tissues of Fabacee, Poacee and tobacco (Paschalidis *et al.*, 2005; Ghuge *et al*., 2015c), in stomata of fava bean (An *et al*., 2008; Qu *et al*., 2014), and in both stomata and vascular tissues of Arabidopsis (Kim *et al.*, 2014; Qu *et al.*, 2014; Ghuge *et al.*, 2015a; Ghuge *et al.*, 2015b; Ghuge *et al.*, 2015c; Alabdallah *et al*., 2017) and grapevine (Paschalidis *et al*., 2010). The expression of *AtCuAOα2/α3* and *AtCuAOγ1/γ2* in both stomata-related hydathode pores and vascular tissues, as well as their regulation by DR stress (Table 4.1) is therefore congruent with the previously reported localization of AOs in tissues and cells involved in water transport, further supporting the hypothesis of their role in water balance regulation.

It has been shown that both apoplastic and peroxisomal AOs contribute to the ABA-induced ROS biosynthesis leading to stomatal closure possibly in cooperation with NADPH oxidases (An *et al*., 2008; Paschalidis *et*

al., 2010; Wimalasekera *et at*., 2011; Qu *et al*., 2014). Furthermore, apoplastic AOs have been involved in early xylem differentiation especially under stress-like conditions, such as those signaled by MeJA treatment (Ghuge *et al*., 2015a; Ghuge *et al*., 2015b) or simulated by treatment with exogenous PAs, AO over-expression (Tisi *et al*., 2011a; Tisi *et al*., 2011b) or a compromised status of cell-wall pectin integrity (Cona *et al*., 2014). Thus, the ROS signature occurring during specific developmental events or in response to biotic/abiotic stress conditions is generated by a complex interplay among AOs with different subcellular localization and possibly NADPH oxidases (Gupta *et al*., 2016). On this basis, it is reasonable to hypothesize that the peroxisomal AtCuAOα3 may cooperate with the apoplastic AtCuAOβ, both positively regulated by MeJA, in a potentially MeJA-signaled maturation of root metaxylem vessels. Therefore, the occurrence of CuAOs with different subcellular localization, tissue specific expression and hormone responsiveness, such as AtCuAOα3 in vascular bundles, the apoplastic ABA- and SA-induced AtCuAOγ1 in vascular tissues of new emerging leaves and the apoplastic AtCuAOγ2 in vascular bundles of cotyledons (Table 4.1), may contribute to developmentally-regulated or stress-induced xylem tissue maturation in these organs. Furthermore, the expression of AtCuAOα2, AtCuAOγ1 and AtCuAOγ2 in hydathodes, which are structures evolutionarily related to stomata and represent sites of high free-auxin levels driving xylem differentiation (Aloni *et al*., 2003), along with the evidence that *AtCuAOα2* and *AtCuAOα3* expression is induced by the wound- associated signal MeJA (Table 4.1), allow to hypothesize that the encoded CuAOs may have a role in xylem differentiation during the auxin-driven xylem regeneration around a wound (Aloni, 2001). Moreover, it is interesting to note that *AtCuAOγ1/γ2* are positively regulated by wounding but insensitive to MeJA suggesting the involvement of these genes in the MeJA-independent wounding-response pathway (Titarenko *et al*., 1997; León *et al*., 1998).

GENE:	SUBCELLULAR LOCALIZAION:	TISSUES SPECIFIC EXPRESSION:	INDUCED BY: Hormones|Ab.stress| PAs		
AtCuAOα2	Peroxisomal	- external border of cotyledon and newly expanding leaf - apical hydathode	IAA MeJA	Water stress Wounding	Spd
AtCuAOα3	Peroxisomal	- stipules - vascular tissues	IAA MeJA	Water stress Wounding	Put
AtCuAOγ1	Apoplastic	- root transition/elongation zone - hydathodes	IAA ABA SA	Water stress Wounding	Put
AtCuAOγ2	Apoplastic	- root cap (columella) - stipules associated with the first emerging leaves	IAA	Water stress Wounding	Put

Table 4.1 Summary table of subcellular localization, tissue-specific expression and inductions (by hormones, abiotic stress and polyamines) of the four genes of the α and γ subbranch families analyzed.

5. REFERENCES

Alabdallah O., Ahou A., Mancuso N., Pompili V., Macone A., Pashkoulov D., Stano P., Cona A., Angelini R., Tavladoraki P. (**2017**). The *Arabidopsis* polyamine oxidase/dehydrogenase 5 integrates cytokinin and auxin signaling to control xylem differentiation. *J. Exp. Bot.* 68:997-1012.

Alcázar R., Altabella T., Marco F., Bortolotti C., Reymond M., Koncz C., Carrasco P., Tiburcio A.F. (**2010**). Polyamines: molecules with regulatory functions in plant abiotic stress tolerance. *Planta.* 231:1237–1249.

Aloni R. (**2001**). Foliar and axial aspects of vascular differentiation: hypotheses and evidence. *J Plant Growth Regul.* 20:22–34.

Aloni R., Schwalm K., Langhans M., Ullrich C.I. (**2003**) Gradual shifts in sites of free-auxin production during leaf-primordium development and their role in vascular differentiation and leaf morphogenesis in Arabidopsis. Planta 216:841–53.

An Z., Jing W., Liu Y., Zhang W. (**2008**). Hydrogen peroxide generated by copper amine oxidase is involved in abscisic acid-induced stomatal closure in Vicia faba. *J Exp Bot.* 59:815–25.

Andrés Z., Pérez-Hormaeche J., Leidi E.O., Schlückingb K., Steinhorstb L., McLachlanc D.H., Schumacherd K., Hetheringtonc A.M., Kudlab J., Cuberoa B., Pardo J.M. (**2014**). Control of vacuolar dynamics and regulation of stomatal aperture by tonoplast potassium uptake. *Proc. Natl. Acad. Sci. U S A.* 111:E1806-14.

Angelini R., Cona A., Federico R., Fincato P., Tavladoraki P., Tisi A. (**2010**). Plant amine oxidases "on the move": An update. *Plant Physiol Biochem*. 48:560–4.

Angelini R., Tisi A., Rea G., Chen M.M., Botta M., Federico R., Cona A. (**2008**). Involvement of polyamine oxidase in wound healing. *Plant Physiol.* 146:162-177.

Apel K. and Hirt H. (**2004**). Reactive oxygen species: metabolism, oxidative stress, and signal transduction. Annu. *Rev. Plant Biol.* 55:373–399.

Ashtamker C., Kiss V., Sagi M., Davydov O., Fluhr R. (**2007**). Diverse subcellular locations of cryptogein-induced reactive oxygen species production in tobacco Bright Yellow-2 cells. *Plant Physiol*., 143:1817–1826.

Baima S., Forte V., Possenti M., Peñalosa A., Leoni G., Salvi S., Felici B., Ruberti, I., Morell, G. (**2014**). Negative feedback regulation of auxin signaling by ATHB8/ACL5 BUD2 transcription module. *Mol. Plant.* 7:1006–1025.

Bak G., Lee E.J., Lee Y., Kato M., Segami S., Sze H., Maeshima M., Hwang J.U., Lee Y. (**2013**). Rapid structural changes and acidification of guard cell vacuoles during stomatal closure require phosphatidylinositol 3,5-bisphosphate. *Plant Cell* 25:2202–2216.

Biegański T., Osińska Z., Maśliński C. (**1982**). Inhibition of plant and mammalian diamine oxidases by hydrazine and guanidine compounds. *Int J Biochem.* 14:949-53.

Brodribb T.J., McAdam S.A.M. (**2017**) Evolution of the stomatal regulation of plant water content. *Plant Physiol*. 174:639-649.

Cai G., Sobieszczuk-Nowicka E., Aloisi I., Fattorini L., Serafini-Fracassini D., Del Duca S. (**2015**). Polyamines are common players in different facets of plant programmed cell death. *Amino Acids* 47:27–44.

Carter C., Pan S., Zouhar J., Avila E.L., Girke T., Raikhel N.V. (**2004**). The vegetative vacuole proteome of Arabidopsis thaliana reveals predicted and unexpected proteins. *Plant Cell*. 16:32853303.

Carucci A. (**2017**). Members of Arabidopsis CuAO gene family exhibit different tissue-specific expression patterns during development and distinct responses to hormone or stress treatments. PhD thesis.

Casamitjana-Martínez E., Hofhuis H.F., Xu J., Liu C.M., Heidstra R., Scheres B. (**2003**). Root-specific CLE19 overexpression and the sol1/2 suppressors implicate a CLV-like pathway in the control of Arabidopsis root meristem maintenance. *Curr Biol*, 13:1435–1441.

Chen L., Wang G., Chen P., Zhu H., Wang S., Ding Y. (**2018**). Shoot-Root Communication Plays a Key Role in Physiological Alterations of Rice (Oryza sativa) Under Iron Deficiency. *Front Plant Sci* 9:757.

Chen Q., Sun J., Zhai Q., Zhou W., Qi L., Xu L., Wang B., Chen R., Jiang H., Qi J., Li X., Palme K., Li C. (**2011**). The basic helix-loop-helix transcription factor MYC2 directly represses PLETHORA expression during jasmonate-mediated modulation of the root stem cell niche in Arabidopsis. *Plant Cell* 23:3335–3352.

Cona A., Rea G., Angelini R., Federico R., Tavladoraki P. (**2006**). Functions of amine oxidases in plant development and defense. *Trends Plant Sci.* 11:80-88.

Cona A., Tisi A., Ghuge S.A., Franchi S., De Lorenzo G., Angelini R. (**2014**). Wound healing response and xylem differentiation in tobacco plants over-expressing a fungal endopolygalacturonase is mediated by copper amine oxidase activity. *Plant Physiol. Biochem.* 82:54–65.

Couée I., Hummel I., Sulmon C., Gouesbet G., Amrani A.E.I. (**2004**). Involvement of polyamines in root development. *Plant Cell Tissue Organ Cult* 76:1–10.

Cui X., Ge C., Wang R., Wang H., Chen W., Fu Z., Jiang X., Li J., Wang Y. (**2010**). The BUD2 mutation affects plant architecture through altering cytokinin and auxin responses in Arabidopsis. *Cell Res.* 20:576-586.

Davies W. and **Zhang J.** (**1991**). Root signals and the regulation of growth and development of plants in drying soil. *Annu. Rev. Plant Physiol. Plant Mol. Biol.* 42:55-76.

de Agazio M., Federico R., Angelini R., De Cesare F., Grego S. (**1992**). Spermidine pretreatment or root tip removal in maize seedlings: effects on K+ uptake and tissue modifications. *J Plant Physiol* 140:741–746.

Dello Ioio R., Nakamura K., Moubayidin L., Perilli S., Taniguchi M., Morita M.T., Aoyama T., Costantino P., Sabatini S. (**2008**). A genetic framework for the control of cell division and differentiation in the root meristem. *Science*, 322:1380–1384.

Fraudentali I., Ghuge S.A., Carucci A., Tavladoraki P., Angelini R., Cona A., Rodrigues-Pousada R.A. (**2019**). The copper amine oxidase AtCuAOδ participates in abscisic acid-induced stomatal closure in Arabidopsis. *Plants* 8: E183, doi: 10.3390/plants8060183.

Fraudentali I., Rodrigues-Pousada R.A., Volpini A., Tavladoraki P., Angelini R., Cona A. (**2018**). Stress-Triggered Long-Distance Communication Leads to Phenotypic Plasticity: The Case of the Early Root Protoxylem Maturation Induced by Leaf Wounding in Arabidopsis. *Plants* 7: E107. doi: 10.3390/plants7040107.

Fukao Y., Hayashi M., Hara-Nishimura I., Nishimura M. (**2003**). Novel glyoxysomal protein kinase, GPK1, identified by proteomic analysis of glyoxysomes in etiolated cotyledons of Arabidopsis thaliana. *Plant Cell Physiol* 44:1002-12.

Gémes K., KimY.J., Park K.Y., Moschou P.N., Andronis E., Valassaki C., Roussis A., Roubelakis-Angelakis K.A. (**2016**). An NADPH-Oxidase/Polyamine Oxidase Feedback Loop Controls Oxidative Burst Under Salinity. *Plant Physiol*. 172:1418–1431.

Ghuge S.A. (**2014**). Plant Amine Oxidases in development and stress responses. PhD thesis.

Ghuge S.A., Carucci A., Rodrigues Pousada R.A., Tisi A., Franchi S., Tavladoraki P., Angelini R., Cona A. (**2015b**). The apoplastic copper AMINE OXIDASE1 mediates jasmonic acid-induced protoxylem differentiation in Arabidopsis roots. *Plant Physiol.* 168:690–707.

Ghuge S.A., Carucci A., Rodrigues-Pousada R.A., Tisi A., Franchi S., Tavladoraki P., Angelini R., Cona A. (**2015c**). The MeJA-inducible copper amine oxidase AtAO1 is expressed in xylem tissue and guard cells. *Plant Signal Behav.* 10:1073872.

Ghuge S.A., Tisi A., Carucci A., Rodrigues-Pousada R.A., Franchi S., Tavladoraki P., Angelini R., Cona A. (**2015a**). Cell Wall Amine Oxidases: New Players in Root Xylem Differentiation under Stress Conditions. *Plants* 4:489-504.

Gupta K., Sengupta A., Chakraborty M., Gupta B. (**2016**). Hydrogen Peroxide and Polyamines Act as Double Edged Swords in Plant Abiotic Stress Responses. *Front Plant Sci.* 7:1343.

Groβ F., Rudolf E.E., Thiele B., Durner J., Astier J. (**2017**). Copper amine oxidase 8 regulates arginine-dependent nitric oxide production in Arabidopsis thaliana. *J Exp Bot.* 68:2149-62.

Hanzawa Y., Takahashi T., Michael A. J., Burtin D., Long D., Pineiro M., Coupland G., Komeda Y. (**2000**). ACAULIS5, an Arabidopsis gene required for stem elongation, encodes a spermine synthase. *EMBO J*. 19:4248–4256.

Heyman J., Canher B., Bisht A., Christiaens F., De Veylder L. (**2018**). Emerging role of the plant ERF transcription factors in coordinating wound defense responses and repair. *J Cell Sci*. 29: 131(2).

Hilleary R. and Gilroy S. (**2018**). Systemic signaling in response to wounding and pathogens. *Curr Opin Plant Biol.* 43:57-62.

Hou Z.H., Liu G.H., Wang L.X., Liu X. (**2013**). Regulatory function of polyamine oxidase-generated hydrogen peroxide in ethylene-induced stomatal closure in Arabidopsis thaliana. *J. Integr. Agricult.* 12:251–262.

Huang J.S. (**1986**). Ultrastructure of bacterial penetration in plants. *Ann. Rev. Phytopathol.* 24:141157.

Huber A.E. and Bauerle T.L. (**2016**). Long-distance plant signaling pathways in response to multiple stressors: the gap in knowledge. *J Exp Bot.* 67:2063-2079.

Imai A., Matsuyama T., Hanzawa Y., Akiyama T., Tamaoki M., Saji H., Shirano Y., Kato T., Hayashi H., Shibata D., Tabata S., Komeda Y., Takahashi T. (**2004**) Spermidine synthase genes are essential for survival of Arabidopsis. *Plant Physiol*. 135:1565–1573.

Jacobs J. and Roe J.L. (**2005**). SKS6, a multicopper oxidase-like gene, participates in cotyledon vascular patterning during Arabidopsis thaliana development. *Planta* 222:652–66.

Jefferson R.A. (**1987**). Assaying chimeric genes in plants: the GUS gene fusion system. *Plant Mol Biol. Rep*. 5:387–405.

Jiménez-Bremont J.F., Marina M., Guerrero-González Mde L., Rossi F. R., Sánchez-Rangel D., Rodríguez-Kessler M., Ruiz O.A., Gárriz A. (**2014**). Physiological and molecular implications of plant polyamine metabolism during biotic interactions. *Front Plant Sci*. 5:95.

Jung C., Seo J.S., Han S.W., Koo Y.J., Kim C.H., Song S.I., Nahm B.H., Choi Y.D., Cheong J.J. (**2008**). Overexpression of AtMYB44 enhances stomatal closure to confer abiotic stress tolerance in transgenic *Arabidopsis*. *Plant Physiol*. 146:623-635.

Kärkönen A. and Kuchitsu K. (**2015**). Reactive oxygen species in cell wall metabolism and development in plants. *Phytochemistry*. 112:22-32.

Katz E. and Chamovitz D.A. (**2017**). Wounding of Arabidopsis leaves induces indole-3-carbinol-dependent autophagy in roots of Arabidopsis thaliana. *Plant J* 91:779-787.

Kim D.W., Watanabe K., Murayama C., Izawa S., Niitsu M., Michael A.J., Berberich T., Kusano T. (**2014**). Polyamine Oxidase5 Regulates *Arabidopsis* Growth through Thermospermine Oxidase Activity. *Plant Physiol*. 165:1575-1590.

Kollist H., Nuhkat M., Roelfsema M.R. (**2014**). Closing gaps: linking elements that control stomatal movement. *NewPhytol*. 203:44–62.

Kwak J.M., Mori I.C., Pei Z.M., Leonhardt N., Torres M.A., Dangl J.L., Bloom R.E., Bodde S., Jones J.D.G., Schroeder J.I. (**2003**). NADPH oxidase AtrbohD and AtrbohF genes function in ROS-dependent ABA signaling in Arabidopsis. *EMBO J.* 22:2623–2633.

León J., Rojo E., Titarenko E., Sánchez-Serrano J.J. (**1998**). Jasmonic acid-dependent and -independent wound signal transduction pathways are differentially regulated by Ca2+/calmodulin in Arabidopsis thaliana. *Mol Gen Genet*. 258:412-9.

Leshem Y., Golani Y., Kaye Y., Levine A. (**2010**). Reduced expression of the v-SNAREs AtVAMP71/AtVAMP7C gene family in Arabidopsisreduces drought tolerance by suppression of abscisic acid-dependent stomatal closure. *J. Exp. Bot.* 61:2615–2622.

Liu J.H., Kitashiba H., Wang J., Ban Y., Moriguchi T. (**2007**). Polyamines and their ability to provide environmental stress tolerance to plants. *Plant Biotechnol*. 24:117-126.

Livak K.J. and Schmittgen T.D. (**2001**). Analysis of relative gene expression data using real-time quantitative PCR and the 2 (Delta Delta C(T)) Method. *Methods*. 25:402–408.

Mähönen A.P., ten Tusscher K., Siligato R., Smetana O., Díaz-Triviño S., Salojärvi J., Wachsman G., Prasad K., Heidstra R., Scheres B. (**2014**). PLETHORA gradient formation mechanism separates auxin responses. *Nature* 515:125–129.

Marco F., Bitrián M., Carrasco P., Alcázar R., Tiburcio A.F. Polyamine Biosynthesis Engineering as a Tool to Improve Plant Resistance to Abiotic Stress. (**2015**). In: Jaiwal PK *et al*. (eds.), Genetic Manipulation in Plants for Mitigation of Climate Change. *Springer*.

Medda R., Belelli A., Pec P., Federico R., Cona A., Floris G (**2009**). Copper amine oxidase from plants. In: Mondovi B., Floris G. (eds). Copper Amine Oxidase: Structures, Catalitics Mechanisms and Role in Pathology. *CRC Press*.

Medda R., Padiglia A., Pedersen J.Z., Agro A.F., Rotilio G., Floris G. (**1997**). Inhibition of Copper Amine Oxidase by Haloamines: A Killer Product Mechanism. *Biochemistry* 36:2595-2602.

Melotto M., Underwood W., He S.Y. (**2008**). Role of stomata in plant innate immunity and foliar bacterial diseases. *Annu Rev Phytopathol*. 46:101-122.

Minocha R., Majumdar R, Minocha SC. (**2014**). Polyamines and abiotic stress in plants: a complex relationship. *Front Plant Sci*. 5:175.

Mittler R. and Blumwald E. (**2015**). The Roles of ROS and ABA in Systemic Acquired Acclimation. *The Plant Cell* 27:64-70.

Mittler R., Vanderauwera S., Gollery M., Van Breusegem F. (**2004**). Reactive oxygen gene networks of plants. *Trends Plant Sci*. 9:490–498.

Møller S.G. and McPherson M.J. (**1998**). Developmental expression and biochemical analysis of the Arabidopsis atao1 gene encoding an H_2O_2-generating diamine oxidase. *The Plant J.* 13:781–91.

Møller S.G., Urwin P.E., Atkinson H.J., McPherson M.J. (**1998**). Nematode induced expression of atao1, a gene encoding an extracellular diamine oxidase associated with developing vascular tissue. *Physiol. Mol. Plant Pathol.* 53:73–79.

Moschou P.N., Sarris P.F., Skandalis N., Andriopoulou A.H., Paschalidis K.A., Panopoulos N.J., Roubelakis-Angelakis K.A. (**2009**). Engineered polyamine catabolism preinduces tolerance of tobacco to bacteria and oomycetes. *Plant Physiol.* 149:1970-1981.

Moschou P.N., Wu J., Cona A., Tavladoraki P., Angelini R., Roubelakis-Angelakis K.A. (**2012**). The polyamines and their catabolic products are significant players in the turnover of nitrogenous molecules in plants. *J Exp Bot.* 63:5003-5015.

Murata Y., Mori I.C., Munemasa S. (**2015**). Diverse stomatal signalig and the signal integration mechanism. *Annu. Rev. Plant Biol.* 66:369–392.

Murray-Stewart T.R., Woster P.M., Casero R.A.Jr. (**2016**). Targeting polyamine metabolism for cancer therapy and prevention. *Biochem J.* 473:2937-53.

Nguyen C.T., Kurenda A., Stolz S., Chételat A., Farmer E.E. (**2018**). Identification of cell populations necessary for leaf-to-leaf electrical signaling in a wounded plant. *Proc Natl Acad Sci U S A.* 115:10178-10183.

Ohkubo S., Mancinelli R., Miglietta S., Cona A., Angelini R., Canettieri G., Spandidos D.A., Gaudio E., Agostinelli E. (**2019**) Maize polyamine oxidase in the presence of spermine/spermidine induces the apoptosis of LoVo human colon adenocarcinoma cells. *Int J Oncol.* 54:2080-2094.

Padiglia A., Medda R., Pedersen J.Z., Lorrap A., Peč P., Frébort I., Floris G. (**1998**). Inhibitors of Plant Copper Amineoxidases. *Journal of Enzyme Inhibition*. 13:311-325.

Paschalidis K.A., Toumi I., Moschou P.N., Roubelakis-Angelakis K.A. (**2010**). ABA-dependent amine oxidases-derived H2O2 affects stomata conductance. *Plant Signal Behav.* 5:1153–56.

Peiter E., Maathuis F.J., Mills L.N., Knight H., Pelloux J., Hetherington A.M., Sanders D. (**2005**). The vacuolar Ca^{2+}-activated channel TPC1 regulates germination and stomatal movement. *Nature* 234:404-8.

Planas-Portell J., Gallart M., Tiburcio A.F., Altabella T. (**2013**). Copper-containing amine oxidases contribute to terminal polyamine oxidation in peroxisomes and apoplast of *Arabidopsis thaliana*. *BMC Plant Biol.* 13:109.

Pradedova E.V., Trukhan I.S., Nimaeva O.D., Salyaev R.K. (**2013**). Hydrogen peroxide generation in the vacuoles of red beet root cells. *Doklady Biological Sciences* 449, 1–4.

Qi Z., Stephens N.R., Spalding E.P. (**2006**). Calcium entry mediated by GLR3.3, an Arabidopsis glutamate receptor with a broad agonist profile. *Plant Physiol*. 142:963-71.

Qu Y., An Z., Zhuang B., Jing W., Zhang Q., Zhang W. (**2014**). Copper amine oxidase and phospholipase D act independently in abscisic acid (ABA)-induced stomatal closure in *Vicia faba* and *Arabidopsis*. *J. Plant. Res.* 127:533–544.

Rea G., Metoui O., Infantino A., Federico R., Angelini R. (**2002**). Copper amine oxidase expression in defense responses to wounding and Ascochyta rabiei invasion. *Plant Physiol.* 128, 865–875.

Rea G., de Pinto M.C., Tavazza R., Biondi S., Gobbi V., Ferrante P., de Gara L., Federico R., Angelini R., Tavladoraki P. (**2004**). Ectopic expression of maize polyamine oxidase and pea copper amine oxidase in the cell wall of tobacco plants. *Plant Physiol.* 134:1414–1426.

Sagor G.H., Zhang S., Kojima S., Simm S., Berberich T., Kusano T. (**2016**). Reducing Cytoplasmic Polyamine Oxidase Activity in Arabidopsis Increases Salt and Drought Tolerance by Reducing Reactive Oxygen Species Production and Increasing Defense Gene Expression. *Front Plant Sci.* 7:214.

Savatin D.V., Gramegna G., Modesti V., Cervone F. (**2014**). Wounding in the plant tissue: the defense of a dangerous passage. *Front Plant Sci.* 5:470.

Schmidt R., Kunkowska A.B., Schippers J.H. (**2016**). Role of reactive oxygen species during cell expansion in leaves. *Plant Physiol.* 172:2098–106.

Sirichandra C., Wasilewska A., Vlad F., Valon C., Leung J. (**2009**). The guard cell as a single-cell model towards understanding drought tolerance and abscisic acid action. *J Exp Bot.* 60:1439-1463.

Song Y., Miao Y., Song C.P. (**2014**). Behind the scenes: the roles of reactive oxygen species in guard cells. *New Phytol.* 201:1121–1140.

Su S.H., Gibbs N.M., Jancewicz A.L., Masson P.H. (**2017**). Molecular mechanisms of root gravitropism. *Curr Biol.* 27:R964-R972.

Tardieu F. and Davies W.J. (**1992**). Stomatal response to abscisic acid is a function of current plant water status. *Plant Physiol*. 98:540-545.

Tavladoraki P., Cona A., Angelini R. (**2016**). Copper-containing amine oxidases and FAD-dependent polyamine oxidases are key players in plant tissue differentiation and organ development. *Front Plant Sci.* 7:824.

Tavladoraki P., Cona A., Federico R., Tempera G., Viceconte N., Saccoccio S., Battaglia V., Toniello A., Agostinelli E. **(2012)** Polyamine catabolism: target for antiproliferative therapies in animals and stress tolerance strategies in plants. *Amino Acids.* 42:411- 426.

Tiburcio A.F., Altabella T., Bitrián M., Alcázar R. (**2014**). The roles of polyamines during the lifespan of plants: from development to stress. *Planta*. 240:1-18.

Tisi A., Angelini R., Cona A. (**2011a**) Does polyamine catabolism influence root development and xylem differentiation under stress conditions? *Plant Signal Behav*. 11:1844–47.

Tisi A., Federico R., Moreno S., Lucretti S., Moschou P.N., Roubelakis-Angelakis K.A., Angelini R., Cona A. (**2011b**). Perturbation of polyamine catabolism can strongly affect root development and xylem differentiation. *Plant Physiol*. 157:200–15.

Titarenko E., Rojo E., León J., Sánchez-Serrano J.J. (**1997**). Jasmonic acid-dependent and -independent signaling pathways control wound-induced gene activation in Arabidopsis thaliana. *Plant Physiol*. 115:817-26.

Todaka D., Zhao Y., Yoshida T., Kudo M., Kidokoro S., Mizoi J., Kodaira K-S., Takebayashi Y., Kojima M., Sakakibara H., Toyooka K., Sato M., Fernie A.R., Shinozaki K., Yamaguchi-Shinozak K. (**2017**). Temporal and spatial changes in gene expression, metabolite accumulation and phytohormone content in rice seedlings grown under drought stress conditions. *The Plant Journal* 90:61–78.

Tsukagoshi H., Busch W., Benfey P.N. (**2010**). Transcriptional regulation of ROS controls transition from proliferation to differentiation in the root. *Cell* 143:606–16.

Valvekens D., Van Montagu M., Van Lijsebettens M. (**1988**). Agrobacterium tumefaciens-mediated transformation of Arabidopsis thaliana root explants by using kanamycin selection. *Proc Natl Acad Sci USA*. 85:5536-40.

Vera-Sirera F., Minguet E.G., Singh S.K., Ljung K., Tuominen H., Blázquez M.A., Carbonell J. (**2010**). Role of polyamines in plant vascular development. *Plant Physiol Biochem* 48:534–539.

Wang P.C., Dua Y.Y., Hou Y.J., Zhao Y., Hsu C.C., Yuan F.J., Zhu X.H., Tao W.A., Song C.P., Zhu J.K. (**2015**). Nitric oxide negatively regulates abscisic acid signaling in guard cells by S-nitrosylation of OST1. *Proc. Natl. Acad. Sci. USA* 112:613-618.

Wimalasekera R., Villar C., Begum T., Scherer G.F.E. (**2011**) *COPPER AMINE OXIDASE1* (*CuAO1*) of *Arabidopsis thaliana* contributes to abscisic acid- and polyamine-induced nitric oxide biosynthesis and abscisic acid signal transduction. *Mol Plant*. 4:663–678.

Winter D., Vinegar B., Nahal H., Ammar R., Wilson G.V., Provart N.J. (**2007**). An "Electronic Fluorescent Pictograph" browser for exploring and analyzing large-scale biological data sets. *PLoS ONE* 2:718.

Yang Z., Liu J., Tischer S.V., Christmann A., Windisch W., Schnyder H., Grill E. (**2016**). Leveraging abscisic acid receptors for efficient water use in Arabidopsis. *PNAS*, 113:6791–6796.

Yoda H., Yamaguchi Y., Sano H. (**2003**). Induction of hypersensitive cell death by hydrogen peroxide produced through polyamine degradation in tobacco plants. *Plant Physiol.* 132:1973–1981.

Yoshimoto K., Takamura H., Kadota I., Motose H., Takahashi T. (**2016**). Chemical control of xylem differentiation by thermospermine, xylemin, and auxin. *Sci Rep.* 6:21487.

Zeng W., Melotto M., He S.Y. (**2010**). Plant stomata: a checkpoint of host immunity and pathogen virulence. *Curr Opin Biotechnol*. 21:599-603.

Zhou L., Hou H., Yang T., Lian Y., Sun Y., Bian Z., Wang C. (**2018**). Exogenous hydrogen peroxide inhibits primary root gravitropism by regulating auxin distribution during Arabidopsis seed germination. *Plant Physiol Biochem.* 128:126-133.